

https://dspace.org/

Investigations into the mechanisms of rock support provided by sprayed liners

Dube, James

2010-09-09
http://hdl.handle.net/10539/8633

Downloaded from a DSpace repository. https://dspace.org/

INVESTIGATIONS INTO THE MECHANISMS OF ROCK SUPPORT PROVIDED BY SPRAYED LINERS

James Dube

A dissertation submitted to the Faculty of Engineering and the Built Environment, University of the Witwatersrand, Johannesburg, in fulfillment of the requirements for the degree of Master of Science in Engineering.

Johannesburg, 2009

DECLARATION

I declare that this dissertation is my own, unaided work. It is being submitted for the Degree of Master of Science in the University of the Witwatersrand, Johannesburg. It has not been submitted before for any degree or examination in any other University.

.....

(Signature of candidate)

..... day of .....(year) .....

at .....

ABSTRACT

An investigation into the mechanisms of rock support provided by sprayed liners was carried out practically at three different mines, namely, South Deep Mine (Gold Fields), Mponeng Mine (Anglo Gold Ashanti) and Impala Platinum Mine (IMPLATS). The monitored sites included tunnels and pillars supported by steel fibre reinforced shotcrete and plain shotcrete.

Underground monitoring provided information on the behaviour of shotcrete over time as the pillars and tunnels responded to mining induced stress changes. The exercise played a role in the identification of the possible failure modes of shotcrete in-situ. Underground in-situ bond strength tests were carried out to give an idea of the shotcrete-rock interface bond strength. The monitoring methods included measurement of strains and displacements of the tunnel walls and pillar walls with the aid of Vibrating Wire Strain Gauges (VWSG), Multi-Point Borehole Extensometers (MPBX), Single-Point Borehole Extensometers (SPBX) and laser targets. Inspection boreholes were drilled, and monitored using camera probes to observe the condition of the rock behind the shotcrete. Also, photographs were taken to give an idea of the failure modes and support mechanisms provided to the rock by shotcrete based on field observations.

Fibre reinforced shotcrete laboratory tests were carried out according to the EFNARC and ASTM standards for shotcrete panel and beam testing. The laboratory tests helped in identifying the effects of fibre incorporation into the shotcrete for the support of underground mining excavations.

The results obtained from the field monitoring exercise, field tests, and laboratory tests were used to analyse and deduce the possible mechanisms of rock support provided by sprayed liners in mining excavations.

ACKNOWLEDGEMENTS

My profound gratitude on the assistance and support for the success in completing this research work is extended to the following people and institutions:

Professor T.R. Stacey for his supervision, guidance and encouragement throughout this research.

SRK Consulting for allowing me to participate in their SIMRAC shotcrete project. SRK Consulting has also been helpful in providing most of the literature resources through their well equipped library and past work done on the shotcrete project.

William Joughin has provided all the information on the past work done on the project, which includes mapping results of the underground sites. He also provided invaluable guidance throughout the monitoring exercise.

Jody Thompson for the invaluable input in the processing of the large volumes of data obtained from the underground monitoring instruments.

Lars Hage of BASF Construction Company and Terry Bean as well as Phillip Walker of Metalloy Company for donating all the fibres used in the laboratory tests.

The Managers and Staff at Mponeng Gold Mine, South Deep Gold Mine and Impala Platinum Mine for the cooperation and affording me the opportunity to use their premises throughout the study.

Tony Ward of Seismogen and his team for carrying out the monitoring exercise of the instruments at all of the underground monitoring sites.

My wife Memory and son Cyril, as well as all my family members and friends for being around in times of need during the research work.

In memory of my mother Esline and brother Komborerai

TABLE OF CONTENTS

CONTENTS **PAGE**

DECLARATION i

ABSTRACT ii

ACKNOWLEDGEMENTS iii

TABLE OF CONTENTS v

LIST OF FIGURES xiii

LIST OF TABLES xxii

LIST OF TERMS xxiii

CHAPTER 1 1

INTRODUCTION 1

1.1 Background 1

1.2 Definition of the problem 3

1.3 Objectives 4

1.4 Research methodology 5

1.5 Content of the dissertation 6

CHAPTER 2 7

LITERATURE REVIEW 7

2.1 Introduction 7

2.2 Functions of shotcrete as a sprayed liner 7

2.2.1 Supporting the Rock Mass 7

2.2.2 Support Pressure 10

2.2.3 Support of Key Blocks 13

2.2.4 Sprayed liners as a sealant 15

2.3 Loading of sprayed liners in underground excavations 15

2.3.1 Gravity loading due to loosened blocks or wedges 16

2.3.2 Sprayed liner loading due to in situ stresses and mining induced stresses 16

2.3.3 Loading of sprayed liners supporting the rock together with rock bolts 17

2.3.4 Loading due to water pressure 18

2.4 Failure modes for sprayed liners 18

2.4.1 Adhesion failure 18

2.4.2 Shear failure 20

2.4.3 Flexural failure of a shotcrete beam 21

2.4.4 Shotcrete tensile failure 22

2.5 Shotcrete Design Methods 23

2.5.1 Empirical design methods 23

2.5.2 Analytical methods 24

2.5.3 Numerical modelling 25

2.6 Properties of sprayed liners 26

2.6.1 Bond strength 26

2.6.2 Shotcrete strength 28

2.6.3 Shotcrete ductility 29

2.6.4 Shotcrete stiffness 30

2.6.5 Shotcrete thickness 30

2.7 Mechanisms of support provided by sprayed liners 31

2.7.1 Promotion of block interlock 31

2.7.2 Shotcrete structural arch support mechanism 31

2.7.3 Shotcrete basket mechanism of rock support 32

2.7.4 Shotcrete beam support mechanism 33

2.7.5 Durability enhancement through sealing action as a support mechanism 35

2.7.6 Rock bolt face plate extension support mechanism 35

2.8 Summary 36

CHAPTER 3 38

UNDERGROUND FIELD MONITORING AND FIELD TESTING 38

3.1 Introduction 38

3.2 Monitoring objectives 39

3.3 Monitoring instruments..... 39

3.3.1 Ground motion monitor (GMM) 39

3.3.2 Vibrating wire strain gauge (VWSG)..... 40

3.3.3 Multi-point borehole extensometer (MPBX)..... 41

3.3.4 Single point borehole extensometer (SPBX) 41

3.3.5 Laser displacement monitoring 42

3.3.6 Borehole monitoring using a borehole video camera 42

3.3.7 Visual monitoring..... 42

3.4 Monitoring sites..... 42

3.4.1 Mponeng Gold Mine Level 109 Test Site 42

3.4.2 Mponeng Gold Mine Level 116 46

3.4.3 South Deep Gold Mine 49

3.4.4 Determination of the in situ shotcrete material properties at South Deep Mine 57

3.4.5 Impala Platinum Mine..... 60

3.5 Monitoring Results 62

3.5.1 South Deep Mine monitoring results 62

3.5.2 Discussion of the monitoring results at South Deep Mine 70

3.5.3 South Deep Laboratory and field test results 71

3.5.4 Impala Platinum Mine Monitoring Results 75

3.5.5 Mponeng Mine Level 109 monitoring results 77

3.5.6 Mponeng Mine Level 116 monitoring results 79

3.6 Shotcrete Failure Mechanisms 82

3.6.1 Tensile failure 82

3.6.2 Adhesion failure 84

3.6.3 Punching failure 86

3.6.4 Shear failure 87

3.6.5 Bending failure 89

3.7 Conclusion 91

CHAPTER 4 93

LABORATORY TESTS 93

4.1 Introduction 93

4.2 Objectives of laboratory testing 93

4.3 Test suitability 94

4.4 Test programme 94

4.5 Fibre specifications 96

4.5.1 Steel Fibres 96

4.5.2 Polypropylene fibres 96

4.6 Control of consistency..... 97

4.7 Determination of shotcrete performance..... 98

4.7.1 ASTM beams 98

4.7.2 EFNARC beams..... 101

4.7.3 EFNARC Panels..... 103

4.7.4 ASTM centrally loaded Round determinate Panels..... 103

4.7.5 Uniaxial Compressive Strength (UCS) tests..... 103

4.7.6 Spraying losses of steel fibres..... 103

4.8 Presentation and discussion of results..... 103

4.8.1 ASTM beams modulus of rupture..... 104

4.8.2 ASTM beams toughness indices..... 106

4.8.3 EFNARC beams flexural strength 108

4.8.4 EFNARC Beams residual strength..... 110

4.8.5 EFNARC panels peak load results..... 112

4.8.6 EFNARC panels energy absorption 114

4.8.7 ASTM Round determinate panels peak loads..... 116

4.8.8 ASTM Round Determinate Panels (RDPs) Energy Absorption ……...117

4.8.9 Uniaxial compressive strength 120

4.8.10 Steel fibre spraying losses 122

4.9 Comments on laboratory testing results 124

4.10 Conclusions 125

CHAPTER 5 126

INVESTIGATIONS INTO THE MECHANISMS OF ROCK SUPPORT PROVIDED BY SPRAYED LINERS BASED ON FIELD OBSERVATIONS 126

5.1 Introduction 126

5.2 Mechanisms of rock support provided by sprayed liners based on field observations 126

5.2.1 Promotion of block interlock through bonding 126

5.2.2 Tensile strength of liner 130

5.2.3 Basket mechanism 133

5.2.4 Shotcrete structural support mechanism 135

5.2.5 Extended faceplate 139

5.2.6 Mechanical protection 140

5.2.7 Durability enhancement 141

5.3 Conclusion 142

CHAPTER 6 143

CONCLUSIONS AND RECOMMENDATIONS 143

REFERENCES 147

BIBLIOGRAPHY 158

APPENDIX A: Load deflection graphs for ASTM beams, ASTM RDPs, EFNARC panels and EFNARC beams 159

APPENDIX B: Table showing the strength, peak load, residual strength and energy absorption results for the laboratory tested shotcrete specimens..... 176

LIST OF FIGURES

Figure 2.1 Types of failure which occur in massive, jointed and heavily jointed rock masses exposed to low and high in situ stress levels (After Hoek et al, 1995) 9

Figure 2.2 Simplified ground-support reaction curve (After Douglas and Arthur, 1983)..... 11

Figure 2.3a Shotcrete interaction with ground reaction curve: Difference between shotcrete applied close to the tunnel face and far from the tunnel face (After Leach, 1998) 12

Figure 2.3b Shotcrete interaction with ground reaction curve illustrating the failure of plain shotcrete (After Leach, 1998) 12

Figure 2.3c Shotcrete interaction with ground reaction curve: Stability with reinforced shotcrete (After Leach, 1998) 13

Figure 2.4 The key block theory diagram illustrating that when the shaded key blocks are stable, then stability around an excavation is maintained (After Barrett and McCreath, 1995) 14

Figure 2.5 Fallout of shotcrete only indicating poor adhesion (After Malmgren and Svensson, 1999) 19

Figure 2.6 Shotcrete shear failure resulting from loose block movement (After Leach, 2002)..... 20

Figure 2.7 Shotcrete failing in tension as loosened block movement occurs causing lining de-bonding (After Leach, 2002)..... 22

Figure 2.8 Simplified shotcrete design chart (Stacey, 2003, modified after Barton et al, 1974)..... 24

Figure 2.9 Adhesion testing equipment 27

Figure 2.10 Shotcrete rock bearing capacity as an arch (After Stille and Franzen, 1990) 32

Figure 2.11 Shotcrete support as a beam, supported by adhesion to the rock or adhesion to the rock and clamping effect offered by rock bolts (After Stille and Franzen, 1990) 34

Figure 2.12 Shotcrete support as flexible retaining panels in a tunnel (After Kaiser and Tannant, 1997) 34

Figure 2.13 Illustration of the extended face plate where shotcrete and rock bolting are used together (After Stacey, 2001) 36

Figure 3.1 Ground motion monitor (GMM) 40

Figure 3.2 Strain gauge rosettes 41

Figure 3.3 Mponeng Mine Level 109 South-East wall showing positions of laser targets and the inspection borehole 44

Figure 3.4 Mponeng Mine Level 109 North-West wall showing the position of laser targets and the inspection borehole 45

Figure 3.5 Mponeng Mine Level 116 site plan (SRK SIMRAC Internal report, 2008) 46

Figure 3.6 Mponeng Mine Level 116 wall A showing the position of laser targets and the Ground Motion Monitor (GMM) 47

Figure 3.7 Mponeng Mine Level 116 wall B showing the positioning of laser targets the Ground Motion Monitor (GMM) 48

Figure 3.8 South Deep Mine plan showing location of test site (SRK SIMRAC Internal report, 2008) 49

Figure 3.9 Test pillar detail at South Deep Mine Site (SRK SIMRAC Internal report, 2008) 50

Figure 3.10 Face and support mapping of Pillar B and Pillar D (SRK SIMRAC Internal report, 2008) 52

Figure 3.11 Photograph showing South Deep Mine Pillar A and positioning of monitoring instruments, values show the thickness of shotcrete at the marked position 54

Figure 3.12 Photograph showing South Deep Mine Pillar B and positioning of monitoring instruments 55

Figure 3.13 Photograph showing South Deep Mine Pillar D and positioning of monitoring instruments and shotcrete cracks marked on the pillar 56

Figure 3.14 Photograph showing South Deep Mine Pillar E positioning of monitoring instruments 57

Figure 3.15 Photograph showing shotcrete-rock bond strength testing at South Deep Mine (Pillar A) 58

Figure 3.16 Photographs showing the location of drilled cores for UCS testing, bond strength testing and fibre density determination at South Deep Mine on pillars A, D and E 59

Figure 3.17 Impala Platinum Mine monitoring site plan (SRK SIMRAC Internal report, 2008) 60

Figure 3.18 Photograph showing the position of the Vibrating Wire Strain Gauge (VWSG) and the Ground Motion Monitor (GMM) on the monitored sidewall of the shotcreted tunnel at Impala Platinum Mine 61

Figure 3.19 South Deep Mine Pillar A displacement and strain results 63

Figure 3.20 South Deep Mine Pillar B displacement results 64

Figure 3.21 South Deep Mine Pillar B laser targets displacement results 65

Figure 3.22 South Deep Mine Pillar D displacement results 66

Figure 3.23 South Deep Mine Pillar D laser targets displacement results 67

Figure 3.24 South Deep Mine MPBX and GMM monitoring results for Pillar E 68

Figure 3.25 Fracture zones identified at South Deep Mine site from borehole inspection (SRK, SIMRAC Internal report, 2008). 69

Figure 3.26 Impala Platinum Mine GMM displacement results 76

Figure 3.27 Impala Platinum Mine vibrating wire strain gauge results . 76

Figure 3.28 Mponeng Mine Level 109 North-West wall displacement results..... 78

Figure 3.29 Mponeng Mine Level 109 South-East wall displacement results..... 79

Figure 3.30 Laser targets displacement results for Mponeng Mine Level 116 81

Figure 3.31 GMM displacement results for Mponeng Mine Level 116 . 82

Figure 3.32 Photograph showing tensile failure of shotcrete on Pillar B at South Deep Mine..... 83

Figure 3.33 Cross-section of a pillar with the solid line showing original pillar profile and dashed line showing the pillar profile after expansion due to increased mining induced stresses. 84

Figure 3.34a Photograph showing adhesion failure of shotcrete on Pillar E at South Deep Mine 85

Figure 3.34b Photograph showing adhesion failure between Pillar D and Pillar E at South Deep Mine 86

Figure 3.35 Photograph showing punching failure of shotcrete on Pillar D at South Deep Mine 87

Figure 3.36 Photograph showing shear failure of shotcrete on Pillar B at South Deep Mine 88

Figure 3.37 Relative displacement of shotcrete block A to shotcrete block B resulting in shotcrete shear failure 89

Figure 3.38a Photograph showing bending failure of shotcrete on Pillar B at South Deep Mine 90

Figure 3.38b Photograph showing bending failure of shotcrete on Pillar B at South Deep Mine 91

Figure 4.1 Metalloy steel fibre dimensions 96

Figure 4.2 Polypropylene fibre dimensions 97

Figure 4.3 Determination of toughness indices (ASTM C1018, 1997). 101

Figure 4.4 P values from the Load-Deflection graph for flexural and residual strengths (EFNARC, 1996) 102

Figure 4.5 Modulus of rupture for the polypropylene fibre reinforced shotcrete ASTM beams 105

Figure 4.6 Modulus of rupture for the steel fibre reinforced ASTM shotcrete beams 105

Figure 4.7 Toughness indices for the polypropylene fibre reinforced shotcrete ASTM beams 107

Figure 4.8 Toughness indices for the steel fibre reinforced shotcrete ASTM beams 107

Figure 4.9 Flexural strength for the polypropylene fibre reinforced EFNARC beams 109

Figure 4.10 Flexural strength for the steel fibre reinforced shotcrete EFNARC beams 109

Figure 4.11 Residual strength for the polypropylene fibre reinforced shotcrete EFNARC beams 111

Figure 4.12 Residual strength for the steel fibre reinforced shotcrete EFNARC beams 111

Figure 4.13 Peak loads for the polypropylene fibre reinforced shotcrete EFNARC panels 113

Figure 4.14 Peak loads for the steel fibre reinforced shotcrete EFNARC panels 113

Figure 4.15 Energy absorption for the polypropylene fibre reinforced shotcrete EFNARC panels 115

Figure 4.16 Energy absorption for the steel fibre reinforced shotcrete EFNARC panels 115

Figure 4.17 Peak loads for the polypropylene fibre reinforced shotcrete round determinate panels 116

Figure 4.18 Peak loads for the steel fibre reinforced shotcrete round determinate panels 117

Figure 4.19 Energy absorption for the polypropylene fibre reinforced round determinate panels 118

Figure 4.20 Energy absorption results for the steel fibre reinforced round determinate panels 118

Figure 4.21 Load-deflection results for the polypropylene fibre reinforced shotcrete round determinate shotcrete panels 119

Figure 4.22 Load-deflection results for the steel fibre reinforced shotcrete round determinate shotcrete panels 120

Figure 4.23 Uniaxial compressive strength test results for the steel fibre reinforced shotcrete cores 121

Figure 4.24 Uniaxial compressive strength test results for the polypropylene fibre reinforced shotcrete cores 122

Figure 4.25 Steel fibre spraying rebound loss results for the steel fibre reinforced shotcrete specimens 123

Figure 5.1a Borehole A and Borehole B in Mponeng Level 109 showing broken rock (about 0.5m) but interlocked in place by the shotcrete 128

Figure 5.1b Broken and loose rock held back by wire mesh and rope lacing and broken rock interlocked behind shotcrete at Mponeng Mine Level 109 129

Figure 5.1c Side view of the loosened blocks (about 0.5m depth) held back by the mesh and lacing a few meters from the intact shotcreted section shown in Figure 5.1a and Figure 5.1b 130

Figure 5.2 Fibres sticking out due to tensile stresses on a shotcrete crack at South Deep Mine..... 132

Figure 5.3a Diagram illustrating the tensile failure of fibres in fibre reinforced shotcrete..... 132

Figure 5.3b Diagram illustrating the pullout (failure) of fibres in fibre reinforced shotcrete..... 133

Figure 5.4 Basket mechanism where shotcrete has been applied together with rock bolts; mesh and lacing support (Mponeng Mine Level 116)..... 134

Figure 5.5a Demarcation between shotcrete, mesh and lacing support on Level 109 at Mponeng Mine. Shotcreted section shows no signs of loosening whereas the mesh and lacing section show signs of rock loosening. 136

Figure 5.5b Close view of Mponeng Mine Level 109 mesh and lacing section (mesh and lace section in Figure 5.5a) showing loosened rock held back by mesh and lacing support 137

Figure 5.5c Close view of Mponeng Mine Level 109 shotcreted roof section (shotcreted roof section in Figure 5.5a) still intact and showing no signs of failure in the shotcrete as the shotcrete provides support through the beam support mechanism.... 138

Figure 5.6 Cracks observed in a borehole showing a possibility of rock slabs forming in the tunnel walls due to mining induced stresses at Impala Platinum Mine..... 139

Figure 5.7 Tensioned cable bolting with face plates on the surface of shotcrete at Mponeng Mine Level 116 140

Figure 5.8 Damaged corner of one of the pillars that were monitored at South Deep Mine..... 141

LIST OF TABLES

Table 2.1 Overview of some of the relevant property requirements for shotcrete depending on ground condition (after Grov and Blindheim, 1997) 26

Table 2.2 The standard test methods to determine the strength properties of shotcrete 28

Table 3.1 Mponeng Mine site rock mass classification (SRK SIMRAC Internal report, 2008) 43

Table 3.2 South Deep Mine site rock mass classification (SRK SIMRAC Internal report, 2008) 51

Table 3.3 Bulk density, fibre density and UCS test results for cores drilled out of an EFNARC Panel spayed at South Deep Mine during pillar shotcreting 72

Table 3.4 In situ shotcrete core drilling and laboratory testing results at South Deep Mine monitoring site 74

Table 4.1 Test programme per fibre density batch 95

Table 4.2 Steel fibre specifications 96

Table 4.3 Polypropylene fibre specifications 97

Table 4.4 Summary of standard test methods for testing shotcrete beams and panels 98

Table 4.5 Suggested toughness indices (After Morgan, 1988) 100

Table 4.6 Fibre content losses for shotcrete specimens sprayed underground and on surface 124

LIST OF TERMS

ASTM	American Society for Testing Materials
GMM	Ground motion monitor
GSI	Geological strength index
MPBX	Multi-point borehole extensometer
N/m^2	Newton per square metre
RDP	Round determinate panel
RMR	Rock mass rating
SIMRAC	Safety in Mines Research Advisory Committee
SPBX	Single point borehole extensometer
SRK	Steffen, Robertson and Kirsten
UCS	Uniaxial compressive strength
VWSG	Vibrating wire strain gauge
µm	micrometre

CHAPTER 1

INTRODUCTION

1.1 Background

Sprayed liners are a form of rock support for mining excavations, mainly underground operations. Hudson and Harrison (1997) defined rock support as the introduction of structural elements into an excavation for the purpose of inhibiting displacements at the excavation boundary to maintain stability. Hoek and Wood (1987) pointed out that the primary objective of a support system is to mobilize and conserve the inherent strength of the rock mass so that it becomes self-supporting. Rock support can be called active support and passive support.

Brady and Brown (1993) defined active support as the type of support that imposes a predetermined load to the rock surface once installed. Examples of active support include tensioned rock bolts or tensioned cables. Passive support is defined as the support that develops its load while the rock mass surrounding the excavation deforms (Brady and Brown, 1993). Henderson and Lewis (2001) indicated that sprayed liners, which are also referred to as containment support, fall into the category of passive support.

The mechanisms of rock support provided by sprayed liners have not been well explained in past literature. Various research carried out has shown that sprayed liners are viewed as ‘containment’ support, as opposed to ‘retainment’ support provided by rock bolts, cables etc (Stacey and Ortlepp, 1999; Ortlepp et al., 1999). The sprayed liners used in mining operations are shotcrete and thin spray-on liners (TSLs).

Shotcrete is a mixture of cement, sand, small aggregate and additives (e.g. accelerators, plasticizers, etc) that is pneumatically sprayed and compacted under high velocity onto a surface (usually rock). When there are no fibres incorporated, it is referred to as plain shotcrete and when there are fibres (mainly steel or polypropylene) incorporated it is called fibre reinforced shotcrete. Shotcrete prevents or minimizes rock displacement by filling large open joints and fractures, transferring the rock load to adjacent stable rock, and sealing the rock face to prevent ravelling and sloughing (Vandewalle, 1992). There are two types of shotcrete in use, namely, dry-mix shotcrete and wet-mix shotcrete. The main difference between the two systems is the stage at which water is applied to the dry ingredients: at the nozzle for dry-mix shotcrete and during mixing for wet-mix shotcrete (Hoek et al, 2000).

Thin spray-on liners (TSLs) are polymer based products applied to the rock with thickness that can be as low as 3mm to 4mm (Spearing and Hague, 2003). TSLs can be classified into reactive or non-reactive liners. Non-reactive TSLs once applied to the excavation surface gain strength over time as a result of hydration. On the other hand, reactive liners once applied gain strength rapidly due to an exothermic reaction brought on by a catalyst. Thin spray-on liners, sometimes referred to as super skins, have been developed to provide replacements to the traditional forms of containment support. Stacey (2001) states that thin spray-on linings have the advantages of low volume, rapid application and rapid curing.

All forms of sprayed liner support are largely dependent on the bonding between the sprayed liner and the rock interface. This calls for thorough cleaning of the rock surfaces during preparation before the sprayed liner support can be applied onto the excavation.

Sprayed liner support is applicable in both the civil and the mining engineering industries. The support requirements in these two different environments differ due to the fact that mining excavation support design aims at stability not longer than the required life of mine. However, for civil engineering purposes, long-term stability is crucial due to access by the public, and the planned cost of support is usually small in relation to the overall project cost. Also, for civil engineering purposes, excavations must be designed with a very low probability of failure.

Swan and Henderson (2001) indicated that the sprayed liner alone may not be adequate for ground support, hence the need to apply sprayed liners in combination with other forms of support, e.g., rock bolts. When used with other forms of support, the order of application of the supports depends on the design preferences and ground conditions.

Stacey (2001) and Tannant (2001) described a range of mechanisms of sprayed liner support behaviour and their loading behaviour. The support mechanisms are said to be occurring individually or in combination. The mechanisms of sprayed liner support behaviour and the common loading mechanisms need to be reviewed to enhance the understanding for practical application purposes.

1.2 Definition of the problem

The actual mechanisms of rock support provided by sprayed liners are extremely complex (Kaiser and McCreath, 1992). Some statements from the industry such as “the rock starts to behave when it sees the shotcrete” (Stacey and Yu, 2004), show that there is need for practical research to investigate some of the mechanisms by which sprayed liners support the rock.

One problem is that most of the mechanisms identified in literature are based on theoretical reasoning due to lack of field photographic illustrations to enhance the understanding of the mechanisms of rock support provided by the sprayed liners. Additionally, there has been controversy concerning whether shotcrete as a sprayed liner offers structural support or not.

Stacey and Yu (2004) argue that, due to thin applications of shotcrete in mining, typically less than 100mm thick, the structural arch support would be theoretically negligible. Thus the mechanisms of support behaviour of the shotcrete must be very different from that of the structural arch assumption on which most designs are said to be based.

Therefore a practically-based approach to investigate the mechanisms of rock support by means of field monitoring and field testing of sprayed liner supported excavations as well as laboratory testing, will give an improved understanding of rock support mechanisms provided by sprayed liners.

1.3 Objectives

The objective of this research is to improve the understanding of the mechanisms by which sprayed liners support the rock in situ in underground mining excavations by means of a practically based approach. The practically based approach shall concentrate on the analyses of field monitoring results of the shotcreted sites. Laboratory testing of shotcrete was also carried out to determine the effects of fibre incorporation in shotcrete on the rock support mechanisms provided by shotcrete as a sprayed liner.

1.4 Research methodology

A literature review of the information relating to the mechanisms of rock support provided by sprayed liners has been included in the research to provide the essential background information. This was followed by underground monitoring of shotcreted tunnels and pillars.

The underground monitoring exercise was carried out at the following mines: South Deep Gold Mine (Gold Fields Mining Company), Mponeng Gold Mine (Anglo Gold Ashanti operation) and Impala Platinum Mine (IMPLATS). At Mponeng Mine, two monitoring sites were established in tunnels on Level 109 and Level 116. The monitoring site at Impala Platinum Mine was established in a tunnel at Level 24 Shaft Number 15. The monitoring site at South Deep Mine was established in a pillar supported area close to a tipping point. Prior to shotcreting, mapping of the pillars and tunnels was carried out to estimate the pre-existing rock mass conditions at each of the underground mine sites.

Various instruments were used to measure strain, displacement and ground conditions in addition to field observations. The instruments used were Ground Motion Monitor (GMM), Single Point Borehole Extensometer (SPBX), Multi-Point Borehole Extensometer (MPBX) and Vibrating Wire Strain Gauge (SPBX).

Additionally, field tests were carried out at South Deep Mine to determine the shotcrete-rock interface bond strength. Shotcrete cores were drilled from the monitored pillars at South Deep Mine for UCS testing and for the determination of fibre density in the sprayed shotcrete.

Lastly, laboratory testing of shotcrete specimens (panels and beams) was carried out according to the ASTM and EFNARC standards.

1.5 Content of the dissertation

The following chapter reviews information relevant to the mechanisms involved in sprayed liner support using past literature. Chapter 3 presents the field monitoring and the field testing activities carried out to determine the behaviour of shotcrete in situ. Chapter 3 also shows photographic illustrations of the possible failure modes of shotcrete in the field. Presented in Chapter 4 are the results of shotcrete laboratory tests carried out using the ASTM and EFNARC standard test methods to determine the behaviour of fibre reinforced shotcrete and the effect of fibre incorporation in the shotcrete. A link between field observations and possible mechanisms of rock support provided by sprayed liners is presented in Chapter 5. The findings of this research and conclusions are found in Chapter 6. Laboratory test results are summarised in Appendix A and Appendix B.

CHAPTER 2

LITERATURE REVIEW

2.1 Introduction

Chapter 1 has provided the definition of rock support; the forms of rock support; definition of sprayed liners; types of sprayed liners and a brief description of each type of sprayed liner; and the objectives of the research as well as the research methodology. It was highlighted in Chapter 1 that the mechanisms of rock support and loading conditions need to be reviewed, and these topics form part of this Chapter. Also reviewed in Chapter 2 are the functions of sprayed liners, load transfer mechanisms of sprayed liners, failure modes of sprayed liners as well as useful physical properties of the sprayed liners. The review has a major focus on shotcrete as a thin sprayed liner for rock support in underground mining.

2.2 Functions of shotcrete as a sprayed liner

2.2.1 Supporting the Rock Mass

The main function of sprayed liners is to assist the rock mass maintain its stability to ensure safety in underground excavations. Langille et al (1995) mentioned that for one to understand how sprayed liners maintain stability in excavations, it is important for one to first understand how the rock fails. This is due to the fact that failure of the rock in excavations can be stress driven and or structurally controlled depending on the rock mass (Hoek et al, 1995). Figure 2.1 shows tunnels in high and low stress environments

with rock mass characteristics ranging from massive rock to heavily fractured rock mass and the failure associated with each rock mass condition. However, Leach (1998) argues that the excavation geometry also contributes to the displacements taking place in excavations which can result in failure of the excavation boundary.

Langille (2001) pointed out that liner application for ground support in a massive rock environment is not likely to provide any benefit. However, in blocky ground sprayed liner support can be very beneficial. Therefore it is important to understand both the rock mass conditions and the stress changes that will occur in the given rock mass conditions due to mining induced stresses. Hoek et al (1995) mentioned that the intention of the ground control system is not to prevent the failure from occurring by supporting the dead weight of the rock that has loosened, but to control and manage the deformations that result from the failure.

Morrison et al (1999) suggested that the ground can be controlled through the application of support and mining practices such as blasting techniques, de-stressing requirements, scaling practice, mining sequencing, orientation and shape of the excavation. In the ground control system, shotcrete is essential in arresting initial rock mass displacement to promote stability of the rock mass.

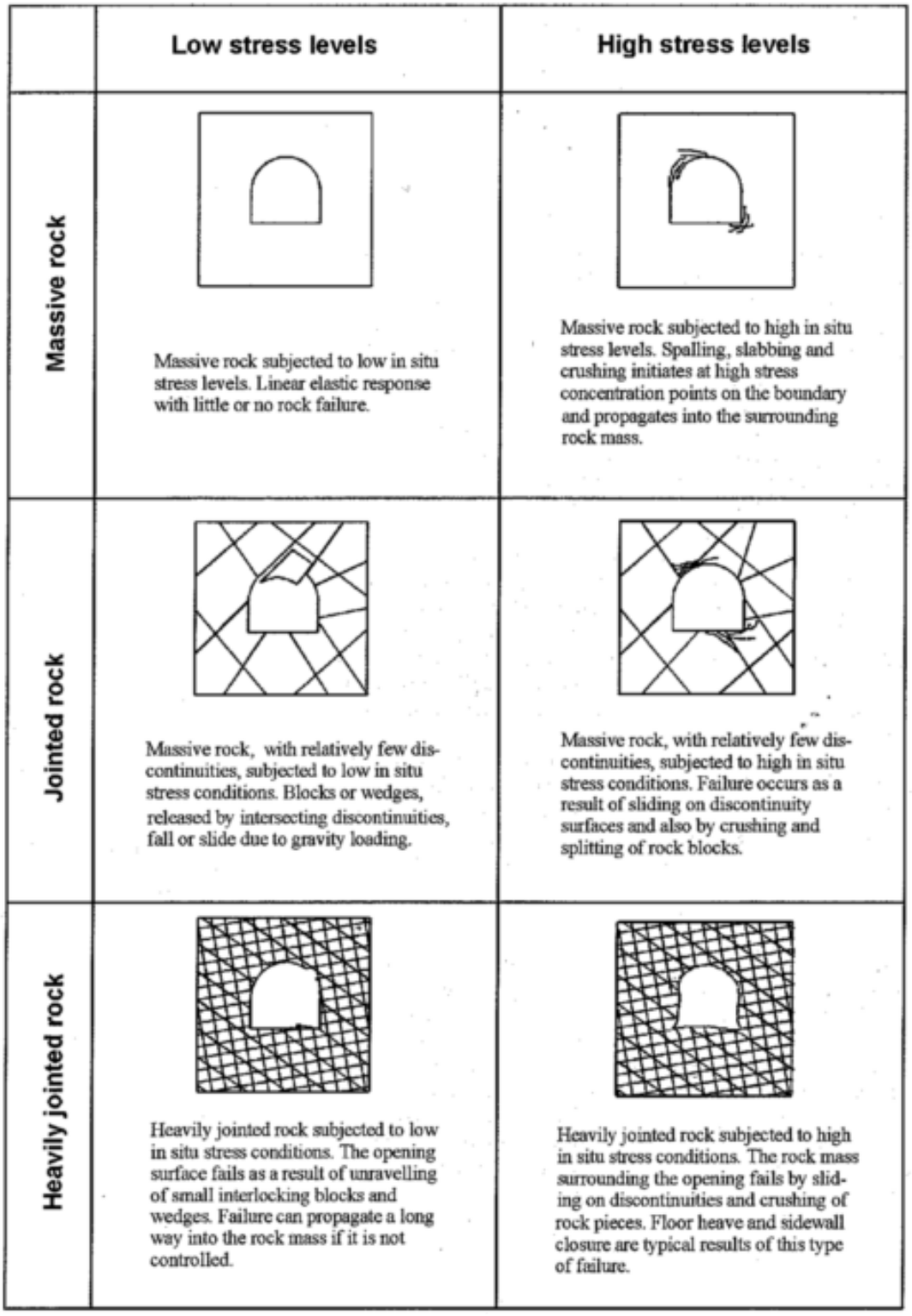


Figure 2.1 Types of failure which occur in massive, jointed and heavily jointed rock masses exposed to low and high in situ stress levels (After Hoek et al, 1995)

2.2.2 Support Pressure

Shotcrete support pressure in support design can be described as the resistance offered by shotcrete to the excavation boundary to control the inward displacement of the excavation walls, thereby preventing the loosening of rock, to ensure stability (Hoek et al, 1995). Mining excavations disturb the original stress patterns in the rock resulting in stress rearrangement and instability of the excavation boundary. Leach (1998) states that support requirements for an excavation can be assessed in terms of support pressure. He also pointed out that support pressure is used to contain the rock in its post failure state thereby attaining the post failure residual strength of the rock mass as the rock fractures are kept closed.

Hudson and Harrison (1997) mentioned that the support pressure required to maintain equilibrium of the excavation boundary at a given displacement value can be presented in a ground-support reaction curve as shown in Figure 2.2. Equilibrium between the stresses induced onto the excavation boundary and the support pressure provided by the sprayed liner is achieved when the support reaction curve intersects the rock mass displacement curve before either of the two curves has displaced too far (line 1 and line 2 marked in Figure 2.2). Line 1 in Figure 2.2 illustrates that if stiff support is installed in an excavation it reaches high support pressures at low excavation displacements and may be less effective. However, line 2 in Figure 2.2 illustrates optimum support that has been installed after some displacement has occurred – it intersects the rock mass displacement curve thereby indicating stability of the excavation. Line 3 in Figure 2.2 illustrates soft support installed after the rock has undergone too much displacement thereby failing to provide effective support to the excavation boundary.

Leach (1998) pointed out that the ground-support reaction curve is dependent on a specific set of conditions for a given mining environment

which include rock strength, excavation size and shape, stress field etc. He developed some curves to illustrate the interaction between shotcrete and the ground reaction curve for a tunnel as illustrated in Figure 2.3a, Figure 2.3b and Figure 2.3c. Figure 2.3a illustrates stability of an excavation attained when the shotcrete is applied close to the face and further away from the face. Figure 2.3c shows the benefit of reinforcement in shotcrete as stability is attained due to its ductility. This can be compared to plain shotcrete in Figure 2.3b, where stability of the tunnel is not attained.

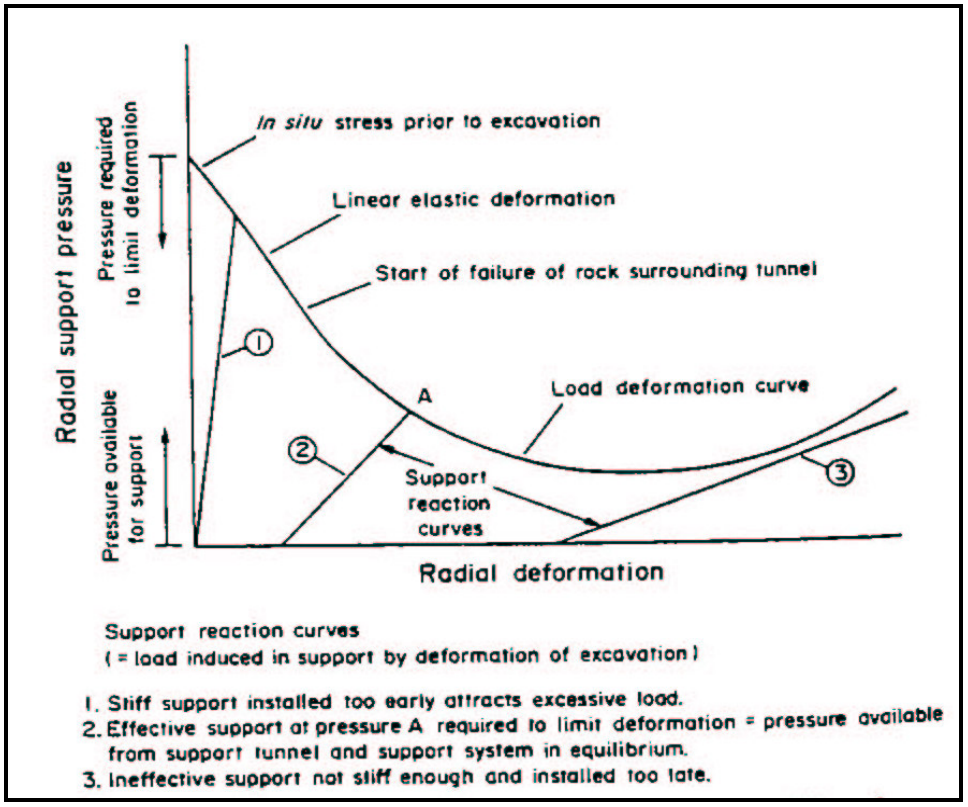


Figure 2.2 Simplified ground-support reaction curve (After Douglas and Arthur, 1983).

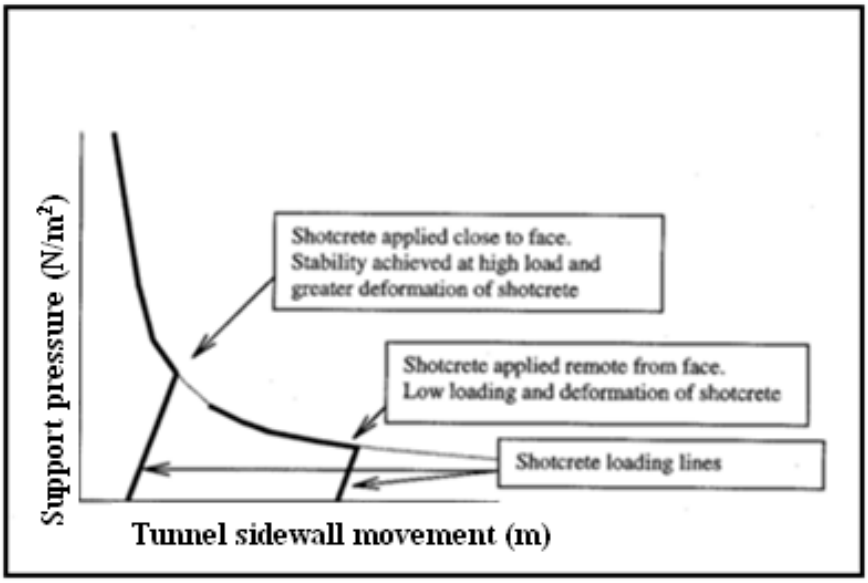


Figure 2.3a Shotcrete interaction with ground reaction curve: Difference between shotcrete applied close to the tunnel face and far from the tunnel face (After Leach, 1998)

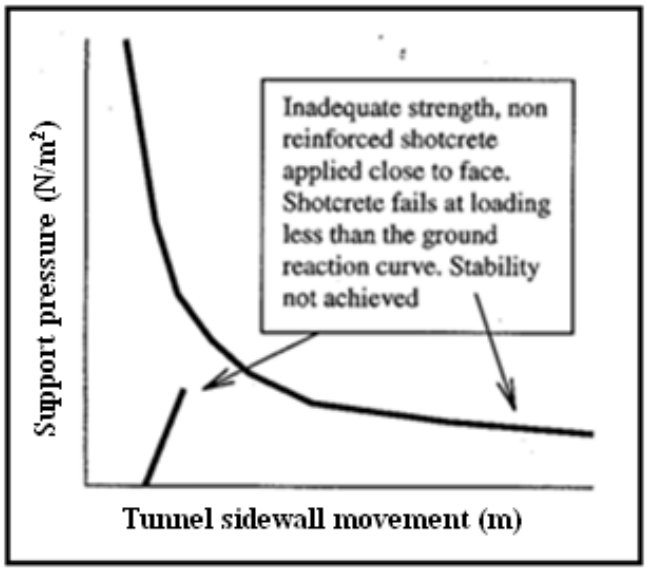


Figure 2.3b Shotcrete interaction with ground reaction curve illustrating the failure of plain shotcrete (After Leach, 1998)

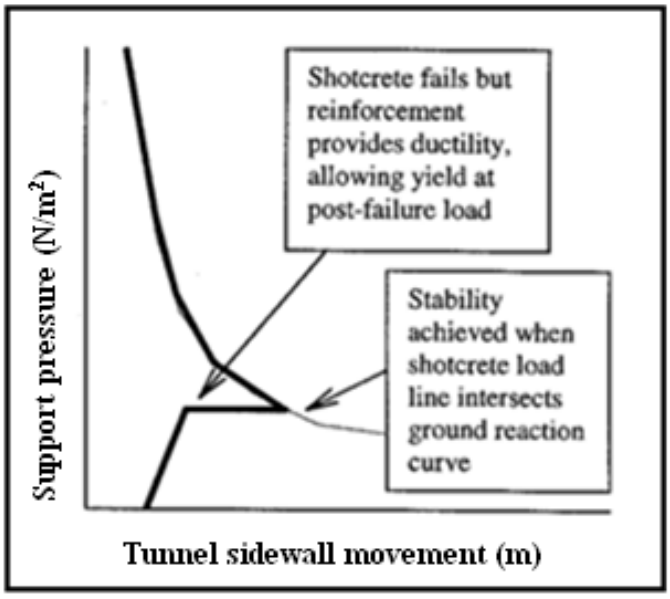


Figure 2.3c Shotcrete interaction with ground reaction curve: Stability with reinforced shotcrete (After Leach, 1998)

According to the support pressure design theory, shotcrete needs to be applied as quickly as possible to freshly exposed rock surfaces. Long delays allow the rock mass to loosen thereby reducing its ability to arch and increasing the potential for dead loads to develop (Stille and Franzen, 1990). Exceptions may occur in highly stressed ground where application is usually delayed to allow large stress-induced deformations to dissipate.

2.2.3 Support of Key Blocks

Shi and Goodman (1981) developed a concept for tunnels developed in blocky ground called the key block theory. The support of key block theory states that if all potentially unstable blocks surrounding a tunnel are supported, then, stability of the tunnel is achieved. Figure 2.4 illustrates the concept of the key block support theory whereby the block numbers demonstrate the order in which the rock mass would unravel once the shaded key blocks are removed. Kuijpers and Toper (2002) pointed out that sprayed liners provide stability to large blocks embedded in relatively

competent rock mass. Kuijpers and Toper (2002) emphasized good adhesion in the sprayed liner-rock interface and provision of sufficient shear and/or tensile resistance by the sprayed liner. However, due to the greater dead weight of the larger key blocks, Rose (1985) pointed out that large blocks are best supported by long rock bolts whereas shotcrete is necessary for the support of small key blocks in between the rock bolts.

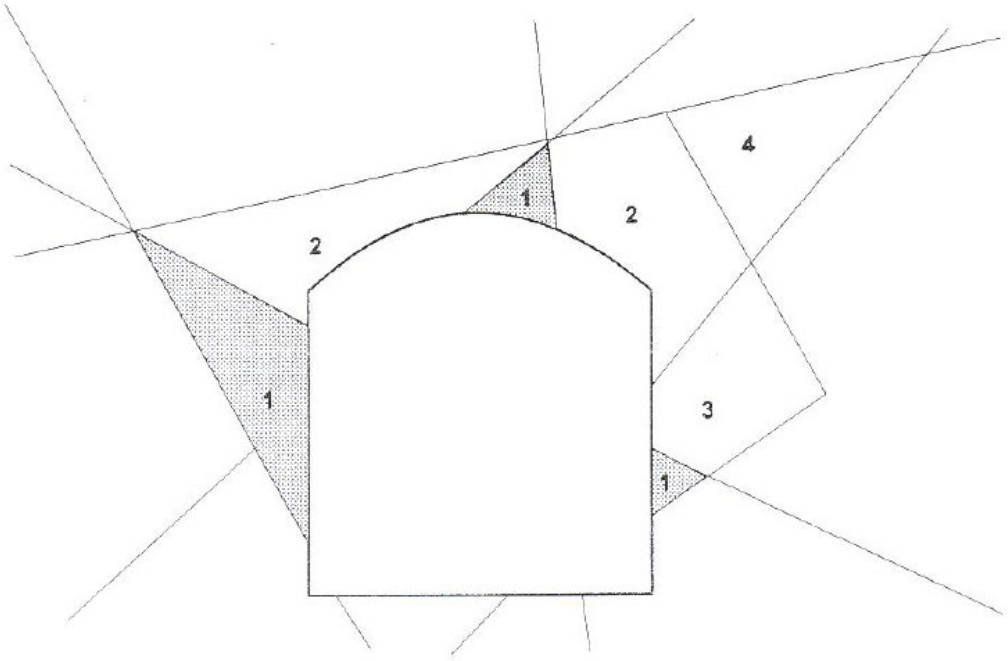


Figure 2.4 The key block theory diagram illustrating that when the shaded key blocks are stable, then stability around an excavation is maintained (After Barrett and McCreath, 1995)

Lang (1961) demonstrated the importance of sprayed liners in the support of small key blocks between rock bolts. Through his inverted bucket experiment, he showed that stability of small blocks can be achieved by a hairnet between the rock bolts. When the hairnet was burnt, the rock collapsed. However, Pells (2008) argued that conclusions drawn from

Lang's experiment can be questioned using simple applied mechanics. He goes on to say that in the experiment, the stresses induced on the rock bolts are too small by several orders of magnitude to have any effect on the rock mass strength in underground excavations.

2.2.4 Sprayed liners as a sealant

Egger (1981) and Morgan and Mowatt (1984) mentioned that shotcrete can help maintain the integrity of the rock by sealing open joints, as it penetrates into the joints during spraying. On the other hand, Speers (1998) considered sprayed liners as a sealant to intact rock that is prone to deterioration by weathering. Some rock types like Kimberlite are prone to deterioration once exposed to water. Stacey (2001) and Bartlett and Borejszo (2002) described the importance of the coating action provided by thin spray-on liners to the exposed Kimberlite as they protect it from water and therefore prevent its decomposition.

2.3 Loading of sprayed liners in underground excavations

The creation of excavations underground through mining activities disturbs the once stable rock in various ways. Supporting the excavations becomes a necessity to restore that stability. Therefore it has been found worthwhile to review the loading of sprayed liners by the rock as the loading determines the mechanism of support and the eventual failure mode of the sprayed liners.

2.3.1 Gravity loading due to loosened blocks or wedges

When blocky ground is excavated, structurally controlled instability of wedges and blocks may take place. The wedges or blocks may displace into the excavation due to gravity when they loosen thereby loading the liner (Stacey and Yu, 2004 and Malmgren, 2005). Kaiser and Tannant (1997) proposed a simplified method whereby the load acting on the shotcrete layer can be estimated as the weight of the loose block or wedge. Failure of the shotcrete takes place when the load bearing capacity of the liner is exceeded by the load exerted by the loose rock.

2.3.2 Sprayed liner loading due to in situ stresses and mining induced stresses

The rock is subjected to uniformly distributed virgin stresses before an excavation is opened up. Once an excavation is made, the original rock stress state is disturbed resulting in the redistribution of stresses in the immediate vicinity of the tunnel (Hoek et al, 1995). Depending on the magnitude of the stresses and the jointing in the rock, stress driven failure of the rock surrounding the excavation may load the sprayed liner applied to the excavation boundary. However, if there is no stress driven rock displacement taking place, only the rock will be stressed and not the sprayed liner. Stacey and Yu (2004) indicated that if there is good adhesion between the shotcrete-rock interface, when the shotcrete is stiffer than the fractured rock, it may result in the premature failure of the shotcrete. Malmgren et al (2004) pointed out that shotcrete applied in high stress environments should be able to deform freely to accommodate some excavation boundary displacements before failure.

When shotcrete has been reinforced with fibres and used together with rock bolts, mining induced stresses may cause distributed loads to act on the shotcrete. Stacey and Yu (2004) pointed out that the distributed loads

may cause the liner to support the rock with a “basket” support mechanism due to the ductility resulting from fibre incorporation which enables the shotcrete to accept some displacement before failure. High stresses on the excavation walls may induce bending loading on the shotcrete.

Stacey and Yu (2004) stated that support in excavations is normally placed on the roof and sidewalls. As a result, high stresses may cause the floor to converge faster than the roof thereby inducing bending loading onto the shotcrete, especially in the haunch areas of the excavation (Stacey and Yu, 2004).

Stresses can also result in a cantilever loading mechanism onto the sprayed liner. Cantilever loading of the sprayed liner support was first discussed by Tannant et al (1999) after carrying out field investigations underground on Thin Spray-on Liners (TSLs). From field observations, Tannant et al (1999) noted two different occasions when the sprayed liner failed due to continuous tearing apart caused by rock slabs that had rotated and cantilevered from the back. Tannant (2002) pointed out that cantilever loading resulting in tearing of the liner can be avoided when there is full areal coverage of the excavation by the sprayed liner.

2.3.3 Loading of sprayed liners supporting the rock together with rock bolts

When rock bolts and shotcrete are used together for rock support, Humphries and Funkhouser (1993) and Malmgren (2001) pointed out that the interaction between the rock bolts and the shotcrete is achieved when face plates are attached to the rock bolts with the face plates placed on the surface of shotcrete. The face plates play a crucial role for effective load transfer between the shotcrete and the rock bolts.

2.3.4 Loading due to water pressure

Aagaard et al (1997) mentioned that water may build up behind the sprayed liner supported excavations thereby loading the sprayed liner. In order to avoid surface support failure due to water pressure loading, Aagaard et al (1997) and Stacey (2001) indicated that provision for draining water collecting behind the sprayed liner is the best solution to ensure there is no water build up behind the sprayed liner.

2.4 Failure modes for sprayed liners

Failure modes for sprayed liners range from adhesion failure, bending failure, shear failure, compressive failure and tensile failure. Fernandez-Delgado et al (1981), Holmgren (1987) and Vandewalle (1992) explored modes of shotcrete failure using falling block tests to simulate the load applied on shotcrete. Their test results indicated that for steel fibre-reinforced and mesh-reinforced linings, direct shear failure tends to occur when adhesion to the rock mass is good, whereas flexural and punching shear failure occur when adhesion is poor and de-bonding has occurred.

2.4.1 Adhesion failure

Adhesion between the sprayed liner and the substrate plays a key role in defining the limiting failure mechanism, provided that cracking parallel to the bonded surface does not occur in the substrate itself (Barrett and McCreath, 1995). If adhesion is maintained, failure of the shotcrete will be controlled by direct shear. However, adhesion loss due to the sprayed liner peeling off from the rock or slabbing of the substrate will see the flexural failure mechanism becoming kinematically possible.

Hahn and Holmgren (1979) and Fernandez-Delgado et al (1976) pointed out that shotcrete-rock interface bond strength is poor on surfaces that have not been cleaned thoroughly with high pressure water. However, Egger (1981) added that adhesion is very much dependent on the type and quality of rock, following a series of tests on different rocks. On the other hand, Kumar et al (2002) proved through a series of tests that the bond strength of shotcrete varies directly with the joint roughness of the rock.

Malmgren and Svensson (1999) and Kuchta (2002) illustrated that adhesion failure occurs when the shotcrete-rock bond strength is weak relative to the dead weight of the shotcrete, resulting in the fallout of shotcrete as shown in Figure 2.5.

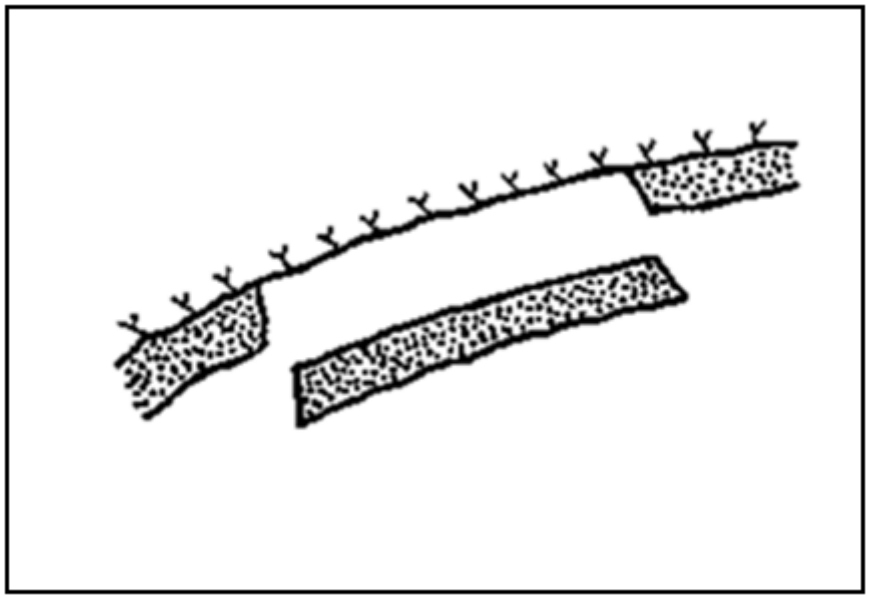


Figure 2.5 Fallout of shotcrete only indicating poor adhesion (After Malmgren and Svensson, 1999)

2.4.2 Shear failure

Barrett and McCreath (1995) indicated that shear failure can occur in two forms, namely direct shear failure or punch shear failure. They described direct shear failure of shotcrete as a process that occurs when the applied loads exceed the shear strength of the shotcrete as illustrated in Figure 2.6. Kuchta (2001) and Barrett and McCreath (1995) highlighted that the shotcrete-rock bond strength should be strong enough such that no bond failure occurs for direct shear of the shotcrete to take place.

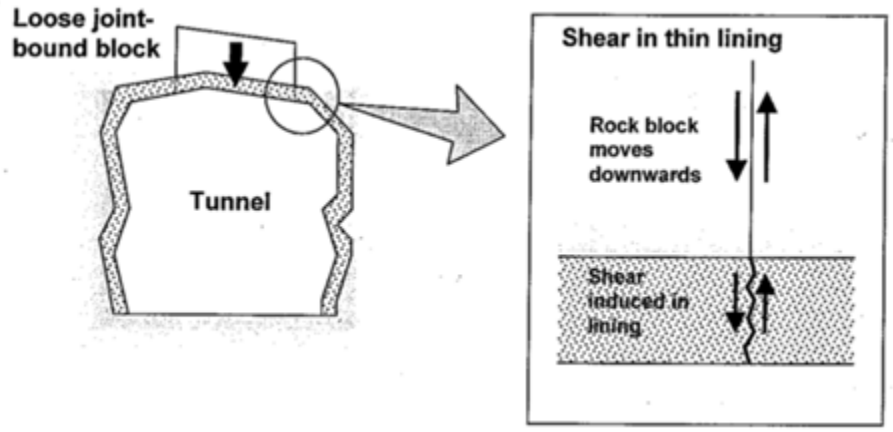


Figure 2.6 Shotcrete shear failure resulting from loose block movement (After Leach, 2002)

Point loading or concentrated loading on the shotcrete by a loosened block which is squeezed out from the excavation boundary due to high stresses may cause punching shear failure of the shotcrete. Punching shear failure usually occurs when the adhesion failure of the shotcrete-rock interface occurs. Failure would occur close to the rock bolts where shear forces are at a maximum. Failure occurs along planes inclined at approximately 45˚ to the horizontal (Barrett and McCreath, 1995).

2.4.3 Flexural failure of a shotcrete beam

Failure in flexure occurs once adhesion between shotcrete and the rock has been lost. When the bond between the rock and the shotcrete interface is strong, the flexural capacity of the rock-shotcrete system may be increased due to the formation of a composite beam, with the reinforced shotcrete on the outside and mechanically interlocked broken rock on the inside.

Barrett and McCreath (1995) estimated that a 50mm thick plain shotcrete lining, having flexural strength of 6 MPa at 28 day strength and supported by 1.2m x 1.2m bolt spacing, could support a bending moment of 1.5 kNm in pure bending.

Steel fibre reinforcement in shotcrete helps to improve the post peak strength of shotcrete in flexure. Morgan and Mowatt (1984) carried out tests on steel fibre reinforced shotcrete slabs to see the effects of steel fibre incorporation. The results obtained from the tests revealed that the steel fibre reinforcement in the shotcrete permits the slab to continue supporting approximately 80% of the peak load over small deformations (less than 10mm) and approximately 60% of the peak load over large deformations of 10 to 50mm. Holmgren (1983) developed the following relationship for the flexural capacity of a steel fibre-reinforced, statically indeterminate concrete slab:

$$C_{flex} = 0.9 \{(R_{10/5} + R_{30/10}) / 200\} \sigma_{flex} t^2/6 \, s/2$$

Where:

C_{flex} = the resistance to moments

$R_{10/5} + R_{30/10}$ are the toughness factors defined in ASTM C1018 (1997)

s = bolt spacing

t = shotcrete thickness

Despite being developed for a concrete slab, Holmgren's equation provides a logical starting point for designing the quantity and type of reinforcement required in a reinforced shotcrete lining (Barrett and McCreath, 1995). Additionally, Holmgren's equation provides a starting point for designing the shotcrete thickness and bolt spacing.

2.4.4 Shotcrete tensile failure

Kuchta (2002) pointed out that good adhesion is important for the overall support characteristics of shotcrete. Therefore if the adhesion strength is low, the weight of loose blocks of rock pushing down on the shotcrete layer may cause sections to separate and gaps can be formed between the shotcrete layer and the rock surface. Kuchta (2002) further indicated that the subsequent bending of the shotcrete will result in pure tensile failure of the shotcrete as shown in Figure 2.7.

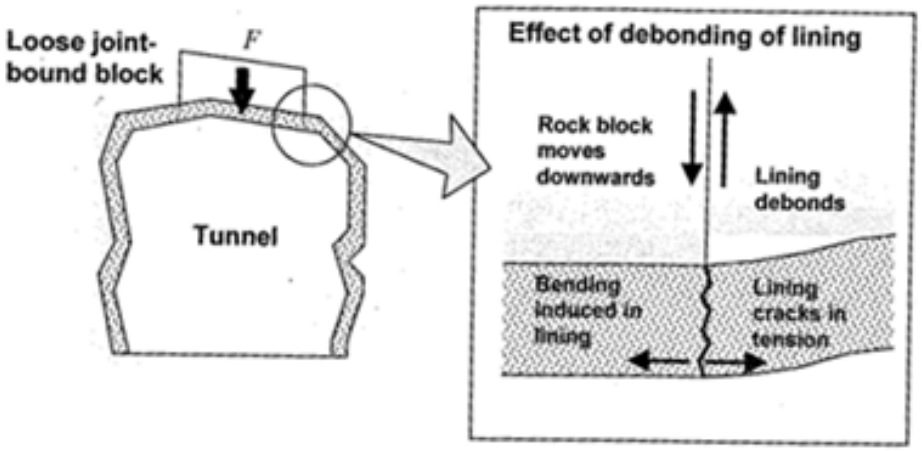


Figure 2.7 Shotcrete failing in tension as loosened block movement occurs causing lining de-bonding (After Leach, 2002)

2.5 Shotcrete Design Methods

This section presents some of the support design methods that can be adopted to determine the thickness of shotcrete and the reinforcement required. In general, design methods were classified by Whittaker and Frith (1990) into three different categories, namely:

(a) Empirical methods,
(b) Analytical methods and
(c) Computational or numerical methods

2.5.1 Empirical design methods

Empirical design methods are based on in situ observations or measurements made on prototype rock (Obert and Duvall, 1967). An example of the empirical design method of shotcrete support is that developed and subsequently refined by Barton et al (1974) and Barton (2002). A simplified version of this empirical design was published by Stacey (2003) for application in the mining environment as shown in Figure 2.8. The design chart encompasses rock mass rating (RMR) and the Q-System of rock mass classification, as well as the span of the excavation to estimate the shotcrete thickness requirements.

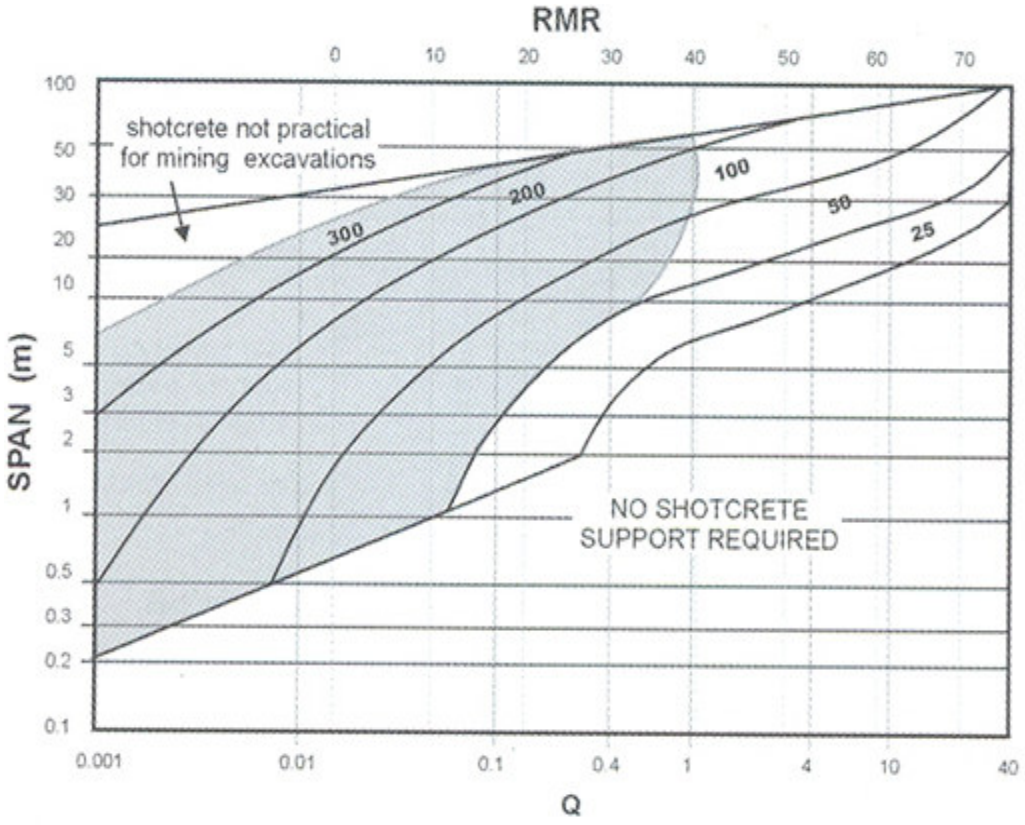


Figure 2.8 Simplified shotcrete design chart (Stacey, 2003, modified after Barton et al, 1974)

2.5.2 Analytical methods

Analytical design methods for shotcrete design consist of resolving a problem into its simplest elements and representing the problem by tractable equations and then solving them (Brown and Bray, 1987). An example is that of the yield line theory first developed by Johansen (1962). The yield line theory provides a simple method to calculate the ultimate load bearing capacity of shotcrete or alternatively the required plastic moment resistance for a given load on a shotcrete panel.

Yield line theory is based on the principle that internal work done by yield lines rotating must equal the external work done by the load moving. A yield line in this context is a line of cracked shotcrete serving as an axis of

rotation for an un-cracked shotcrete panel. Only the energy absorbed by the yield lines rotating is considered, the amount of the energy absorbed by shear or elastic deformation is ignored for calculation purposes. In reinforced shotcrete design, the error introduced by this assumption is very small but in shotcrete, the rock-shotcrete interface may absorb large amounts of energy in shear possibly leading to conservative results. Malmgren et al (2004) compared panel test results with predicted results and found that in general the yield line theory provides conservative estimates of ultimate capacity in panel tests. The under-estimation of the ultimate load bearing capacity was assumed to be the result of arching in the shotcrete panel. In practice this arching effect may not always be relied upon and the results may be less conservative. Detailed information on the topic is available in Johansen (1962) and Kennedy and Goodchild (2004).

2.5.3 Numerical modelling

Numerical modelling in rock engineering can be used for support design. The software packages are available in 2 dimensional and 3 dimensional versions.

Whittaker and Frith (1990) argue that the assumptions made in formulating a mathematical solution as introduced in the previous subsection, are far too simple to provide a solution to the real situation. However, support design using a combination of empirical methods, analytical methods and numerical analysis can give a solution best suited to reality (Whittaker and Frith, 1990).

2.6 Properties of sprayed liners

The relative importance of shotcrete material properties for ground support purposes depends on the type of ground stability problem. A summary of some of the relevant shotcrete properties has been prepared by Grov and Blindheim (1997) and is reproduced in Table 2.1.

Table 2.1 Overview of some of the relevant property requirements for shotcrete depending on ground condition (after Grov and Blindheim, 1997)

Ground conditions	Good bond	High stiffness	High ductility
Jointed and blocky	Required	Required	Not required
Squeezing Ground	Required	Not required	Required
Spalling	Required	Not wanted	Required
Water seepage	Required	Not applicable	Not applicable

2.6.1 Bond strength

Saiang et al (2004) have indicated that the shotcrete-rock interface bond strength is one of the most important sprayed liner properties. However, Melbye (1994) indicated that little control can be exercised as far as the bond strength value is concerned since it largely depends on the nature and roughness of the surface on which the shotcrete is applied. Bond strength is also dependent on the mixing process and the application techniques (Malmgren, 2001). However, Melbye (1994) and Kuchta et al (2004) indicated that control should not only focus on the application process but also on the level of cleaning the face before application.

There are various physical tests to determine bond strength which include the EFNARC (1996) standard test method whereby an in situ core of shotcrete is drilled to a certain depth together with the rock. Still bonded together, the shotcrete-rock core is then taken to the laboratory to determine the bond strength by pull testing. Another method, illustrated in Figure 2.9, involves drilling a shotcrete core until the rock is reached. Then a metal disc is installed onto the shotcrete core using high strength glue. Once the glue sets, the disc is pulled out and the bond strength value is read off the equipment. Bond strength tests carried out by various researchers have indicated that shotcrete-rock bond strength varies between 0.5 – 3.0 MPa. At the moment, design is not based on bond strength since it is difficult to measure and varies over short distances (Grov and Blindheim, 1997 and Melbye et al., 1995).

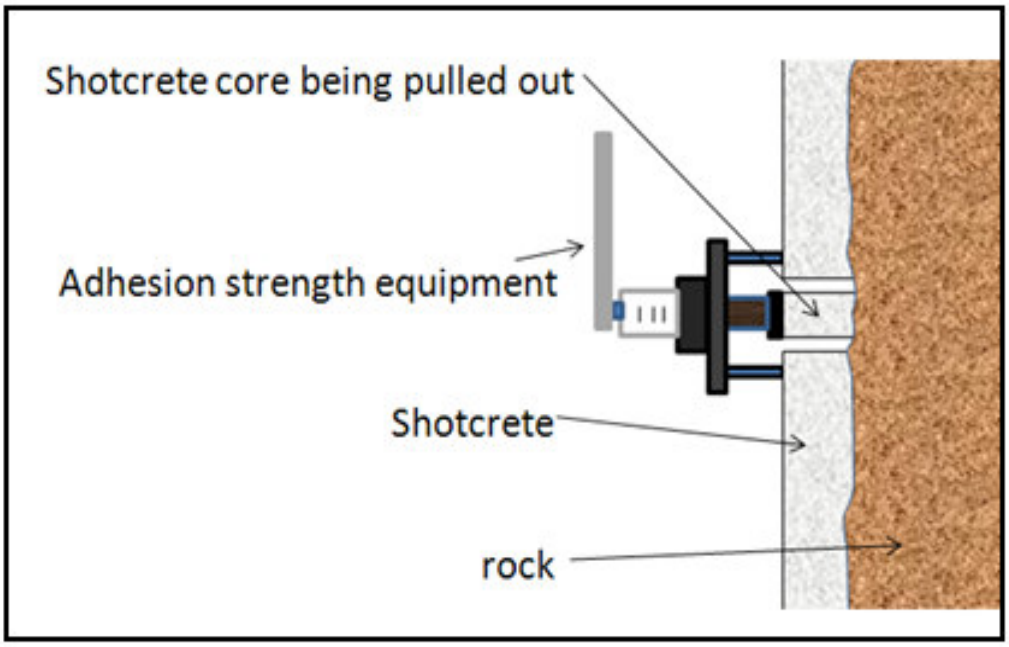


Figure 2.9 Adhesion testing equipment

2.6.2 Shotcrete strength

The most commonly used strength properties of shotcrete are compressive strength, flexural strength and tensile strength. There are standard test methods for each of the above mentioned strength properties and these are summarised in Table 2.2.

The compressive strength of shotcrete on its own is regarded as a less important property but provides a measure of the Young's modulus of shotcrete (Grov and Blindheim, 1997). Grov and Blindheim (1997) and Melbye et al (1995) indicated that the Young's modulus of shotcrete follows the shotcrete compressive strength closely. However, MacKay and Trottier (2004) argue that compressive strength is the primary factor in structural concrete design. This may be true for civil engineering where the sprayed liners are designed for structural support purposes. However, in mining, since the thicknesses of shotcrete are typically less than 100mm, structural support offered by shotcrete is often negligible (Stacey and Yu, 2004). MacKay and Trottier (2004) indicated that fibre addition may increase the compressive strength of concrete by 20 percent. However, Morgan (1988) has noted that the compressive strength of shotcrete is not significantly influenced by the addition of fibres.

Table 2.2 The standard test methods to determine the strength properties of shotcrete

Strength Property	Standard Test Method
Compressive strength	ASTM C39
Flexural strength	ASTM C496
Tensile strength	ASTM C1018

Flexural strength is a measure of the bending capacity of shotcrete at first crack. Knowing first crack stress enables the designer to perform the correct design calculation for the expected shotcrete failure mechanism.

MacKay and Trottier (2004) have pointed out that the flexural strength of fibre reinforced shotcrete is known as residual strength post the first crack. Residual strength is not a true strength because it is based on a linear elastic response and uses the gross properties of the uncracked section in the beam testing of shotcrete (MacKay and Trottier, 2004). Ray (1997) has pointed out that the flexural strength is the most ideal design criterion for plain shotcrete. Ray's (1997) argument was based on the fact that once the plain shotcrete section has cracked, its load carrying capacity is destroyed and the brittle failure is almost instantaneous. However, Morgan (1988) performed several flexural strength tests and concluded from the results he obtained that the flexural strength of shotcrete slightly improves with the addition of fibres in the shotcrete. Additionally, Morgan (1988) indicated that a remarkable improvement in the shotcrete flexural strength of shotcrete can be achieved by the addition of super plasticisers.

The third strength property of shotcrete is its tensile strength. The tensile strength of shotcrete indicates its capacity to resist forces pulling the shotcrete in opposite directions. Melbye (1994) has pointed out that the tensile strength of the shotcrete is not so important due to the likelihood of shrinkage cracks that may develop while the sprayed shotcrete cures.

2.6.3 Shotcrete ductility

Shotcrete ductility provides an indication of its ability to maintain load while undergoing deformation (Ratcliffe, 1999). The main reason for incorporating fibres in shotcrete is to impart ductility to an otherwise brittle shotcrete thereby improving the fibre reinforced shotcrete load bearing capacity (Papworth, et al., 1996). Vandewalle (1998) indicated that the load bearing capacity of shotcrete is improved by the process of load redistribution as a result of fibre incorporation. Grov and Blindheim (1997) and Ray (1997) also pointed out that the ductility of shotcrete is affected by fibre type, shape, length and quantity.

Ductility of shotcrete can be measured as residual strength, toughness or energy absorption. Energy absorption is defined as the area under the load-deflection curve of a beam or panel test. Energy absorption is also called toughness. The residual strength provides the load bearing capacity post the peak strength or peak load of shotcrete. The methods for testing ductility include ASTM C1018, JSCE-SF4 Japanese Standard, Norwegian Standard and the Template Method proposed by Morgan et al (1995). The strengths and weaknesses of each of the above mentioned methods were discussed by Ray (1997) and Papworth et al (1996).

2.6.4 Shotcrete stiffness

The stiffness of shotcrete indicates its resistance to bending. Stiffness increases with an increase in shotcrete compressive strength. Also, an increase in stiffness is related to increased brittleness of shotcrete (Ray, 1997). Stiffer shotcrete in blocky ground mainly helps to arrest initial rock movement (Stacey and Yu, 2004). However, stiffer shotcrete is less effective in squeezing ground conditions where sustained resistance, toughness or ductility are most required (Ray, 1997). Stacey and Yu (2004) also pointed out that the stiffer the sprayed liner the smaller the rock movements it can withstand before failure. Therefore design considerations should cater for ground condition assessment before the final support design can be implemented.

2.6.5 Shotcrete thickness

Chen et al (1994) indicated that the thickness of a shotcrete layer is important in that it dictates the maximum width of cracks occurring during failure thereby influencing the performance of the shotcrete. The thickness of shotcrete in situ can be determined by using depth pins or probing of the shotcrete while still wet. The thickness of dried shotcrete can be tested using a Hilti drilling machine. The drawback for this method is that

sometimes it can be difficult to determine the inter-change from shotcrete to rock thereby jeopardising the accuracy of the method. A more accurate method would involve measuring the thickness of in situ drilled cores. The thickness of shotcrete may determine whether the support offered to the rock is structural or not.

2.7 Mechanisms of support provided by sprayed liners

2.7.1 Promotion of block interlock

Shotcrete is applied to the rock under high pressure. As a result, mortar and fines penetrate into joints and cracks thereby producing a wedge effect between the rock blocks (Egger, 1981, Melbye, 1994 and Stacey, 2001). The wedge effect interlocks the rock blocks thereby inhibiting rock displacement. Stacey (2001) also explained how good bonding on the shotcrete-rock interface, shear strength and tensile strength properties of shotcrete assist in the promotion of block interlock to maintain excavation stability. The promotion of block interlock by sprayed liners may not be feasible where there are large loose blocks which may require much stiffer support.

2.7.2 Shotcrete structural arch support mechanism

Sutcliffe and McClure (1969) and Stille and Franzen (1990) pointed out that sprayed liners can support the rock through the structural arch support mechanism. Melbye (1994) explained that shotcrete prevents the differential movement of crushed rock thereby causing a generally even inward displacement of the rock. As the rock moves inwards, the length of the excavation contour decreases resulting in compressive forces acting on the shotcrete-rock composite as illustrated in Figure 2.10. Sutcliffe and

McClure (1969) pointed out that the early strength of the liner plays an important role if the shotcrete is to achieve a structural arch support mechanism. Stacey (2001) also mentioned that such a liner should have high flexural rigidity. Stille and Franzen (1990) indicated that the arch would be stressed by pure compression and that the stability of the excavation relies on the strength of the arch. However, Fredriksson and Stille (1992) and Alberts and Backstrom (1971) have indicated that the shotcrete only prevents the loosening of the rock thereby transforming the surrounding rock into a self supporting arch. Each of the explanations may be true, but this suggests considerable uncertainty in the structural arch support mechanism.

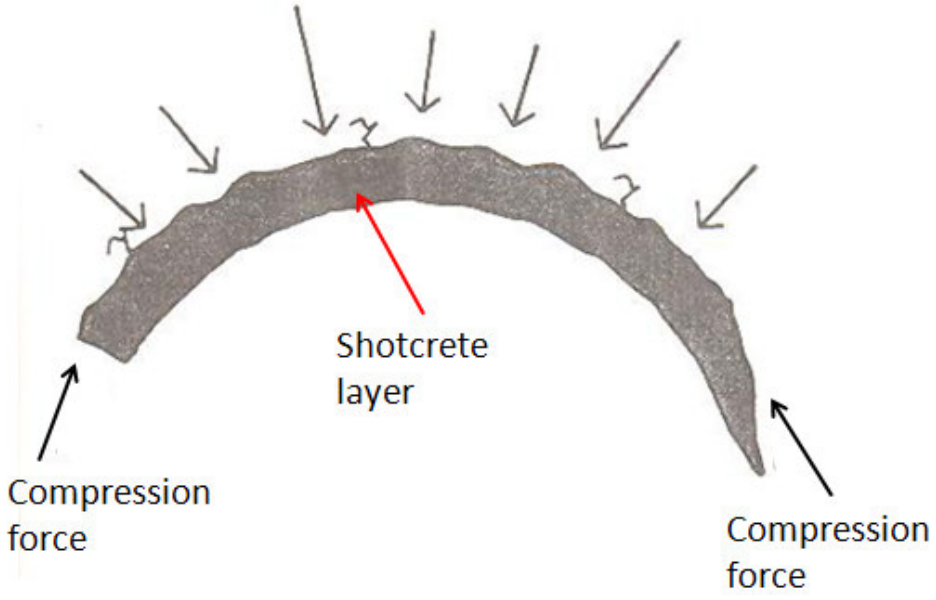


Figure 2.10 Shotcrete rock bearing capacity as an arch (After Stille and Franzen, 1990)

2.7.3 Shotcrete basket mechanism of rock support

The basket mechanism of rock support provided by sprayed liners occurs when the sprayed liners develop some form of basket into which the failed

rock is collected (Stacey, 2001). The sprayed liner needs to have ductility so that it has the capability to undergo some deflection without failing. The incorporation of fibres in the shotcrete is important in offering the shotcrete increased ductility.

2.7.4 Shotcrete beam support mechanism

An illustration of shotcrete acting as beam is shown in Figure 2.11. When shotcrete supports the rock as a beam, Banton et al (2004) pointed out that the shotcrete can be treated as a beam in bending. As a result, beam theory can be used to estimate the driving moments and the resisting moments to determine bending capacity of the shotcrete in design.

Melbye (1994) pointed out that shotcrete adhesion to the rock is essential when the shotcrete enhances the bending capacity of the rock. He added that rock bolting with face plates clamping the shotcrete to the rock will improve the bearing capacity provided by the combined support.

Kaiser and Tannant (1997) suggested that the beam action support by shotcrete can be enhanced when the shotcrete is applied in the form of flexible panels as illustrated in Figure 2.12. The flexible panels prevent the generation of tangential stresses in the shotcrete thereby preserving its bending capacity. When there is good bonding between the shotcrete and the rock, the result can be a stronger rock-shotcrete composite beam.

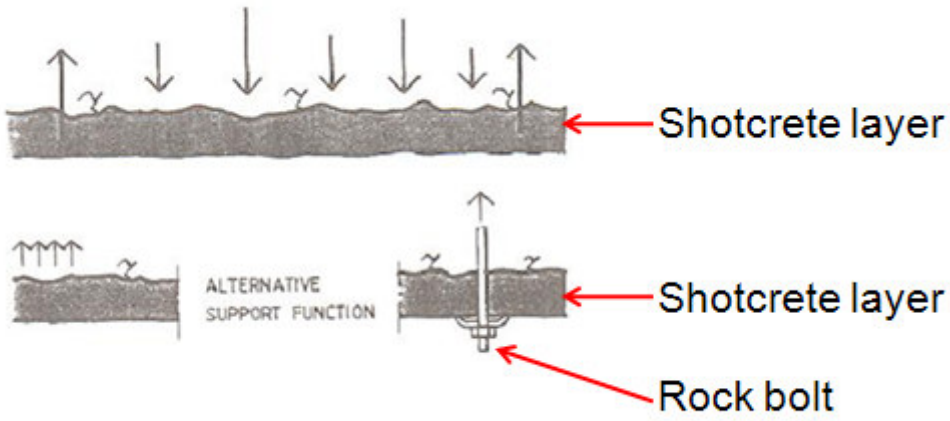


Figure 2.11 Shotcrete support as a beam, supported by adhesion to the rock or adhesion to the rock and clamping effect offered by rock bolts (After Stille and Franzen, 1990)

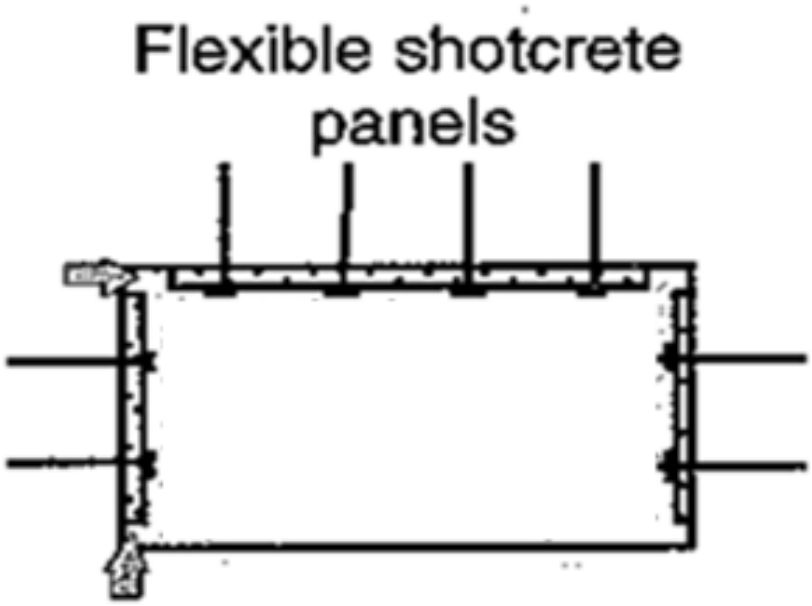


Figure 2.12 Shotcrete support as flexible retaining panels in a tunnel (After Kaiser and Tannant, 1997)

Banton et al (2004) described how a rock-shotcrete composite beam can be formed resulting in a much stronger beam compared to the beam consisting of the layer of shotcrete only. Banton et al (2004) mentioned

that the improvement in carrying capacity is a result of the increase in the thickness of the rock-shotcrete composite beam.

2.7.5 Durability enhancement through sealing action as a support mechanism

Sprayed liners can be used to protect support units from equipment damage or the rock mass itself from the damage by equipment. Player (2004) reported the success in using fibre reinforced shotcrete in protecting pillars and the previously installed mesh and bolt support from damage by remote controlled loaders underground. Finn et al (1999), Bartlett and Nesbitt (2000) and Stacey (2001) also indicated that rocks like Kimberlite, which is prone to weathering on exposure to wetting and drying, will have their life prolonged by the coating action provided by sprayed liners.

2.7.6 Rock bolt face plate extension support mechanism

Humphries and Funkhouser (1993) and Malmgren (2001) have shown that the interaction between shotcrete and rock bolts can be improved when a face plate connected to the rock bolt is placed on the outer surface of the sprayed liner. Stacey (2001) demonstrated how the area of influence of the rock bolt is increased when the face plate interacts with the shotcrete as illustrated in Figure 2.13.

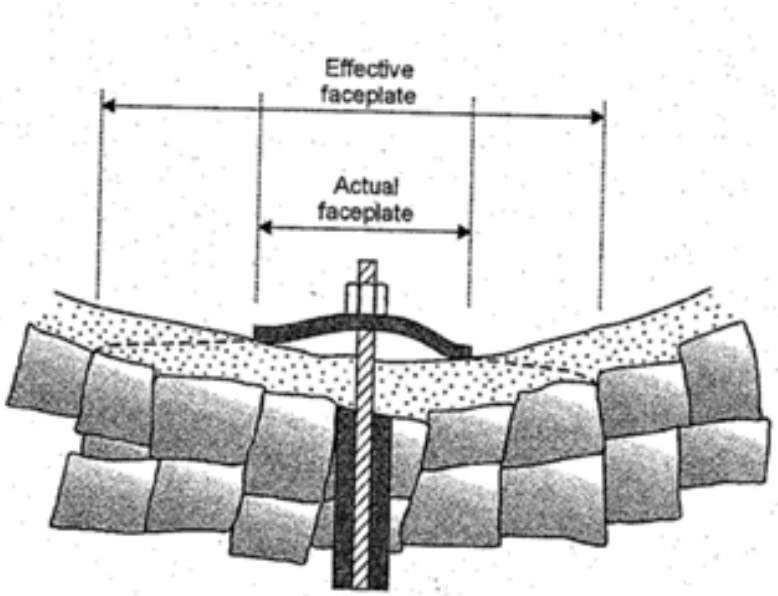


Figure 2.13 Illustration of the extended face plate where shotcrete and rock bolting are used together (After Stacey, 2001)

2.8 Summary

It has been noted that the primary function of sprayed liners, like any other form of support, is to help the rock maintain stability. The stability is achieved in a number of ways which included providing support pressure to an excavation, holding up key blocks to maintain stability and providing sealing action to the rock. Shotcrete failure modes reviewed include tensile failure, adhesion failure, shear failure and flexural failure. A review of the shotcrete properties has shown that properties such as the bond strength cannot be controlled since it is dependent on cleanliness of the rock surface and roughness of the rock surface onto which the shotcrete is applied. Also reviewed are the design methods for surface support which have been classified into empirical, analytical and numerical modelling methods. The design methods have a direct bearing on the properties of shotcrete to be achieved for different ground conditions. Various

mechanisms of rock support provided by sprayed liners have been identified in literature. They shall be used in analysing the mechanisms of rock support provided by sprayed liners in the field. Therefore the literature survey has provided invaluable information for use in the subsequent chapters.

CHAPTER 3

UNDERGROUND FIELD MONITORING AND FIELD TESTING

3.1 Introduction

The previous chapter has provided a review of the aspects that have been found relevant to the investigation of the mechanisms of rock support provided by spayed liners. Some of these aspects include failure modes of shotcrete, methods of shotcrete design, mechanisms of surface support loading and the identified mechanisms of support provided by the sprayed liners. The review has provided information useful for the practical underground monitoring of shotcreted sites at three different mine sites, namely, South Deep Mine, Impala Platinum Mine and Mponeng Mine. This chapter starts by identifying the objectives of the field monitoring exercise and giving a brief description of the instruments used for the in situ monitoring. Additionally, a brief description is provided for each monitoring site followed by the monitoring results. Rock-shotcrete bond strength tests were carried out at South Deep Mine. Cores were drilled from South Deep Mine pillars for fibre content determination and uniaxial compressive strength testing. Of the two EFNARC panels that were sprayed at the time of spraying the South Deep Mine pillars, one was used for energy absorption testing and shotcrete cores were drilled for UCS testing and fibre content determination from the other.

3.2 Monitoring objectives

Monitoring of the test sites was carried out to achieve the following objectives:

- To identify the failure mechanisms of shotcrete in situ,
- To identify the mechanisms of rock support provided by sprayed liners.

3.3 Monitoring instruments

3.3.1 Ground motion monitor (GMM)

The GMMs are high precision digital extensometers used to measure sidewall displacement of the shotcreted pillars. They were end-anchored at a depth of 3.5m into the pillars. Figure 3.1 shows a section through a GMM installed in a hole. Displacement results from the GMM can be read directly using a manual readout unit that will be connected to the GMM. Alternatively, the GMM can be connected to a data logger or slug, which is an instrument that can continuously store displacement measurement results at user pre-set time intervals. The slug or data logger has the facility to download the stored results into a computer database. Two data loggers or slugs can be used interchangeably to enable continuous monitoring using the GMMs when one slug has been taken to surface for the purpose of downloading the recorded displacement results.

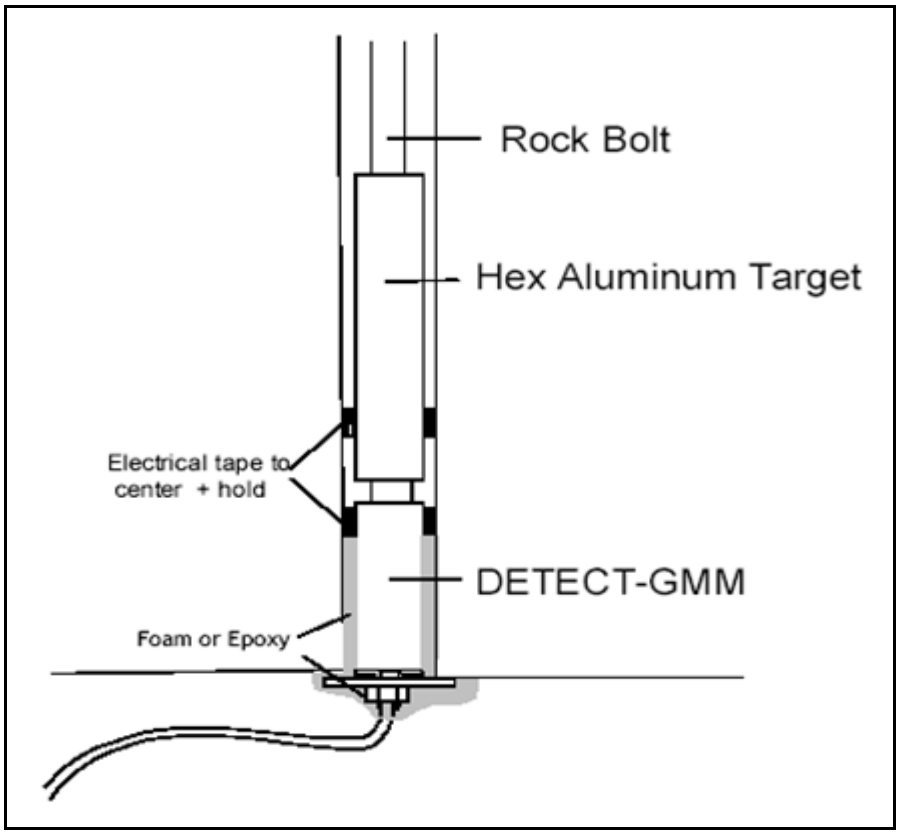
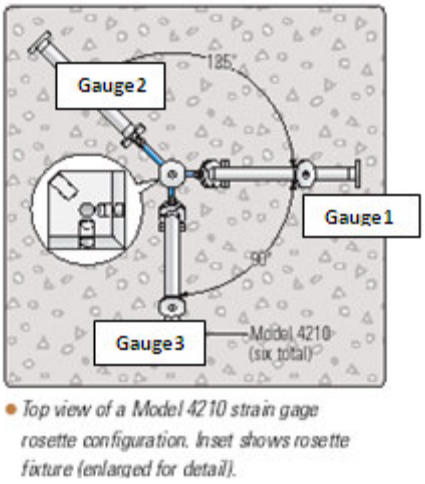


Figure 3.1 Ground motion monitor (GMM)

3.3.2 Vibrating wire strain gauge (VWSG)

Vibrating wire embedment strain gauges are normally used to measure strain in shotcrete. However, during the monitoring exercise, the strain gauges were used to measure strain in the rock. Figure 3.2 shows a strain gauge rosette configuration showing three gauges (flanges) oriented in three different directions. The gauges were installed in the vertical plane with each rosette consisting of 3 gauges installed at depths of 1.5 m, 2.5 m and 3.5 m respectively. Strain was then calculated by applying calibration factors to the frequency measurement.



Top view of a Model 4210 strain gage rosette configuration. Inset shows rosette fixture (enlarged for detail).

Figure 3.2 Strain gauge rosettes

3.3.3 Multi-point borehole extensometer (MPBX)

The MPBX is used to determine the stability and movement behaviour of the rock. A typical rod extensometer consists of a reference head, usually installed at the collar of each drill hole and one or more in-hole anchors. Each anchor is fixed in place at a known depth in the borehole namely, 1.8m, 2.8m and 3.8m depths. As the rock deforms, the distance between the individual anchors change. Displacement will be determined by the difference between the initial reading and successive readings. The results are taken using a manual readout unit that reads data directly in mm. This allows an accurate determination of the magnitude, rate and acceleration of deformation in the rock.

3.3.4 Single point borehole extensometer (SPBX)

The Single point borehole extensometer has the same principle of operation as the multi-point borehole extensometer. The only difference is that the SPBX has one anchor whereas the MPBX has more than one. They both provide displacement as output. The SPBXs were end anchored at 3.5m depth.

3.3.5 Laser displacement monitoring

Laser displacement monitoring was carried out using a laser distometer which was set at a fixed position, with distance being measured using a laser beam directed at fixed targets on a pillar or tunnel sidewall. During the monitoring exercise, laser targets were mounted on pillars of interest and each target displacement was recorded over a period of time.

3.3.6 Borehole monitoring using a borehole video camera

Boreholes with a diameter of 100mm were drilled into pillars and tunnel sidewalls to a depth of 10m and a borehole video camera was used for profiling the boreholes over a period of time. This was done to observe changes in the rock behind the applied shotcrete, to assist in the interpretation of the results from the other monitoring instruments.

3.3.7 Visual monitoring

Visual monitoring involved taking photographs using a digital camera to record the changes in the state of the shotcreted pillars and tunnels over time. The photographs were routinely taken from set positions on each site to create a database for the visual state of the shotcrete, and the dates were recorded.

3.4 Monitoring sites

3.4.1 Mponeng Gold Mine Level 109 Test Site

The test site was established at the end of 2005 and is located on 109 Level 44 cross-cut, which is a 4.5m x 4.5m crosscut at 3037m below the

surface. Steel fibre-reinforced dry-mix shotcrete was sprayed on a selected 10m portion of the crosscut adjacent to areas supported by wire mesh and lacing. The test site was chosen because it was expected that it would be subjected to increased levels of stress due to mining. However, changes in the mining sequence after initial site establishment resulted in the expected stress levels not being reached. The site has instead been exposed to a reducing stress field as the crosscut was over-stoped. This site was closed in September 2007. Mapping of both sides of the tunnel was carried out to determine the rock mass characteristics.

The rock type at the Mponeng Mine site is very hard unweathered Alberton lava. The rock mass classification ratings are shown in Table 3.1.

Table 3.1 Mponeng Mine site rock mass classification (SRK SIMRAC Internal report, 2008)

Rock mass classification method	Rock mass rating
Laubscher Mining Rock Mass Rating	55
Bieniawski Mining Rock Mass Rating	54
Q-system	3.1

The site was sprayed with steel fibre reinforced shotcrete. However, before the shotcrete was applied, the following support could be noted:

- 20 mm thick re-bars spaced on a 1.4m by 1.3m pattern and
- Swellex with a square pattern of 1.4m spacing.

Figure 3.3 and Figure 3.4 show the position of the laser targets and the boreholes.

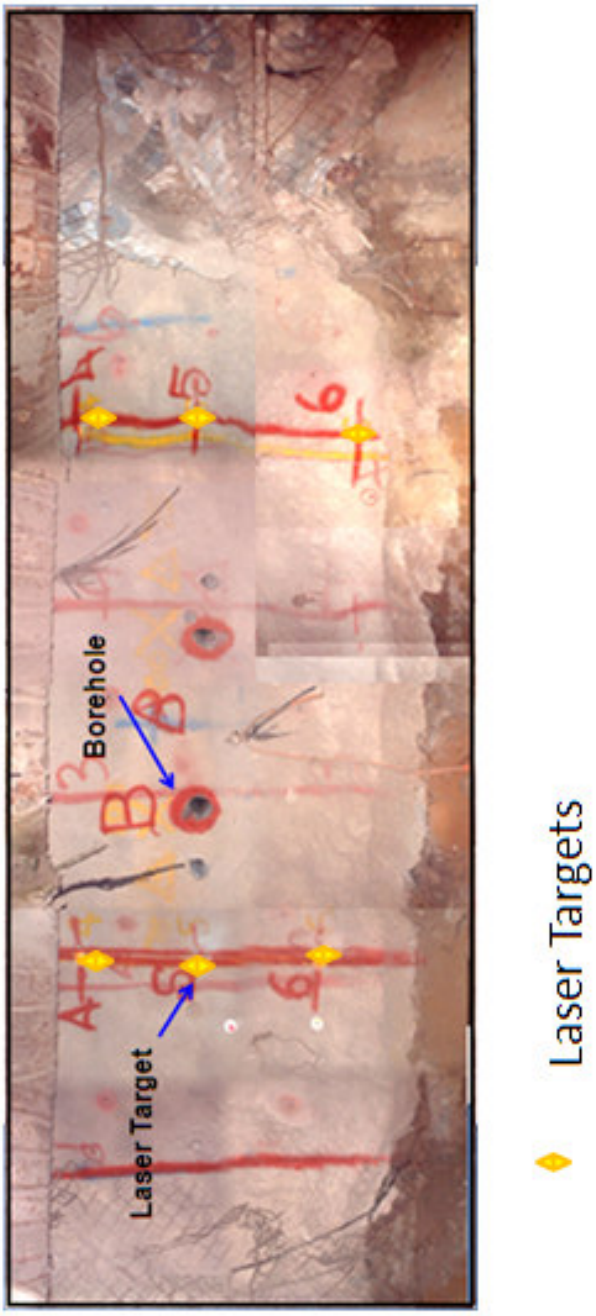


Figure 3.3 Mponeng Mine Level 109 South-East wall showing positions of laser targets and the inspection borehole

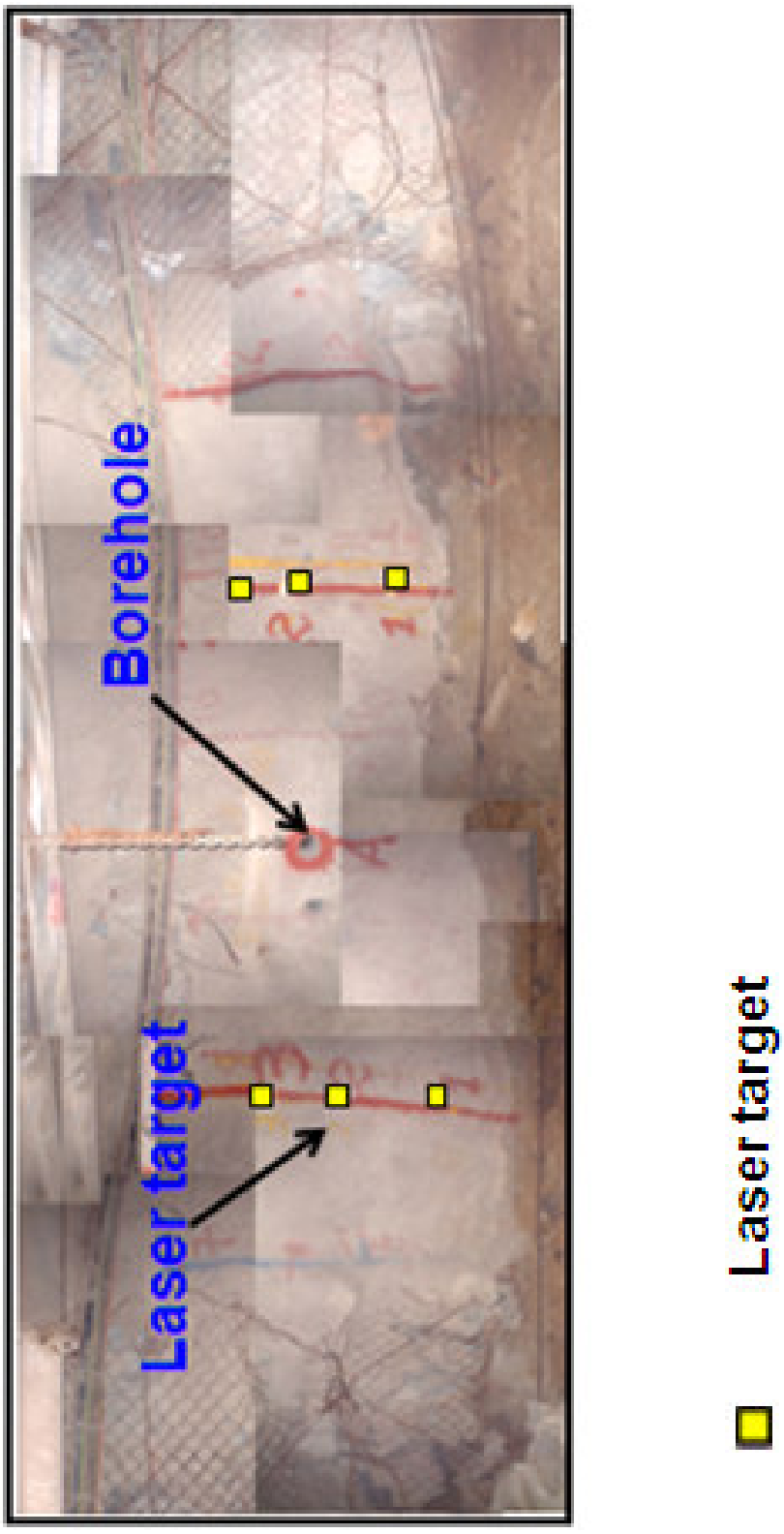


Figure 3.4 **Mponeng Mine Level 109 North-West wall showing the position of laser targets and the inspection borehole**

3.4.2 Mponeng Gold Mine Level 116

The second monitoring site at Mponeng Mine was set up on Level 116, 45 cross-cut in October 2006. Mponeng Mine Level 116 is situated at 3271m below the surface in a highly seismically active area. This location was chosen specifically to measure shotcrete performance under dynamic loading. The area was supported with 50mm steel fibre reinforced shotcrete that was covered by wire mesh and tensioned lacing and 38 tonne anchors. 116 Level 45 cross-cut has rock mass and rock conditions similar to those for Mponeng Mine Level 109. The location of the site is shown in Figure 3.5.

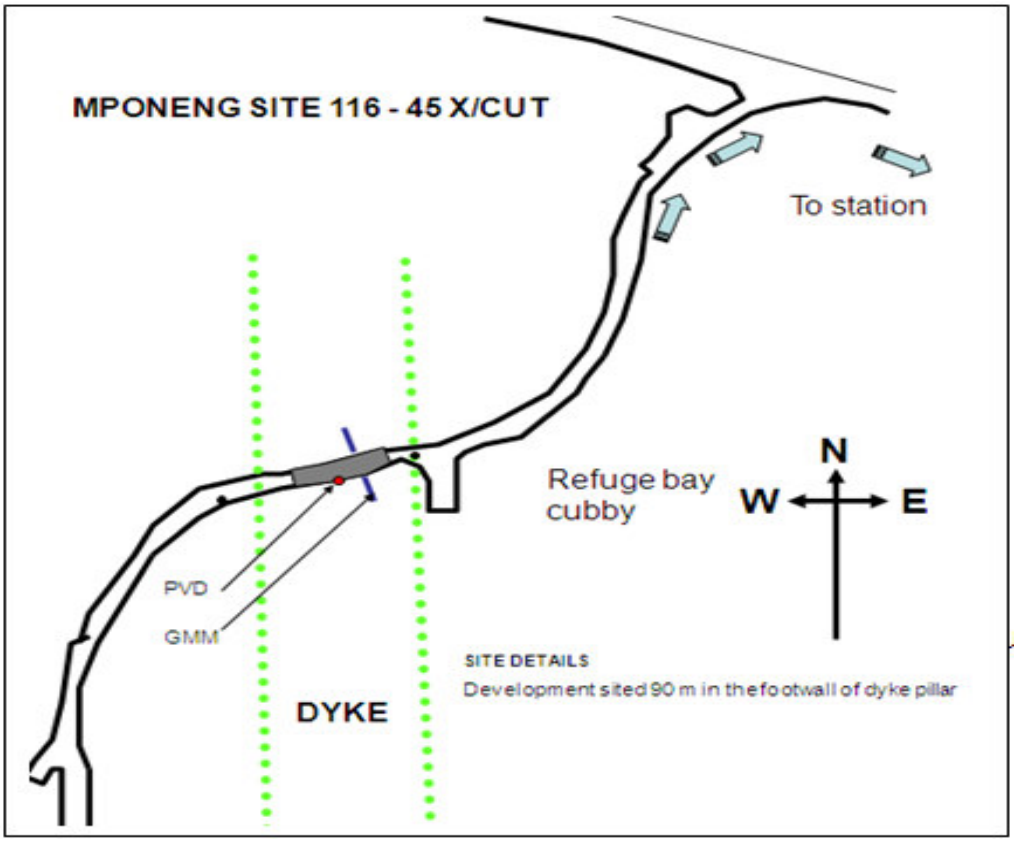


Figure 3.5 Mponeng Mine Level 116 site plan (SRK SIMRAC Internal report, 2008)

The position of boreholes, laser targets and the Ground Motion Monitor (GMM) are shown in Figure 3.6 and Figure 3.7.

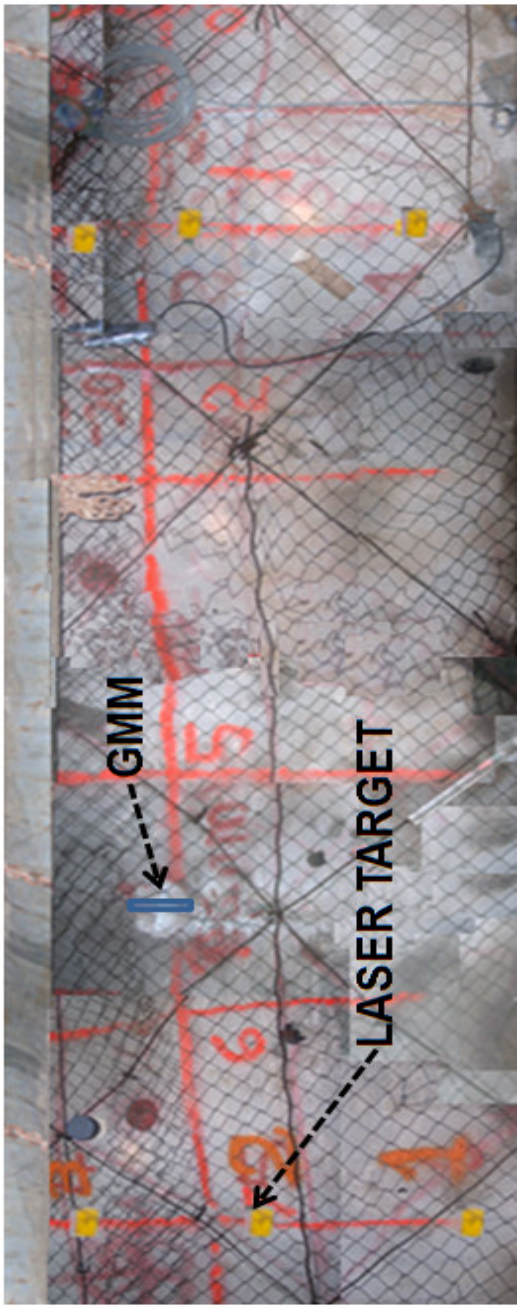


Figure 3.6 Mponeng Mine Level 116 wall A showing the position of laser targets and the Ground Motion Monitor (GMM)

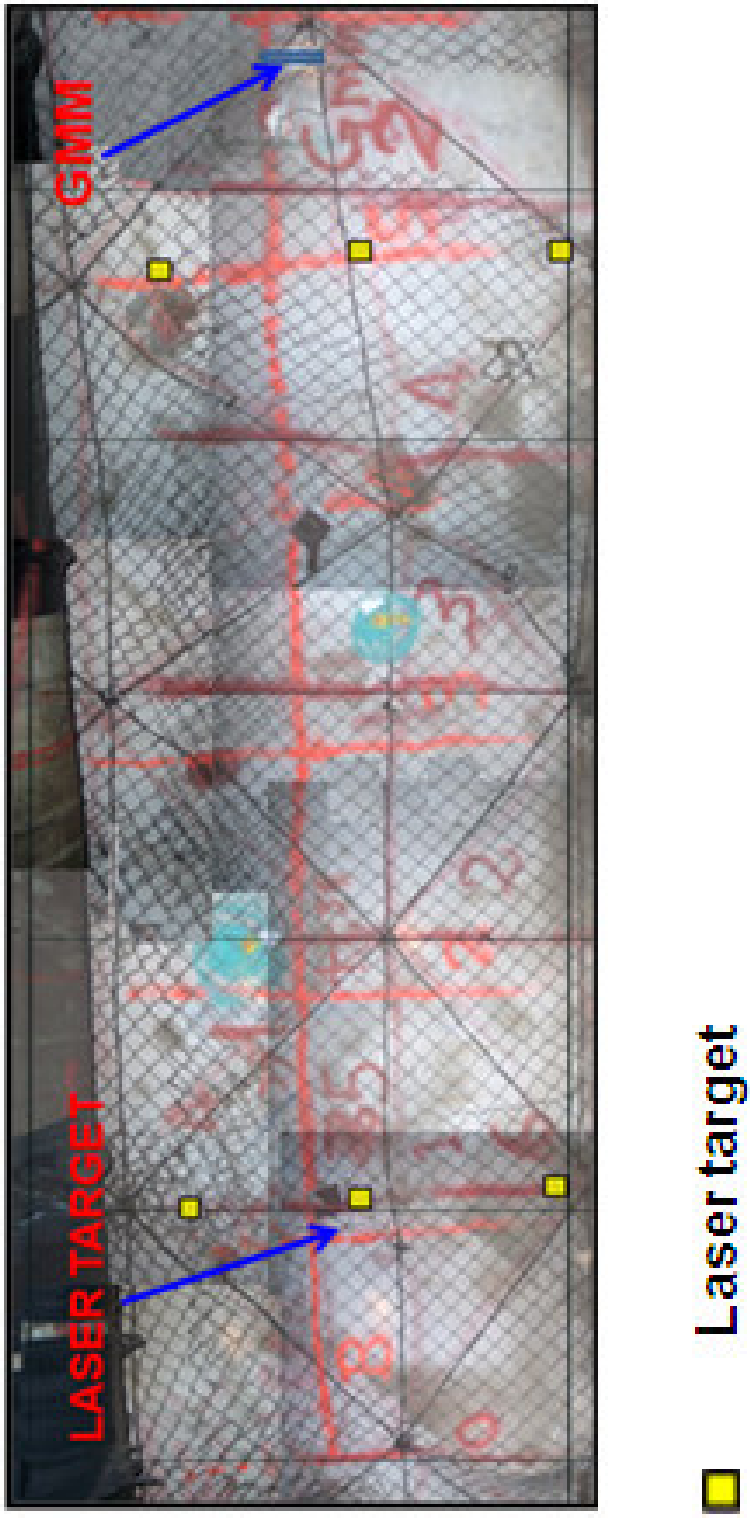


Figure 3.7 **Mponeng Mine Level 116 wall B showing the positioning of laser targets the Ground Motion Monitor (GMM)**

3.4.3 South Deep Gold Mine

The test site was situated on Level 87-2 West. This site was established in February 2007 and is situated in a trackless mechanized mining area that was in the final stages of extraction. The site is approximately 2600m below the surface. The test site was also situated close to a tipping area. Stresses in the remaining pillars were high making the South Deep Mine site the most ideal site for the monitoring of failure mechanisms of shotcrete in situ. High stress levels were indicated by dog earing of drilled boreholes as well as numerous locations of sidewall spalling on nearby pillars. Seismic events were also recorded in the area and some seismic damage was evident in some areas. Figure 3.8 shows a regional plan of the test site and the four pillars that were monitored. Figure 3.9 shows the pillars that were monitored and their dimensions.

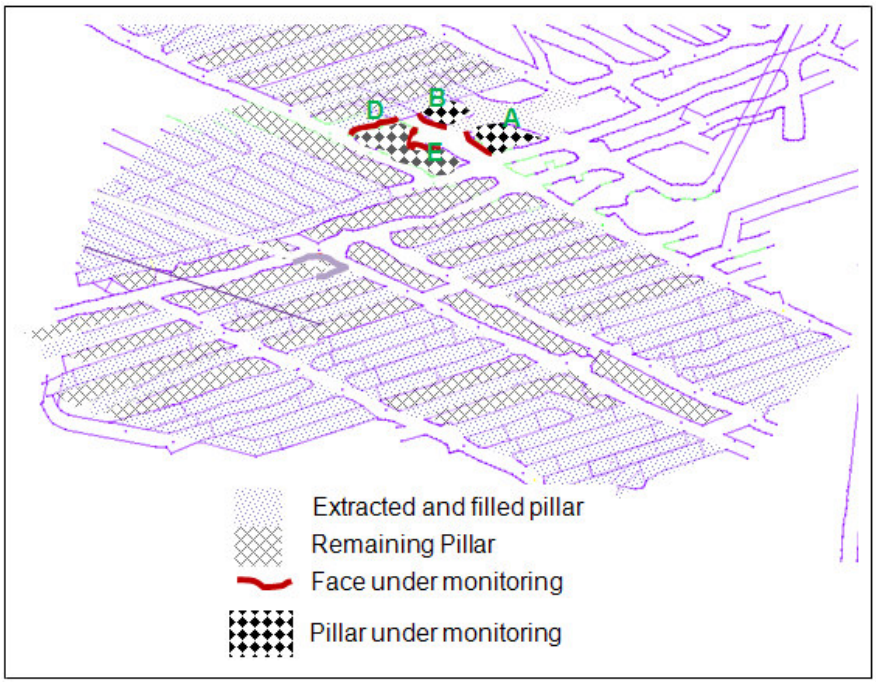


Figure 3.8 South Deep Mine plan showing location of test site (SRK SIMRAC Internal report, 2008)

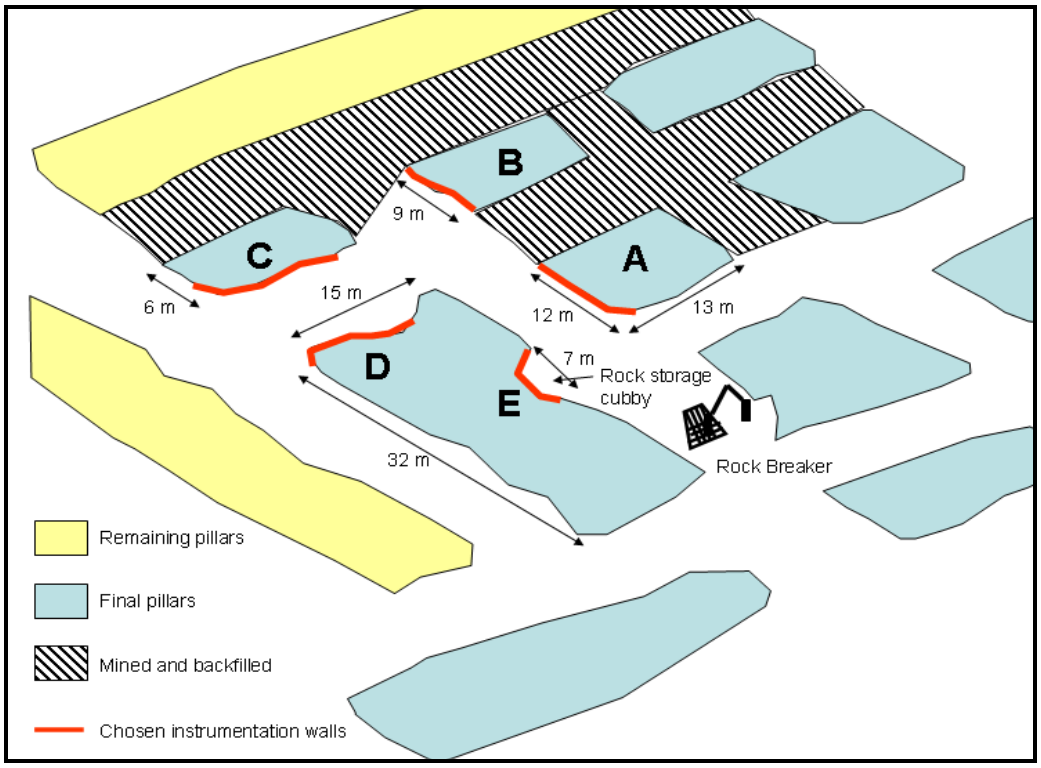


Figure 3.9 Test pillar detail at South Deep Mine Site (SRK SIMRAC Internal report, 2008)

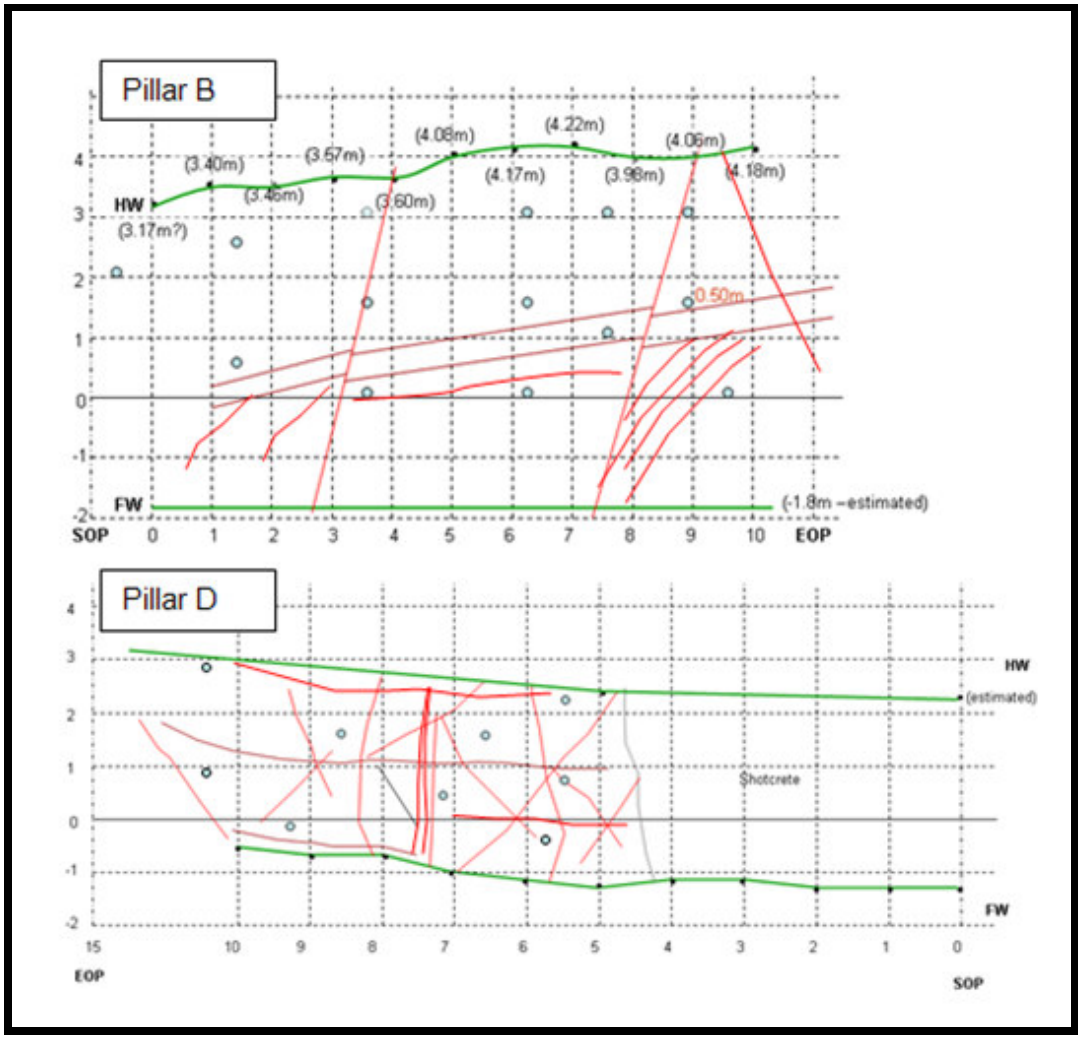
The mechanised trackless section is mined above a 1.8m wide tabular de-stress cut that has been backfilled. Backfilling was applied to help reduce the vertical field stress acting on the 3 pillars in order to prevent violent seismic failure of the pillars during pillar extraction. The pillars were extracted using the mechanised drift and fill mining method. Despite the significant reduction in field stress brought on by the de-stressing, pillar stresses in the trackless sections were high as noted during the monitoring exercise of the pillars.

The pillars were located in brittle, massive conglomerate. Pillars B and D were classified using the following rock mass classification methods: Rock Mass Rating after Laubscher (1990) and Bieniawski (1989), the Q-System after Barton et al (1974) and the Geological Strength Index (GSI). The results obtained are shown in Table 3.2. According to Barton et al (1974), the rock condition can be described as good.

Mapping of the pillars was carried out and Figure 3.10 shows the profiles of the mapped structure and the initial rock support on pillars B and D. Flat dipping bedding planes were found to be common in all the pillars. All the pillars had natural weakness planes and sidewalls showed stress induced fracturing with varying degrees of fracture intensity.

Table 3.2 South Deep Mine site rock mass classification (SRK SIMRAC Internal report, 2008)

Rock mass Rating Method	Pillar B	Pillar D
RMR_L after Laubscher (1990)	71	66
Q after Barton et al (1974)	25	25
RMR_B after Bieniawski (1989)	73	73
GSI = RMR_B - 5	68	68



○ 25mm resin grouted rebar

0.50m Scaling around tendon

• (4.08m) Measured elevation above and below "grade" line

——— Faults, jointing and bedding planes

Figure 3.10 Face and support mapping of Pillar B and Pillar D (SRK SIMRAC Internal report, 2008)

The mapped locations showed 20mm diameter, 2.4m long resin rebar support units in the sidewall of the test pillars. In both Pillars A and B, support units were approximately on a 1.5 m x 1.5 m support grid pattern.

The height of the pillars ranged between 5m and 6m. The site was sprayed with steel fibre-reinforced shotcrete. Photographs of the shotcreted pillar faces are shown in Figure 3.11 to Figure 3.14. In Figure 3.11, the thickness of the shotcrete is indicated and was determined using a battery operated hand held Hilti Drilling machine. The thickness was measured using the probe end of a vernier callipers and the results showed that the thickness ranged between 41 and 81mm on all pillars. However, the average sprayed thicknesses of 55, 66, 59 and 53 millimetres apply to pillars A, B, D and E respectively.

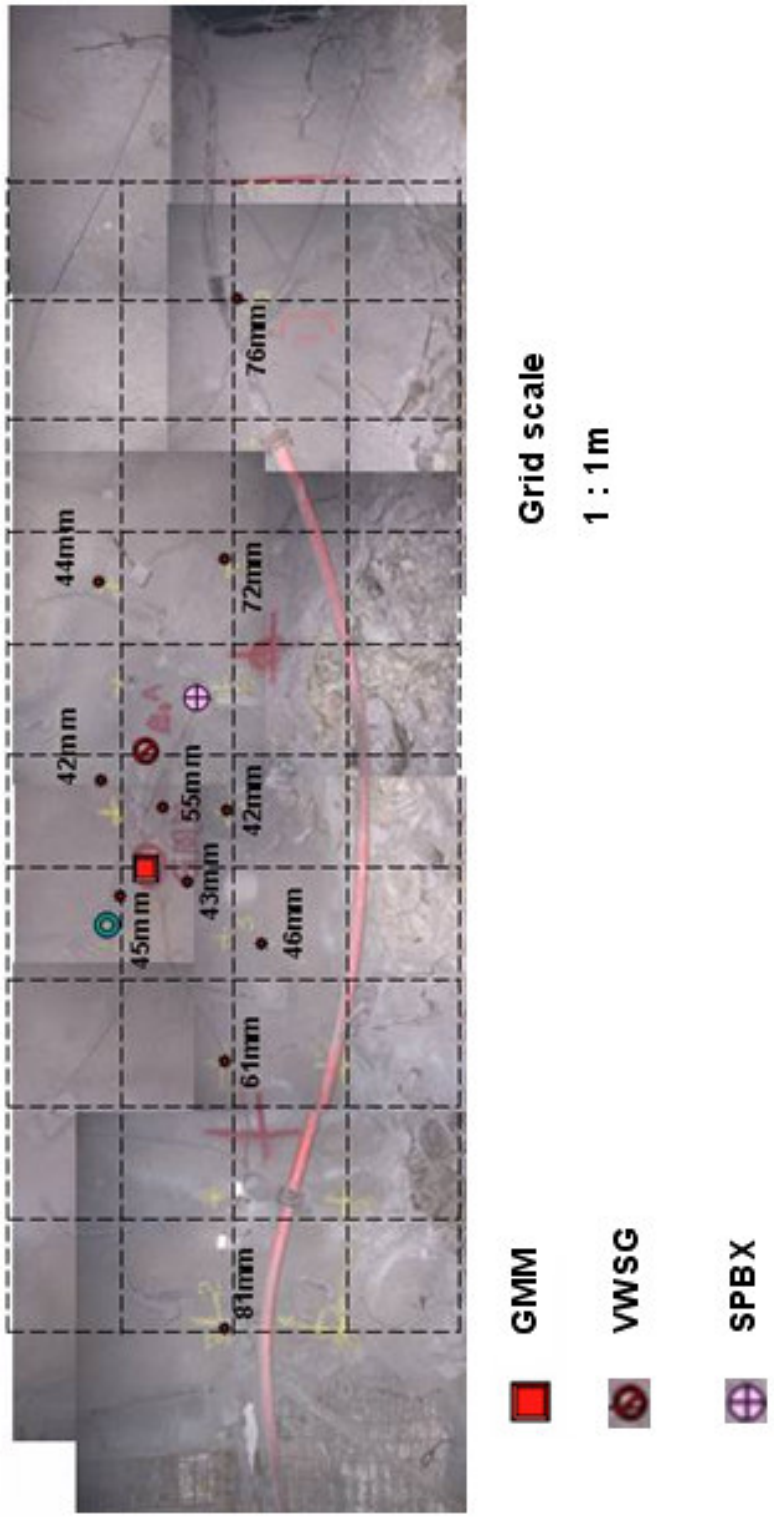


Figure 3.11 Photograph showing South Deep Mine Pillar A and position of monitoring instruments, values show the thicknesses of shotcrete at the marked position

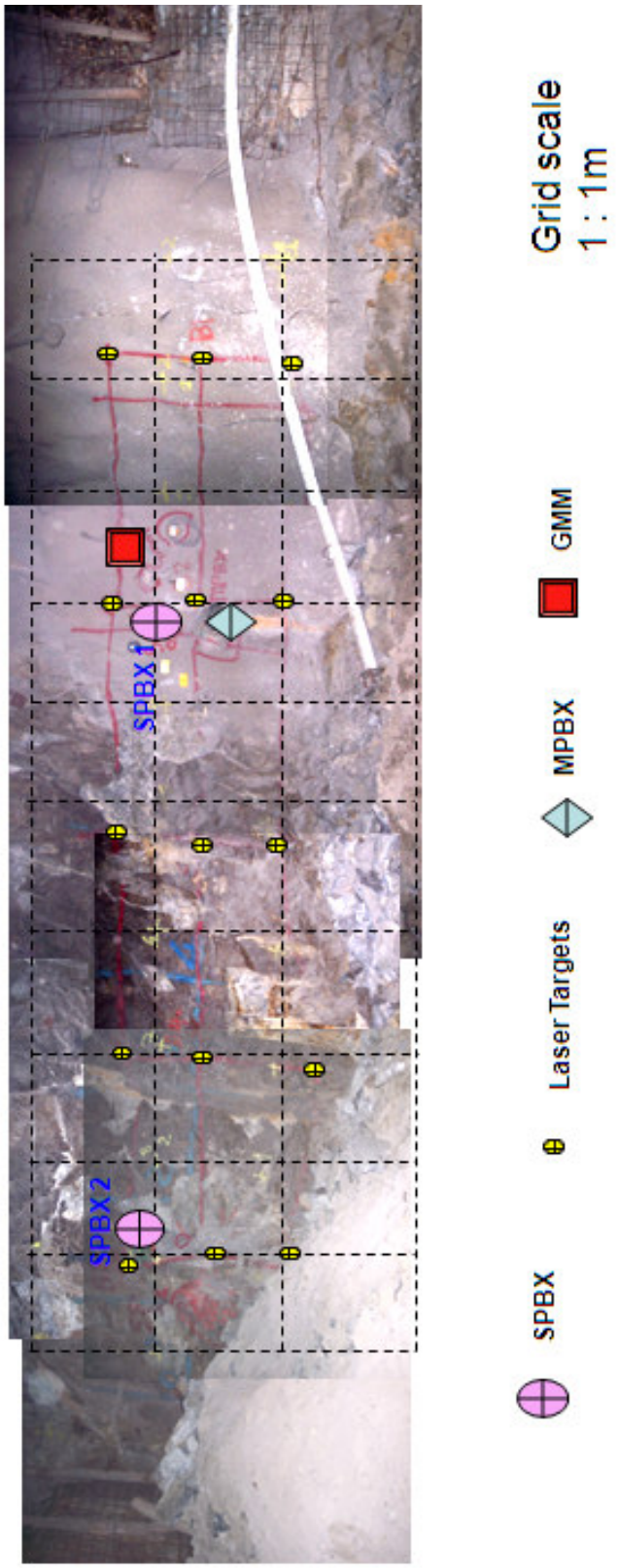


Figure 3.12 Photograph showing South Deep Mine Pillar B and positioning of monitoring instruments

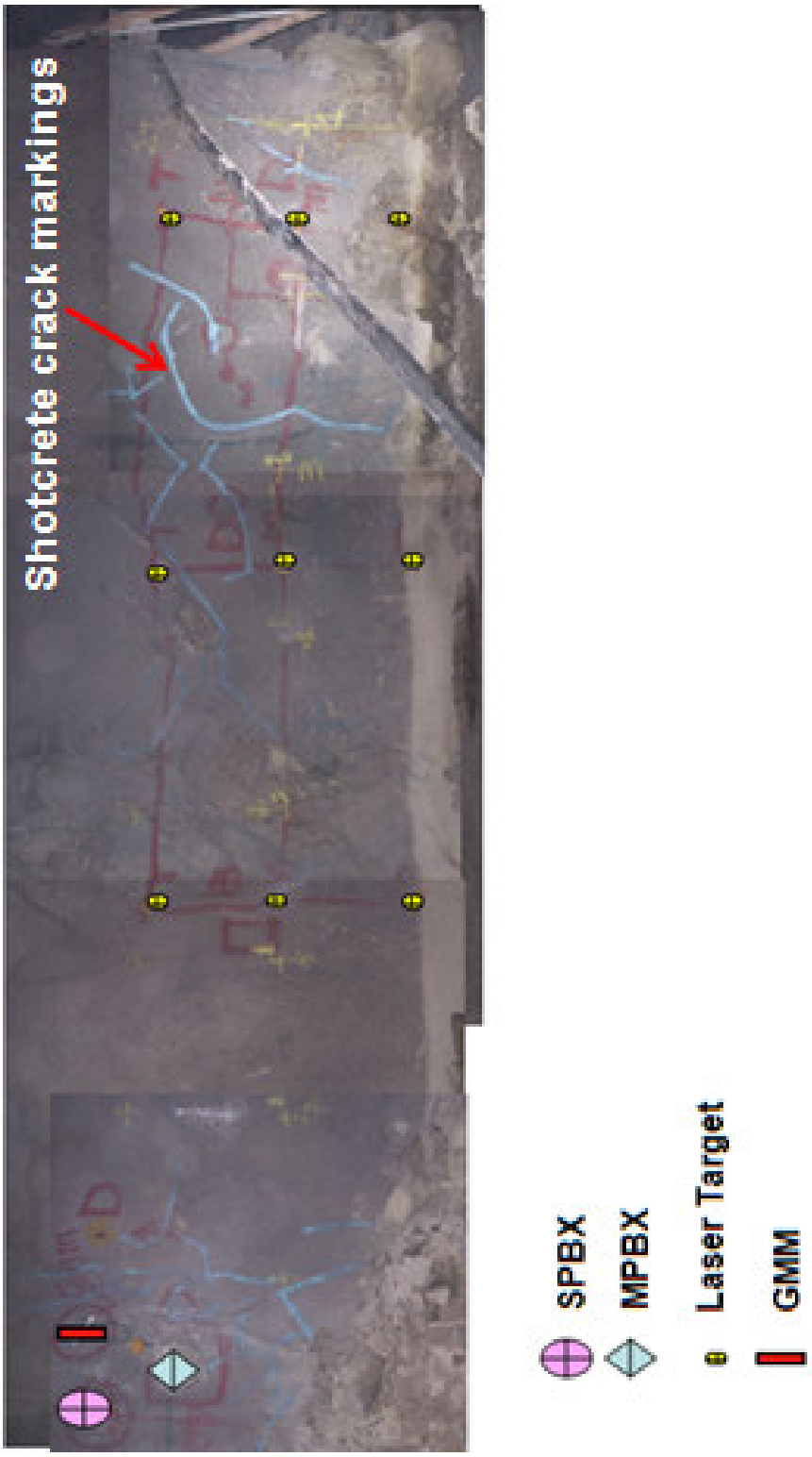


Figure 3.13 Photograph showing South Deep Mine Pillar D and positioning of monitoring instruments and shotcrete cracks marked on the pillar

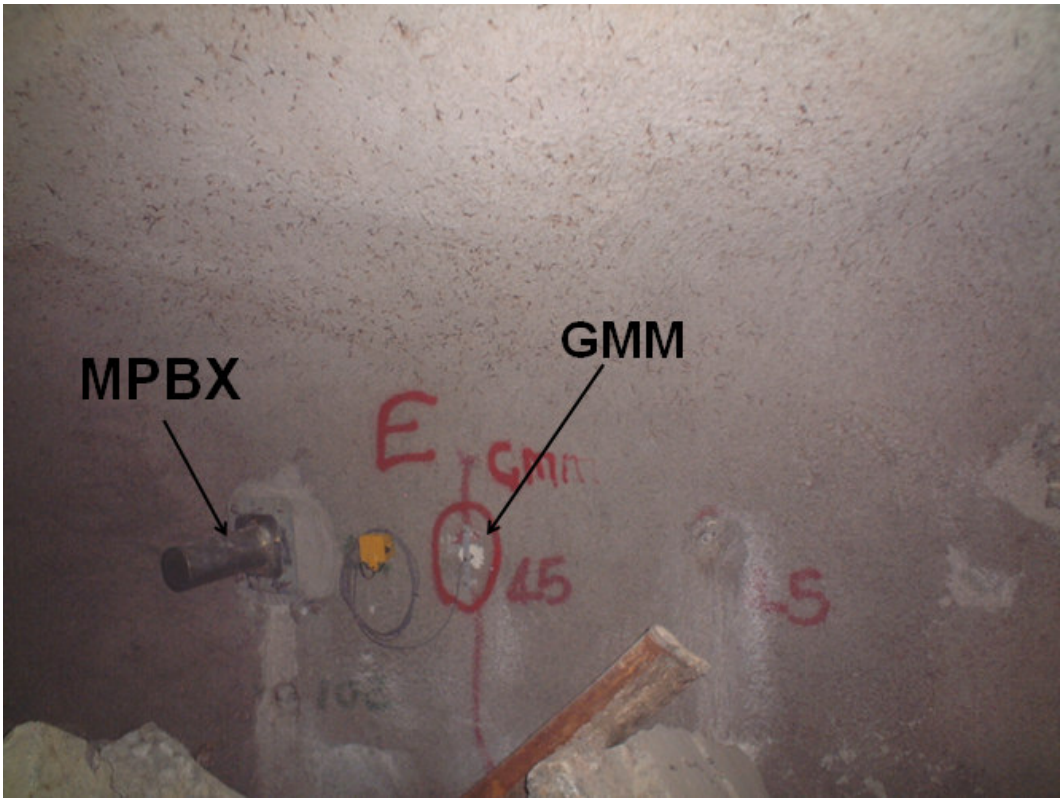


Figure 3.14 Photograph showing South Deep Mine Pillar E positioning of monitoring instruments

3.4.4 Determination of the in situ shotcrete material properties at South Deep Mine

Two EFNARC panels were sprayed underground at the time of spraying the pillars with shotcrete for laboratory testing. The first panel was tested for energy absorption according to the EFNARC (1996) standard. Results obtained indicate that the shotcrete had an energy absorption of 393 joules. Shotcrete cores were drilled from the second EFNARC panel to determine UCS, bulk density and steel fibre density of the shotcrete mix. The samples were tested more than a year after spraying. UCS, bulk density and steel fibre content results for the six core samples drilled from the second panel are presented in Table 3.3 in Section 3.5.3.

Shotcrete cores were drilled from pillars A, D and E. Cores for steel fibre content were drilled using a 50 mm diameter barrel. The cores for UCS testing were drilled using a 75 mm diameter barrel. Due to safety considerations, no cores were drilled from pillar B. UCS, steel fibre density and in situ adhesion (bond) strength tests were conducted on cores obtained from the pillars.

Bond strength testing cores were drilled using a 50mm diameter barrel. The bond strength tests were performed in situ. Figure 3.15 (a) and (b) shows the adhesion (bond) strength testing. The bond strength value was read off the bond strength testing machine shown in Figure 3.15b. The positions from which the bond strength tests were carried out are shown in Figure 3.16 for pillars A, D and E.

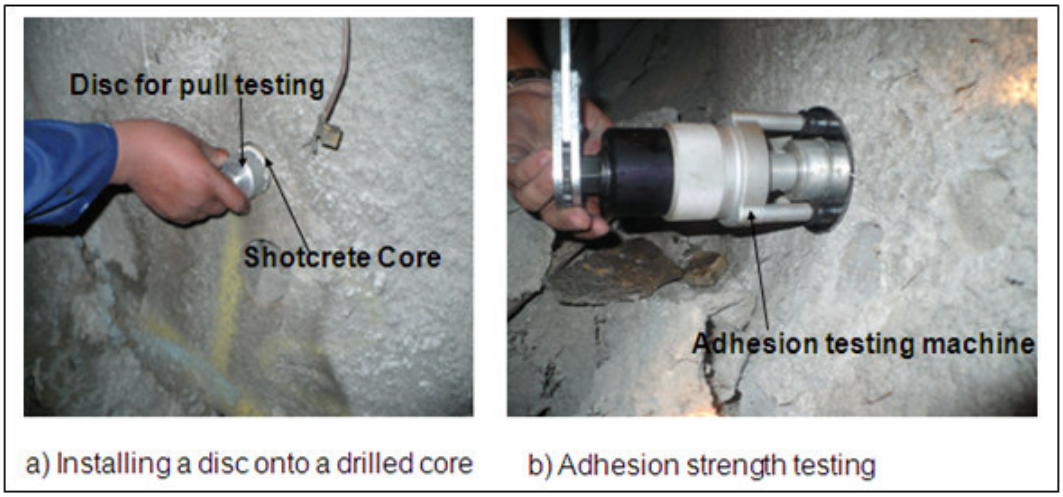


Figure 3.15 Photograph showing shotcrete-rock bond strength testing at South Deep Mine (Pillar A)

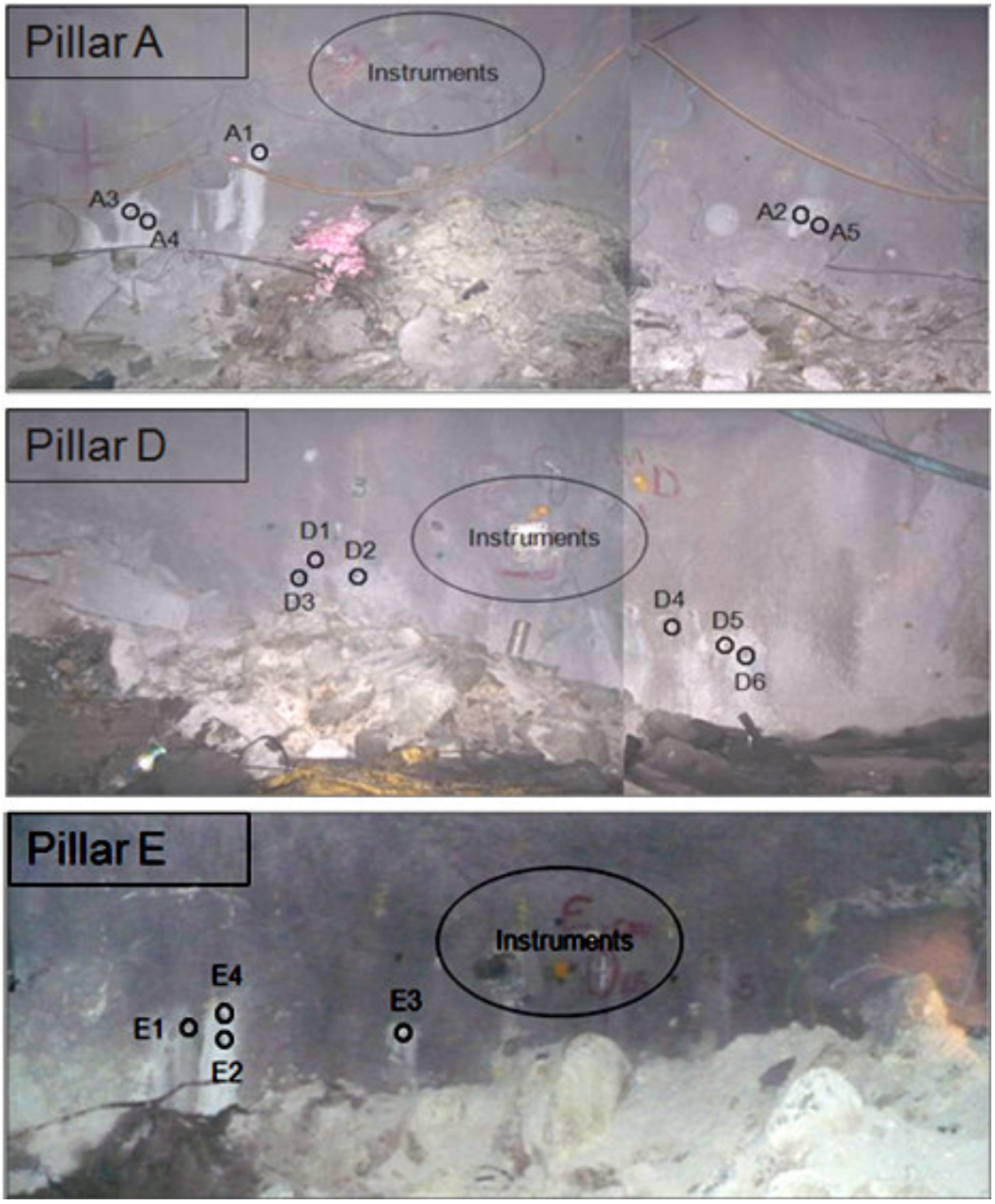


Figure 3.16 Photographs showing the location of drilled cores for UCS testing, bond strength testing and fibre density determination at South Deep Mine on pillars A, D and E

3.4.5 Impala Platinum Mine

The site was located at Number 14 Shaft and was established in March 2006. The site is a 3m x 3m footwall drive at 1200m below the surface on Level 24. It is separated from the stope above by a 7m middling. The tunnel was sprayed with wet-mix plain shotcrete on both sidewalls at an average thickness of 50mm. Figure 3.17 shows the test site location on a regional plan and Figure 3.18 shows the test site sidewall that was being monitored.

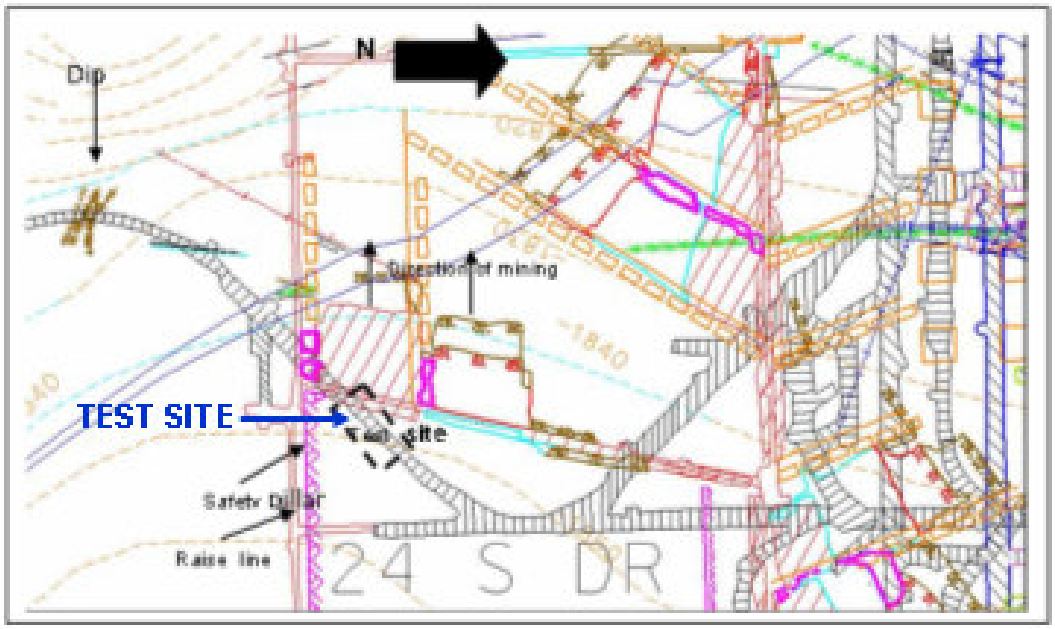


Figure 3.17 Impala Platinum Mine monitoring site plan (SRK SIMRAC Internal report, 2008)

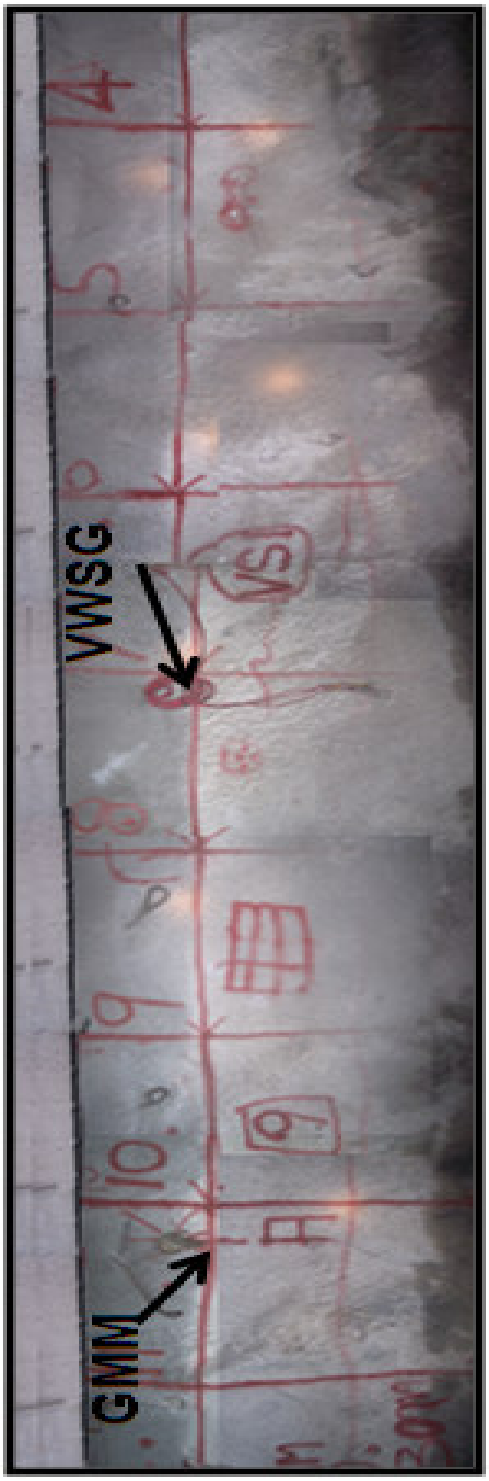


Figure 3.18 **Photograph showing the position of the Vibrating Wire Strain Gauge (VWSG) and the Ground Motion Monitor (GMM) on the monitored sidewall of the shotcreted tunnel at Impala Platinum Mine**

The test site was located in spotted anorthosites which have a high feldspar content. Intense sidewall fracturing and “onion peeling”, was noticeable on the sidewalls, which may indicate high vertical stresses, was effectively controlled using a systematic application of shotcrete close to the tunnel face.

3.5 Monitoring Results

Monitoring results obtained from each mine site have been presented in graphical format showing changes in strain or displacement over time. Also presented are the boreholes monitoring results for South Deep Mine only, as the other sites experienced very little or no changes from the time when the monitoring exercise commenced. Visual monitoring results are presented in Section 3.6, which gives attention to the failure modes of shotcrete observed during the monitoring exercise.

3.5.1 South Deep Mine monitoring results

Monitoring results from South Deep Mine are presented in Figures 3.19 – 3.24. The borehole monitoring results are shown in Figure 3.25.

Figure 3.19 shows the single point borehole extensometer (SPBX), ground motion monitor (GMM) and the vibrating wire strain gauge (VWSG) results for pillar A. The GMM and the SPBX results show a similar displacement trend throughout the monitoring period. They also show a sudden jump in displacement between July 2007 and August 2007. The sudden jump in displacement resulted from the mining of benches close to the monitoring area between July 2007 and August 2007, which increased the mining induced stresses in the pillars. However, the GMM recorded a larger displacement compared to the SPBX. The larger displacement recorded

by the GMM may be attributed to the difference in positioning of the instruments.

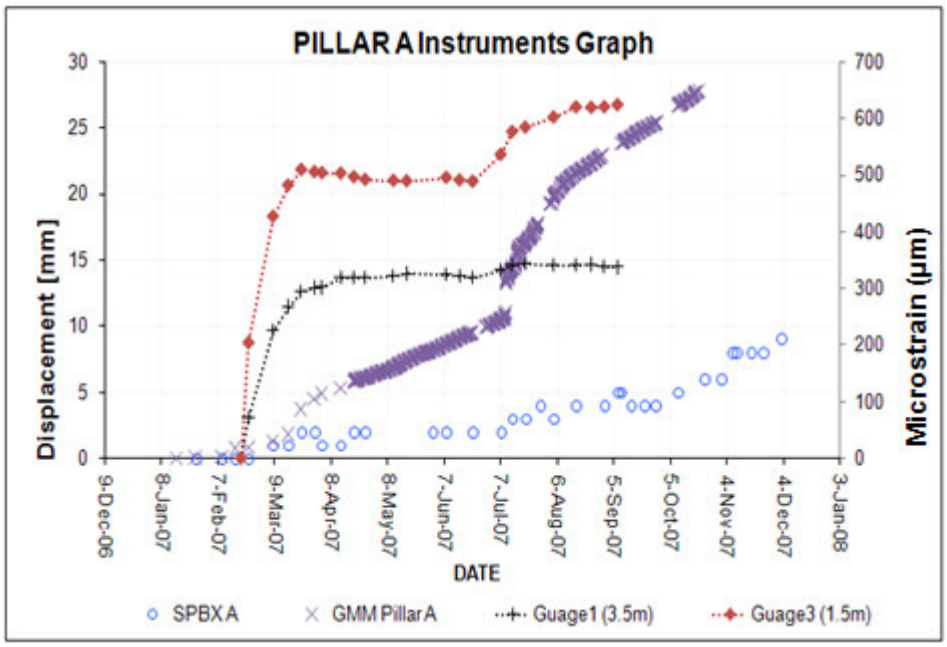


Figure 3.19 South Deep Mine Pillar A displacement and strain results

The vibrating wire strain gauges (VWSG) were inserted in boreholes to measure strain in the pillars. Only two of the VWSG for pillar A were functional as the third was discovered to be faulty after installation. The results for the two gauges show a sudden jump in the strain readings between February 2007 and March 2007. The reason for this sudden jump is not known, but may be a result of the cement grout curing used when installing the vibrating wire strain gauges in the borehole. The distribution of the readings, and the response of the other instruments, indicate that the initial jump does not represent real behaviour. The strain gauge results show no significant change in strain between March 2007 and June 2007. However, between mid-June 2007 and mid-July 2007, there is a gradual increase in strain which is more noticeable in gauge number 3. The increase in strain between mid-June 2007 and mid-July 2007 is likely to

have resulted from an increase in mining induced stresses as the mining of benches close to the monitoring site took place.

Pillar B monitoring results are shown in Figure 3.20 and Figure 3.21. The single-point borehole extensometer (SPBX), multi-point borehole extensometer (MPBX), ground motion monitor (GMM) and laser displacement monitoring results in Figure 3.20 and Figure 3.21 show similar trends. They all show a gradual increase from February 2007 to July 2007. They also show a sudden jump between July and August 2007 when benches close to the monitoring site were mined resulting in increased mining induced stresses in the pillars. The GMM, laser monitoring, MPBX and SPBX B1 show greater displacement compared to the displacement measured by SPBX B2. The SPBX B2 was positioned close to the backfill confined section of the pillar whereas the other instruments were positioned in the middle of the pillar where more displacement could be experienced.

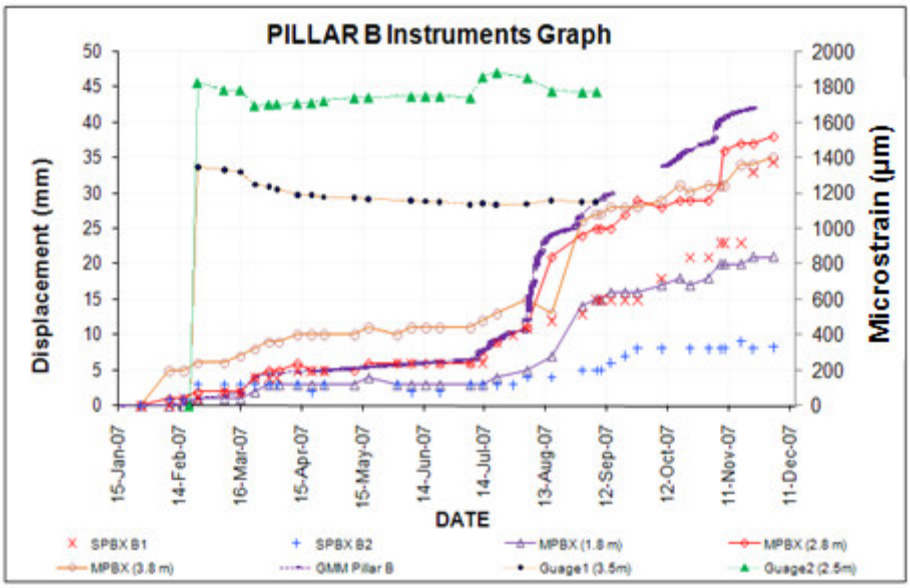


Figure 3.20 South Deep Mine Pillar B displacement results

The vibrating wire strain gauge (VWSG) for pillar B was inserted in a borehole to measure strain in the pillar. The VWSG results shown in Figure 3.20 show a sudden jump in strain between February 2007 and March 2007. As indicated above, these sudden changes are not considered to be real, but probably have resulted from the curing of the cement grout used when installing the vibrating wire strain gauges in the boreholes. VWSG number 1 shows no increase in strain throughout the monitoring period. The lack of strain increase in VWSG number 1 may be due to the fact that at 3.5m depth into the pillar there was stability and this location did not experience any appreciable deformation. However, VWSG number 2 anchored at 2.5m depth and therefore closer to the surface of the pillar shows an increase in strain between July 2007 and August 2007 when the MPBX, SPBX and the GMM also start showing an increase in displacement. The increase in strain between July and August resulted from the increase in mining induced stresses as the mining of benches close to the monitoring site commenced.

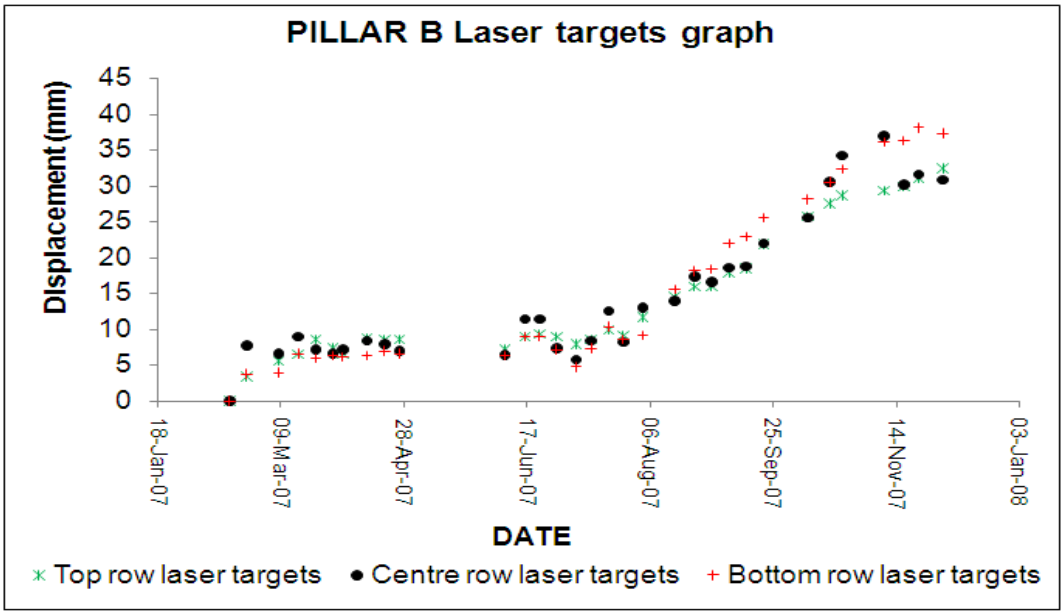


Figure 3.21 South Deep Mine Pillar B laser targets displacement results

Pillar D results shown in Figure 3.22 indicate lower displacement results compared to the displacement results obtained from laser monitoring of the pillar shown in Figure 3.23. The laser targets show displacements above 70mm whereas the SPBX, MPBX and the GMM results show displacements less than 8mm.The difference is likely to have been caused by the smaller pillar C onto which the laser distometer was mounted, with the laser beam directed at the laser targets placed on the larger pillar D. Therefore the displacement results may represent the relative closure of both pillar D and pillar C.

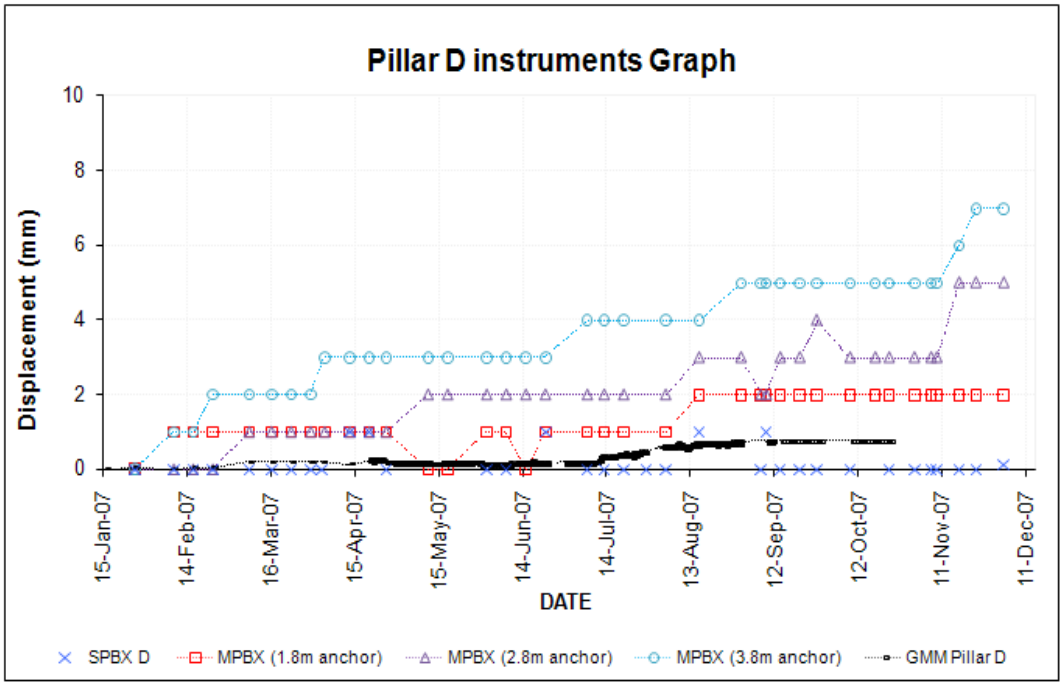


Figure 3.22 South Deep Mine Pillar D displacement results

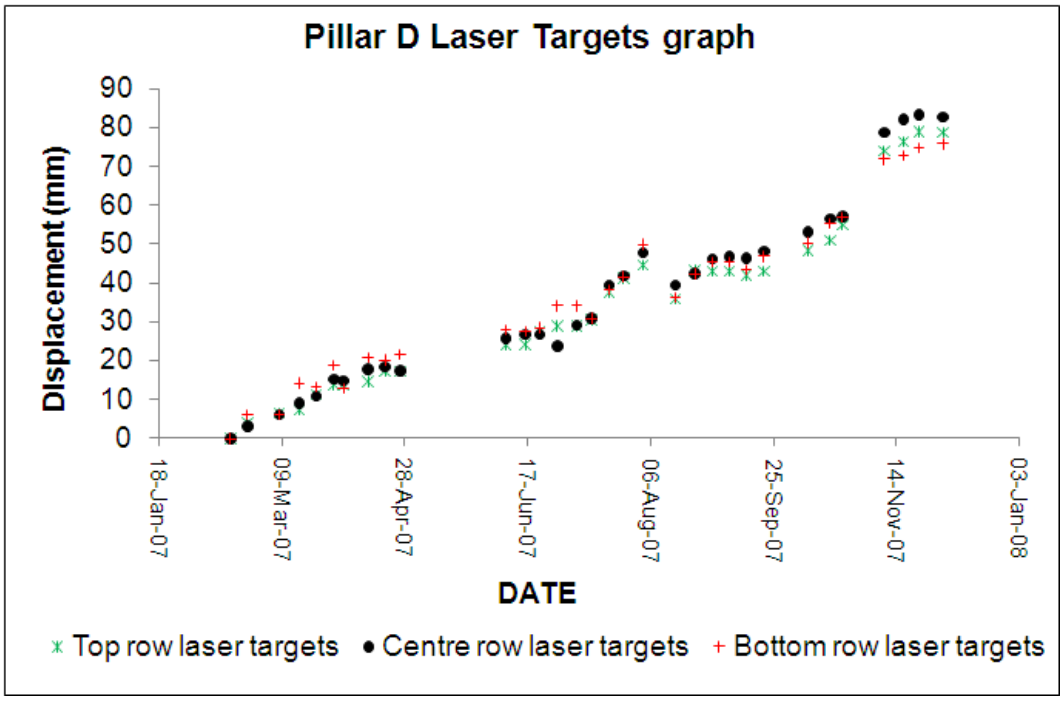


Figure 3.23 South Deep Mine Pillar D laser targets displacement results

The displacement results obtained for pillar E are shown in Figure 3.24. The displacement results show that the pillar experienced the least deformation as the MPBX and the GMM recorded less than 2mm change in displacement. The GMM results in Figure 3.24 show a sudden increase in displacement of about 1.4mm in March 2008. The sudden increase may be attributed to the mining of a tunnel situated about 10m from pillar E. Pillar E instruments recorded the lowest displacement results because pillar E was the largest pillar of those monitored and the instruments were located in the concave section of the pillar which may be more resistant to displacement.

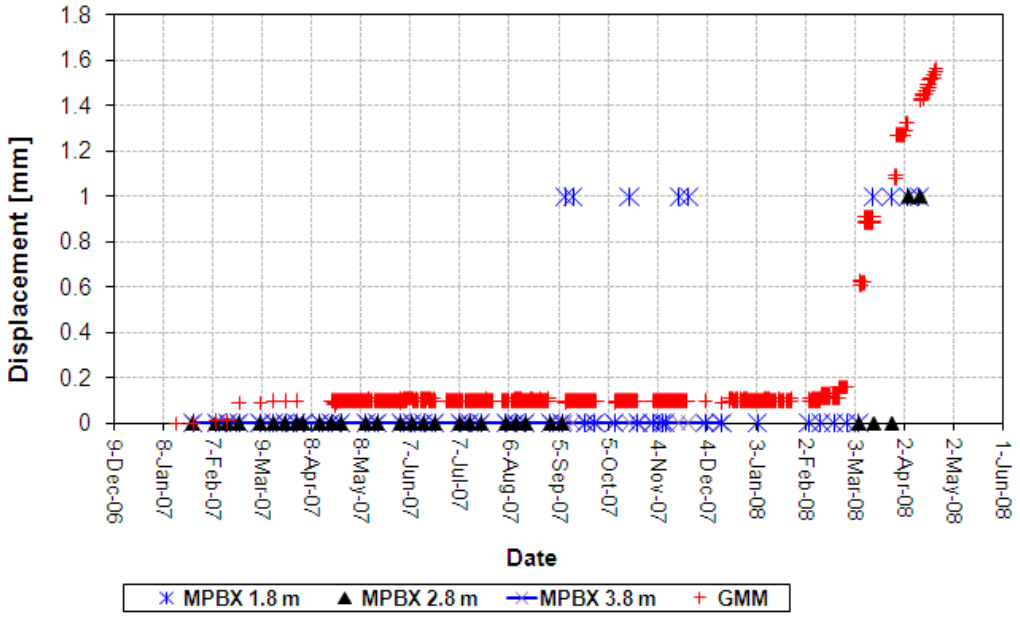


Figure 3.24 South Deep Mine MPBX and GMM monitoring results for Pillar E

Borehole monitoring results at South Deep Mine are shown in Figure 3.25. The condition of the rock was classified into three distinct zones, namely, zone 1 consisting of crushed material; zone 2 which comprised of fractured material and zone 3 consisting of intact rock.

Figure 3.25 shows that in pillar A, crushed rock (zone 1 category) was to a depth of 0.9m. Fractured rock falling in zone 2 was between 0.9 and 2.2m in the borehole and beyond 2.2m the rock was intact.

Pillar D borehole monitoring results in Figure 3.25 show crushed rock to a depth of 0.3m and fractured rock between 0.3m and 1.4m depths. Beyond 1.4m depth, the borehole showed intact rock.

Pillar E borehole monitoring results in Figure 3.25 show that crushed rock was noticed to a depth of 0.1m. Fractured rock was noticed between 0.2m and 0.9m. Beyond 0.9m, the rock was intact.

Pillar A had a larger proportion of crushed and fractured rock due to its smaller size relative to pillar D and pillar E. Therefore it experienced higher average pillar stresses than pillar D and pillar E. Pillar E recorded the least fracturing since the borehole was located in a more stable concave section of the pillar which experienced less deformation due to mining induced stresses.

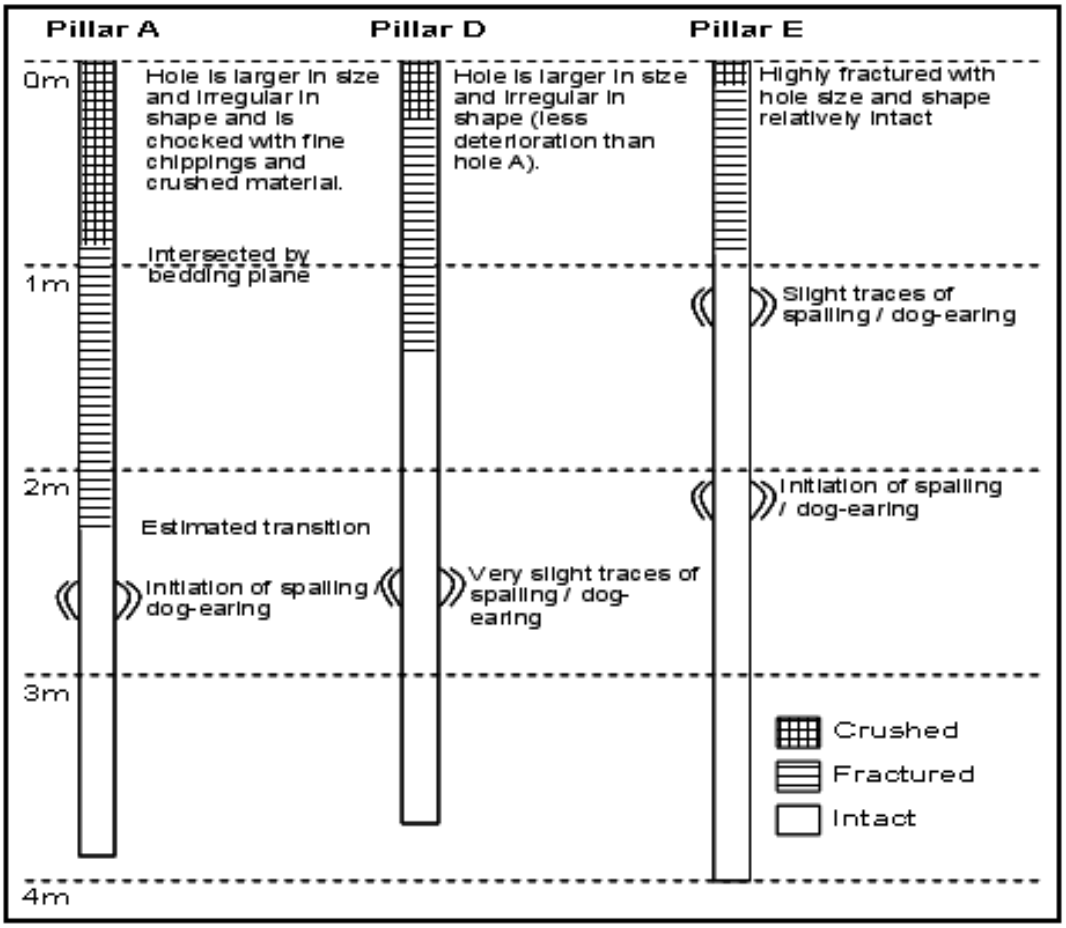


Figure 3.25 Fracture zones identified at South Deep Mine site from borehole inspection (SRK, SIMRAC Internal report, 2008).

3.5.2 Discussion of the monitoring results at South Deep Mine

The displacement results for pillars A, B, D and E show that most instruments recorded a sudden jump between the months of July and August 2007 as the mining of the benches close to the monitoring site commenced. It was also noted that between July and August 2007 shotcrete cracks started forming on pillars B and D. Pillar B instruments recorded the greatest displacement at the South Deep Mine site and this could be due to its smaller size compared to the other pillars and its location closer to the benches that were mined.

When mining of the benches close to the monitoring site started between July and August 2007, various failure modes of the shotcrete were identified and they are presented and discussed in section 3.6.

Borehole monitoring results show that pillar E experienced the least deformation compared to pillar A and pillar D. Monitoring results also showed that pillar E experienced the least displacement amongst the other pillars at South Deep Mine site. However, pillar A borehole, which showed the greatest damage of the rock, showed little cracking in the shotcrete at the end of the monitoring exercise. This could be an indication that the shotcrete was able to hold back the fractured rock thereby maintaining the strength of the pillar. Alternatively, the rock was fractured and therefore destressed before the application of the shotcrete. Therefore shotcrete was not subjected to stresses as the pillar deformed.

Amongst the pillars that were monitored, Pillar B experienced the greatest damage due to mining induced stresses compared to the other pillars. Firstly, pillar B was the smallest of all the pillars which is likely to have caused it to have higher average pillar stresses compared to the other pillars. Therefore the high average pillar stress contributed to the damage of the pillar as the mining of benches close to the site was being carried out.

The vibrating wire strain gauges were placed at different depths in the pillars to measure strain changes in the pillars. However, they did not show significant changes in strain except for the period between July 2007 and August 2007 when there was a slight increase recorded by some of the gauges. The slight increase was a result of the mining of benches close to the test site. Probably, the pillar experienced greater deformation at the periphery as compared to the centre of the pillar resulting in low strain values being recorded by the vibrating wire strain gauges at 1.5m, 2.5m and 3.5m depths.

3.5.3 South Deep Laboratory and field test results

Table 3.3 shows the bulk density, fibre density and the uniaxial compressive strength results of the shotcrete used at South Deep Mine. The steel fibre density in the shotcrete varies between 19 – 23 kg/m^3. The applied steel fibre density during spraying was 30 kg/m^3, therefore spraying fibre losses experienced in the shotcrete range between 23 – 37%.

The shotcrete applied to the pillars had a designed uniaxial compressive strength (UCS) of 30MPa. The results in Table 3.3 show that the shotcrete sprayed at South Deep Mine, after 1 year of curing had UCS results ranging from 30 – 45 MPa, showing an increase in UCS of up to 50% greater than the design value. UCS tests on plain shotcrete would have indicated the effect of fibre addition in the shotcrete. However, no tests on plain shotcrete were carried out. The panel from which the cores were drilled was stored on surface in shade which may have played a role in preserving the compressive strength of the shotcrete.

Table 3.3 Bulk density, fibre density and UCS test results for cores drilled out of an EFNARC Panel spayed at South Deep Mine during pillar shotcreting

Description	Sample ID	Bulk Density (kg/m^3)	Fibre Density (kg/m^3)	UCS (MPa)
EFNARC panel testing	1	2123	19.9	36
	2	2055	19.3	45
	3	2051	22.9	45
	4	2048	20.1	39
	5	2070	23.1	38
	6	2063	20.4	43.5
	Average	2068.3	20.9	41.1

In situ bond strength test results obtained at South Deep Mine are shown in Table 3.4. The bond strength results vary between 0.1 MPa and 2.0 MPa. The bond strength results confirm the point raised by Melbye (1994) that little control can be exercised on the rock-shotcrete bond strength.

The fibre density results from the cores drilled from one of the EFNARC panels varied between 13 – 26 kg/m^3. Therefore fibre losses in the shotcrete panel were slightly higher than the in situ shotcrete by 6%. Probably, there was more rebound from the EFNARC trays compared to the fibre rebound losses from the pillars.

The UCS test results obtained from the in situ cores are shown in Table 3.4. Only one UCS test result per pillar from the South Deep Mine pillars is shown in Table 3.4 because most of the cores drilled from the pillars did not meet the standard dimensions for UCS testing. The UCS test results obtained are not sufficient to draw conclusions regarding the in situ UCS of the shotcrete used at South Deep Mine. The core drilled from pillar A

had a UCS of 30 MPa, the core drilled from pillar D had a UCS of 46 MPa and the core drilled from pillar E had a UCS of 25 MPa. More samples are required for better UCS interpretation of the shotcrete in situ. However, the UCS results from the cores drilled from one of the EFNARC panels sprayed at the time of shotcreting the pillars averaged 41 MPa which is higher than the design compressive strength of 30 MPa.

Table 3.4 In situ shotcrete core drilling and laboratory testing results at South Deep Mine monitoring site

Description		Sample ID	Bond Strength (MPa)	Fibre Density (kg/m³)	UCS (MPa)
Underground core testing	Pillar A	A1	0.7	-	30
		A2	1.5	-	-
		A3	-	25.3	-
		A4	-	12.8	-
		A5	-	-	NTS
		Average	**1.1**	**19.1**	**30**
	Pillar D	D1	0.5	14.8	-
		D2	2	-	-
		D3	-	-	NTS
		D4	-	14.2	-
		D5	-	15.4	-
		D6	-	-	46
		Average	**1.3**	**14.8**	**46**
	Pillar E	E1	0.2	-	-
		E2	0.1	-	-
		E3	-	17.4	25
		E4	-	19.6	-
		Average	**0.2**	**18.5**	**25**
OVERALL AVERAGE			**0.8**	**17.1**	**33.4**

* NTS – Core not to standard

3.5.4 Impala Platinum Mine Monitoring Results

The ground motion monitor (GMM) displacement and the vibrating wire strain gauge (VWSG) monitoring results for Impala Platinum Mine are shown in Figures 3.26 and 3.27 respectively.

Figure 3.26 showing results for GMM1 and GMM2 indicate a gradual increase in displacement results over time. However, both GMMs show displacement results that are less than 1mm in total. Mining of the stope above was abandoned after bad ground conditions were encountered and the anticipated stress changes did not occur in the tunnel that was being monitored. As a result, minimal displacement results were recorded.

The vibrating wire strain gauges (VWSG) at Impala Platinum Mine were installed at a depth of 3.5m in the borehole, with gauge 1 oriented horizontally, gauge 2 oriented at 45˚ to the horizontal and gauge 3 oriented vertically. The strain gauges were used to measure strain changes in the rock and not in the shotcrete. Figure 3.27 shows the VWSG results obtained from Impala Platinum Mine monitoring site. As found for the VWSG results described previously, the results in Figure 3.27 show a sudden jump in strain a month after installation of the strain gauges, probably caused by the curing of the cement grout used in the installation of the strain gauges in the boreholes. However, further monitoring shows no further increases in strain in the rock behind the shotcrete. The expected stress changes due to mining were not experienced because the planned mining of a stope above the tunnel being monitored stopped several metres away from the tunnel. Therefore due to lack of mining induced stress changes around the tunnel, no significant strain changes would be expected, and none were recorded by the vibrating wire strain gauges. Also, no signs of shotcrete cracking were observed throughout the monitoring period.

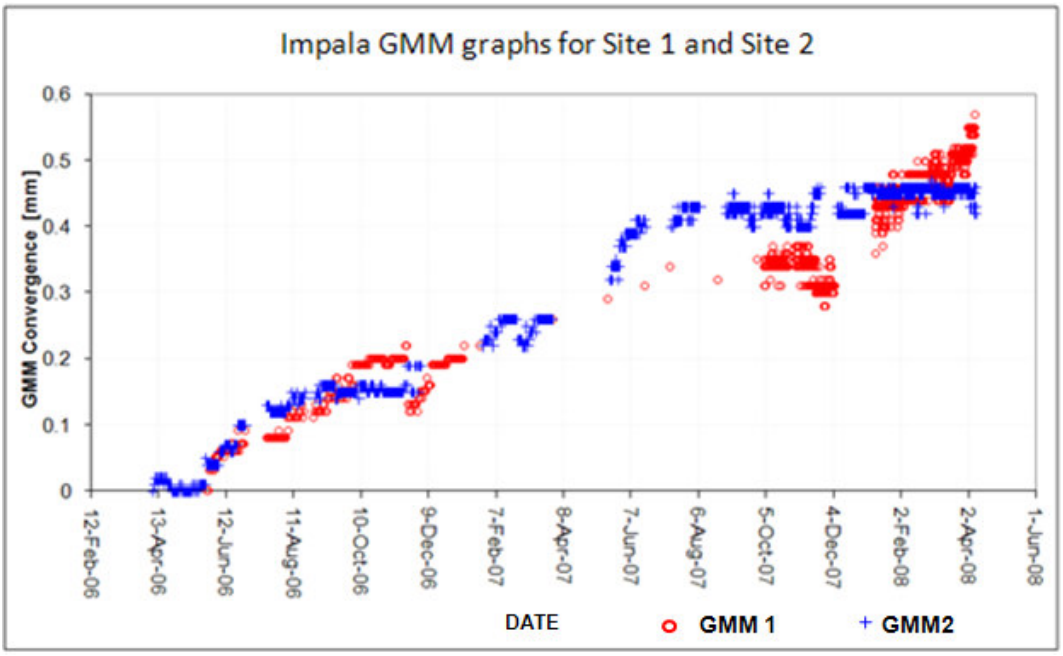


Figure 3.26 Impala Platinum Mine GMM displacement results

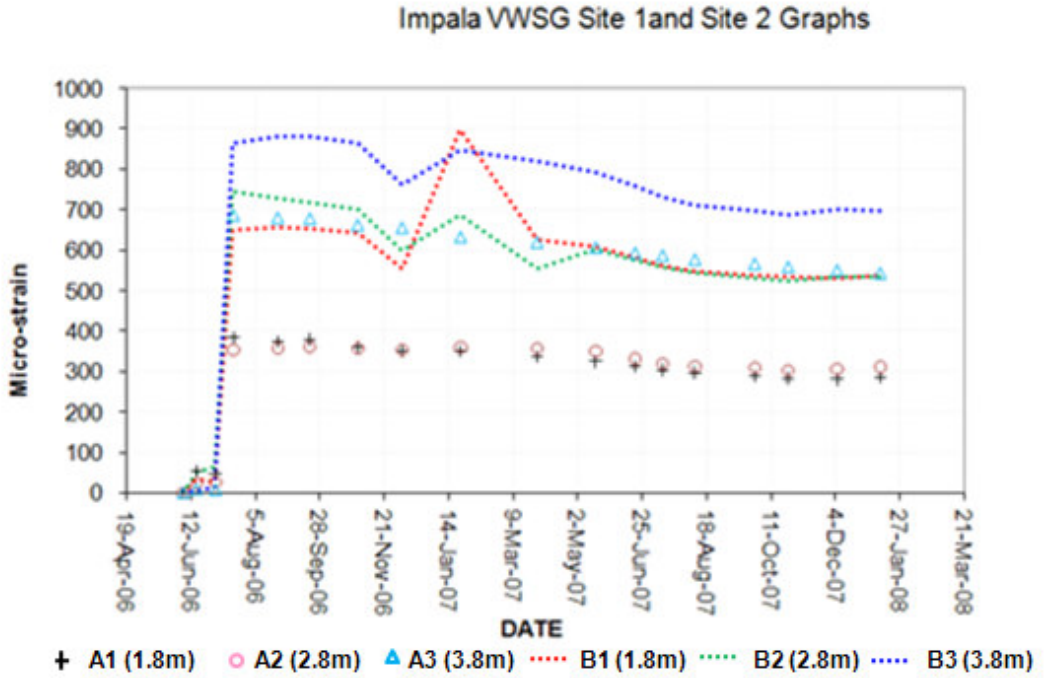


Figure 3.27 Impala Platinum Mine vibrating wire strain gauge results

3.5.5 Mponeng Mine Level 109 monitoring results

Displacement monitoring results for Mponeng Mine Level 109 are shown in Figure 3.28 for the North-West wall and in Figure 3.29 for the South East Wall. The displacement results in these figures display an almost linear trend in displacement with time for both the North-West wall and the opposite South-East wall. Both graphs in Figure 3.28 and Figure 3.29 show that the laser targets in the middle row experienced the greatest displacement compared to the top row and the bottom row laser targets. When the tunnel is exposed to high compressive stresses, the middle section is likely to deform more than the bottom corner or top corner of the tunnel sidewall. The monitoring results therefore conform to the expected behaviour. The top row laser targets and the bottom row laser targets experienced almost similar displacements for both sides of the tunnel. Very little cracking of the shotcrete was observed throughout the monitoring period as there were no mining induced stress changes. The tunnel was in a destressed state since mining of the stope above had progressed past the tunnel when shotcreting was done and monitoring started.

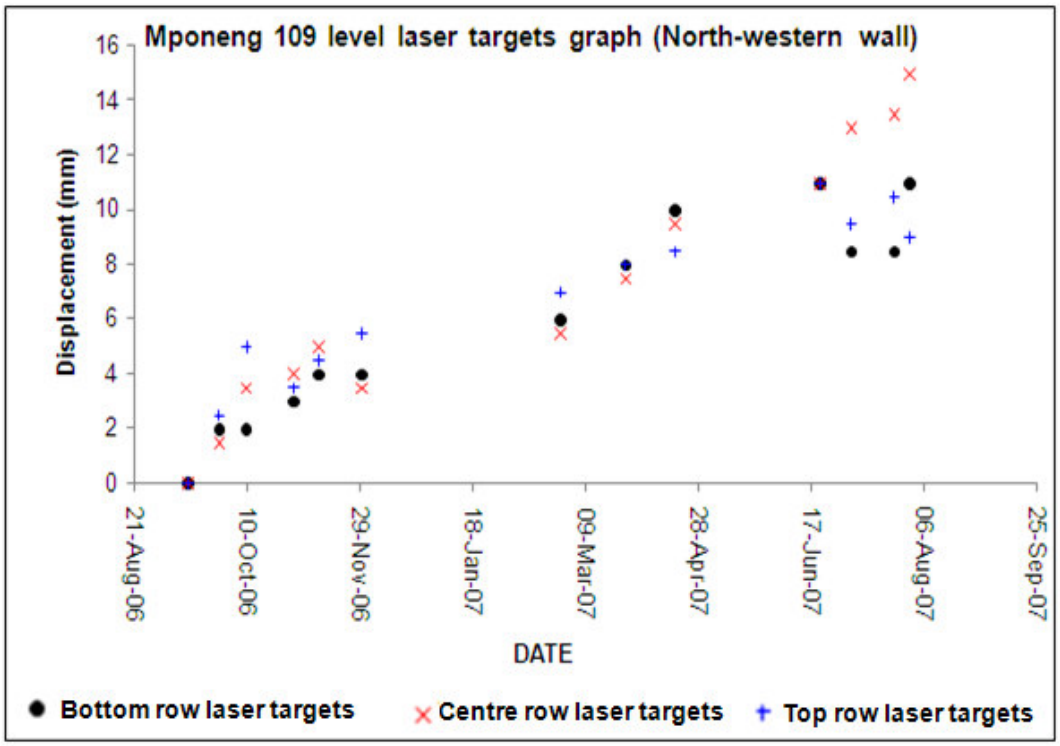


Figure 3.28 Mponeng Mine Level 109 North-West wall displacement results

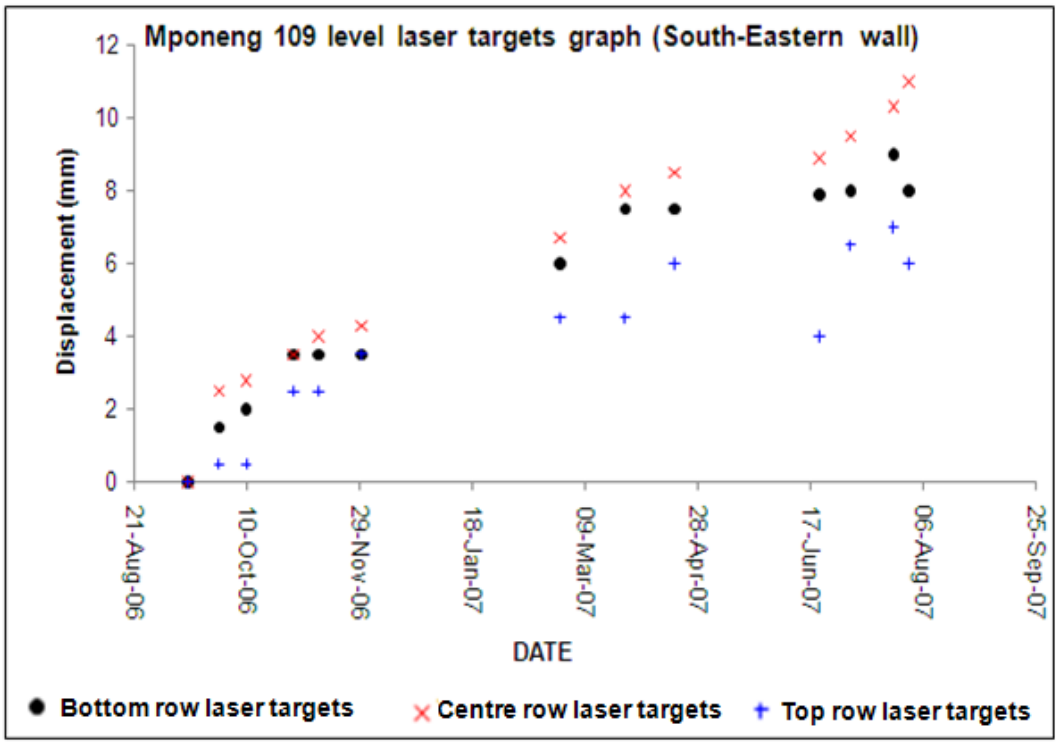


Figure 3.29 Mponeng Mine Level 109 South-East wall displacement results

3.5.6 Mponeng Mine Level 116 monitoring results

Monitoring results obtained from the monitoring instruments at Mponeng Mine are shown in Figure 3.30 and Figure 3.31.

The laser target displacement results shown in Figure 3.30 reveal that the opposite sides of the tunnel sidewalls were each undergoing displacement in the opposite direction relative to the other. The results in Figure 3.30 show sudden jumps in the displacements of the right hand side laser targets. The maximum displacement recorded was up to 450mm. For such displacements, physical damage in the shotcrete would be expected. However, no damage was observed in the shotcrete throughout the monitoring exercise. It was discovered that since the laser distometer was mounted on rails when taking displacement readings for the laser targets, the rails may have possibly shifted sideways when the production wagons

pass through the monitoring site during the ore handling shifts. Therefore the results obtained do not reflect the true sidewall movement but rather, the sideways movement of rails. Also, after the first jump, the laser targets displacements are almost constant. This is probably due to the fact that the rock was in a destressed state when the shotcrete was applied and no significant displacement occurred in the tunnel sidewalls. This is confirmed by the two ground motion monitor (GMM) results that show very small displacements. These reflect the true displacement of the tunnel sidewalls, as there was no physical damage noted on the shotcrete.

There was no major mining of the areas surrounding Mponeng Mine Level 116 monitoring site. Therefore there were no major stress changes anticipated around the tunnel. Rather, Mponeng Mine Level 116 monitoring site was located in a seismically active section and the reason for the location was to observe the changes in the behaviour of the shotcrete after a seismic event. However, there were no remarkable seismic events recorded during the monitoring exercise and the shotcrete was in good condition at the end of the monitoring exercise.

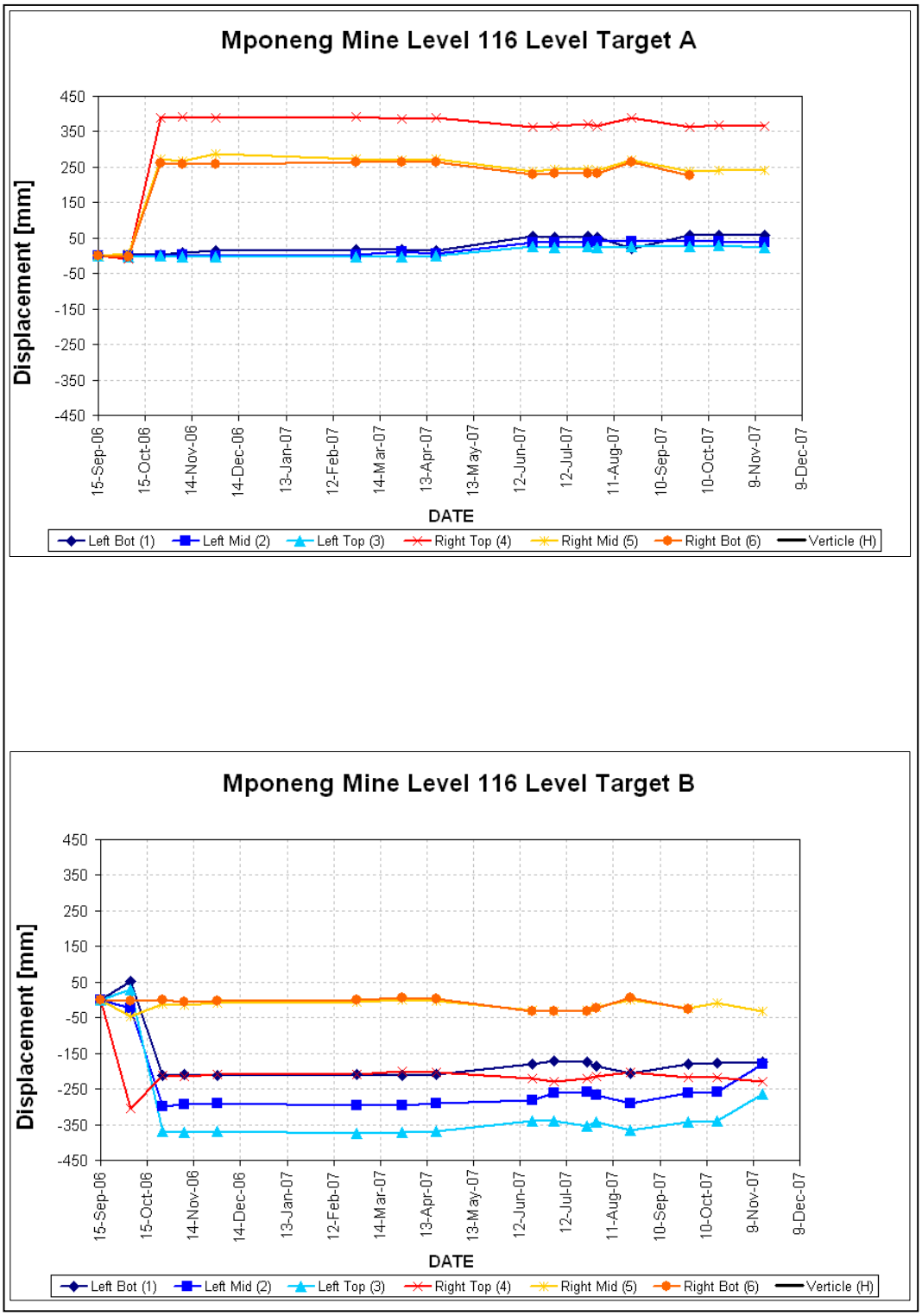


Figure 3.30 Laser targets displacement results for Mponeng Mine Level 116

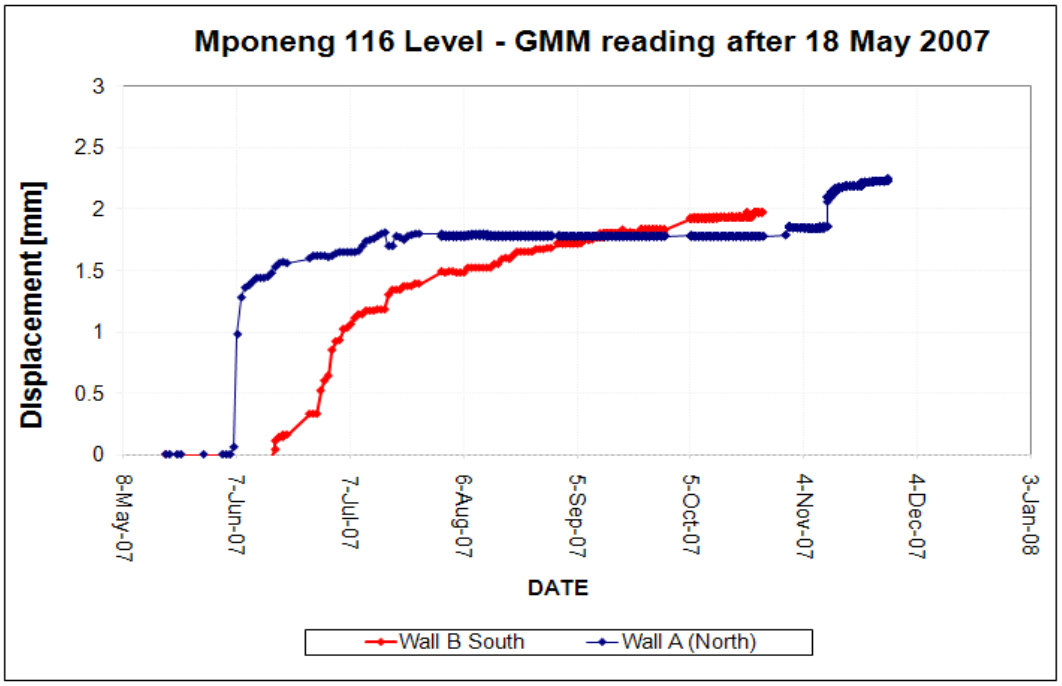


Figure 3.31 GMM displacement results for Mponeng Mine Level 116

3.6 Shotcrete Failure Mechanisms

Shotcrete failure mechanisms were observed mainly at the South Deep Mine site which underwent the expected stress changes due to mining of the surrounding benches. The dominant failure mode of the shotcrete observed on most pillars was tensile failure.

3.6.1 Tensile failure

Figure 3.32 shows a shotcrete crack that runs from the bottom of the pillar upwards. The crack is likely to have developed from pure tension in the shotcrete since the shotcrete layer shows that it has been pulled apart horizontally. Figure 3.32 shows an offset in the red line crossing the crack which may imply shear failure of the shotcrete. However, the fibres sticking out between the cracks were oriented perpendicular to the crack which

shows that the offset was a result of subsequent displacement of the shotcrete slab together with the rock behind after tensile failure of the shotcrete had already occurred. The crack is wider at the bottom and narrows as it progresses upwards indicating greater deformation on that part of the pillar than as one goes up the pillar. It was also noted that the wider part of the shotcrete crack is not at the true bottom of the pillar but was about 1.5m above the true floor since there was muck and rock toes left at the bottom of the pillar due to lack of smooth blasting.

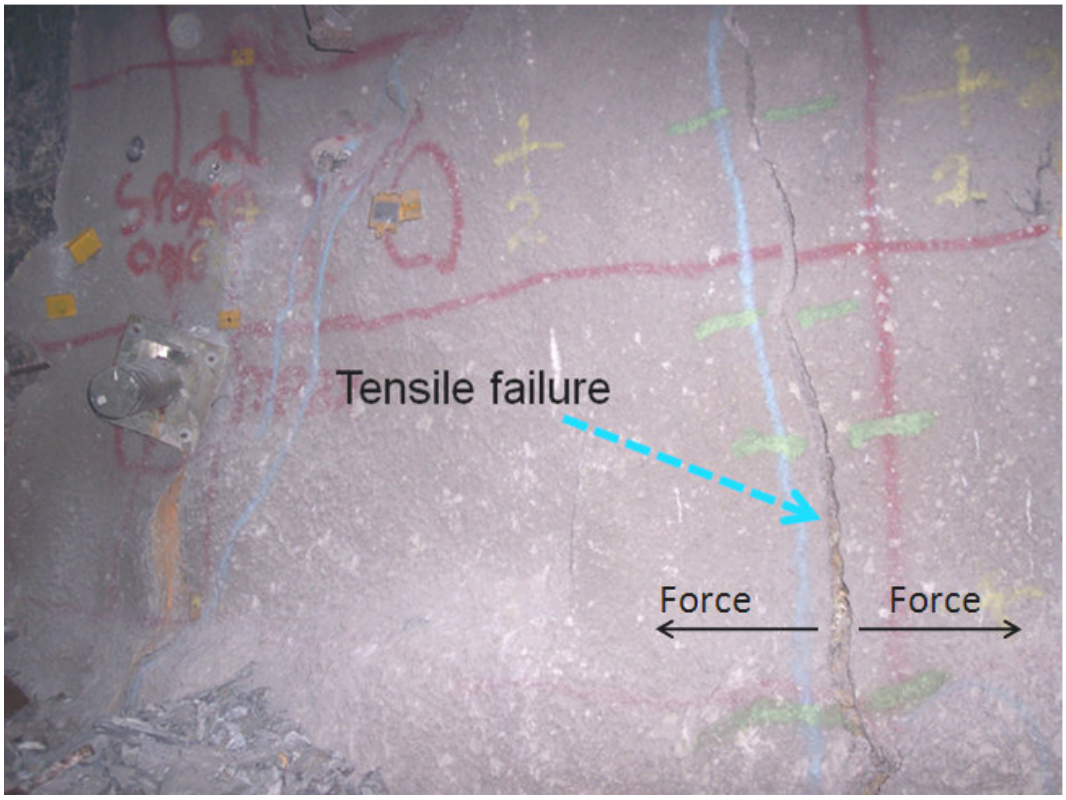


Figure 3.32 Photograph showing tensile failure of shotcrete on Pillar B at South Deep Mine

Tensile failure can be explained by the fact that as the pillar experiences increased mining induced stresses, it will be loaded in compression. As it responds to the mining induced compressive stresses, it will expand

laterally outwards as indicated by the dashed lines in Figure 3.33. The lateral expansion of the pillar stretches the outer skin of the pillar thereby inducing a tensile stress in the shotcrete. The tension induced in the shotcrete may have caused the tensile failure indicated in Figure 3.32. The crack in Figure 3.32 is wider at the bottom because the shotcrete was not applied on the lower part of the pillar but only from about 1.5m above the actual floor.

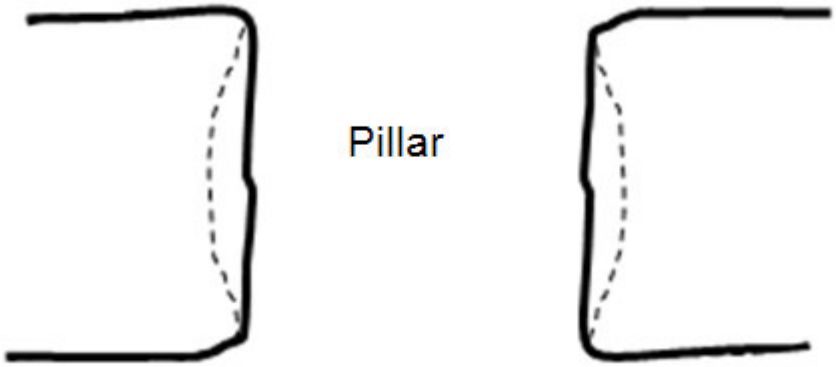


Figure 3.33 Cross-section of a pillar with the solid line showing original pillar profile and dashed line showing the pillar profile after expansion due to increased mining induced stresses.

3.6.2 Adhesion failure

Adhesion failure of the shotcrete-rock interface occurs when the shotcrete separates from the rock as shown in Figure 3.34a and 3.34b. In both of these figures, adhesion failure could have resulted from poor surface preparation of the pillar prior to shotcreting. Alternatively, shrinkage cracking of the shotcrete as the shotcrete cured may have resulted in the weakening of the shotcrete-rock bond strength. Therefore the weak

adhesion strength on the shotcrete-rock interface resulted in shotcrete adhesion failure.



Figure 3.34a Photograph showing adhesion failure of shotcrete on Pillar E at South Deep Mine



Figure 3.34b Photograph showing adhesion failure between Pillar D and Pillar E at South Deep Mine

3.6.3 Punching failure

Punching failure of shotcrete is illustrated in Figure 3.35. Punching failure of the shotcrete is likely have resulted from localised squeezing of some loosened rocks behind the shotcrete due to high stresses as the mining of benches close to the monitoring site took place. In Figure 3.35, small broken rocks behind the shotcrete can be observed showing that the stresses were quite high in that portion of the pillar. However, this failure mode was not common to most pillars.



Figure 3.35 Photograph showing punching failure of shotcrete on Pillar D at South Deep Mine

3.6.4 Shear failure

Shear stresses in the rock can cause shear failure of the shotcrete as illustrated in Figure 3.36. Shown in Figure 3.36 is a sub-vertical crack that was observed on pillar B at South Deep Mine. The shotcrete crack is likely to have been formed when a block of shotcrete labelled A moved out relative to the block labelled B. The shotcrete crack can be seen outcropping between the two blocks of shotcrete labelled A and B. Due to the increase in mining induced stresses, the pillar may have deformed resulting in rock blocks forming. One block of failed rock may have been squeezed out, shearing through the shotcrete layer. The relative movement of the shotcrete blocks A and B has been illustrated in Figure 3.37.



Figure 3.36 Photograph showing shear failure of shotcrete on Pillar B at South Deep Mine

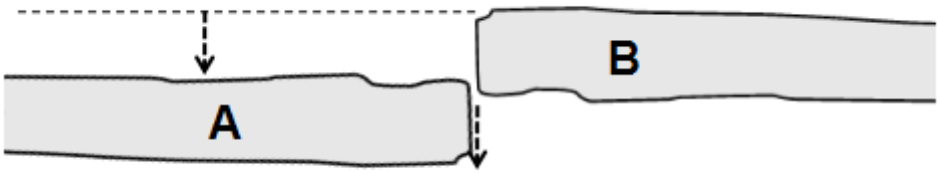


Figure 3.37 Relative displacement of shotcrete block A to shotcrete block B resulting in shotcrete shear failure

3.6.5 Bending failure

Shotcrete failure due to bending is illustrated in Figure 3.38a. Figure 3.38b shows a closer view of the bending failure. The failure of shotcrete in bending may have occurred as the pillar became exposed to increased mining induced stresses. Tensile failure of the shotcrete is likely to have occurred first resulting in the crack marked A in Figure 3.38a. The orientation of the fibres was found to be perpendicular to the crack as illustrated in Figure 3.38b. The tensile failure may have been due to the outward expansion of the pillar. Thereafter, broken rocks seen behind the shotcrete are likely to have been squeezed out causing localised bending of the shotcrete. The crack marked B in Figure 3.38a is likely to have been caused by the localised bending of the shotcrete as the broken rocks were squeezed out due to increasing mining induced stresses in the pillar. The mining induced stresses increased due to the mining of benches close to the monitoring site.

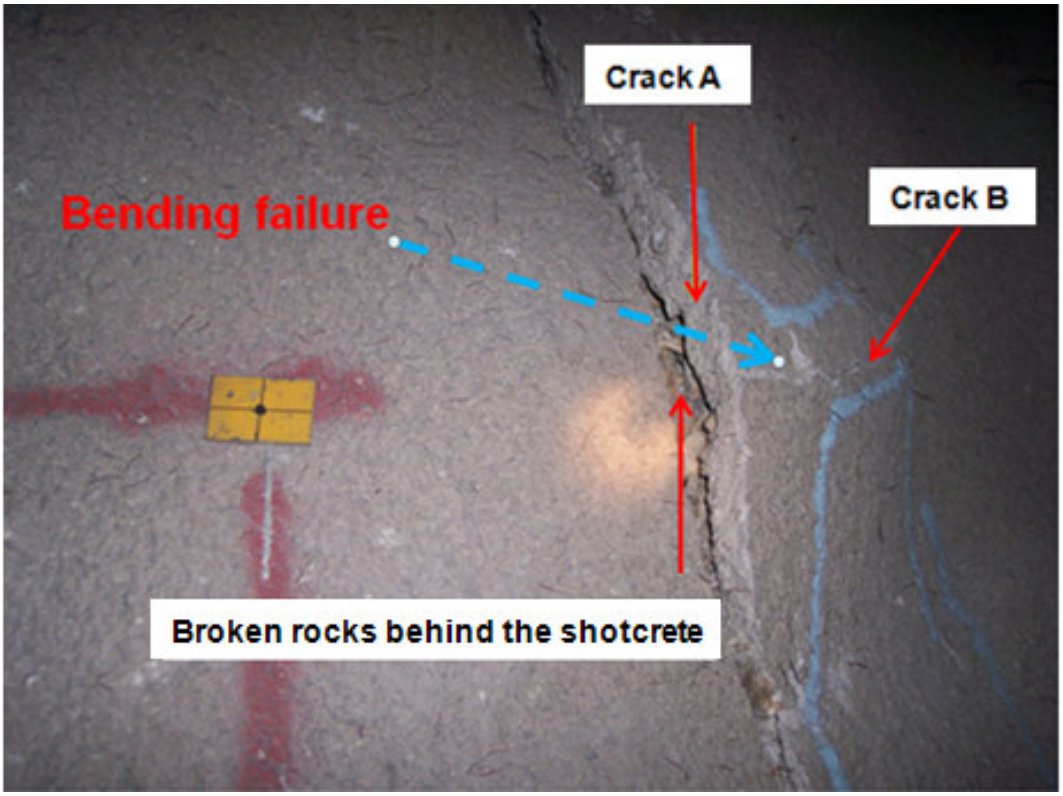


Figure 3.38a Photograph showing bending failure of shotcrete on Pillar B at South Deep Mine

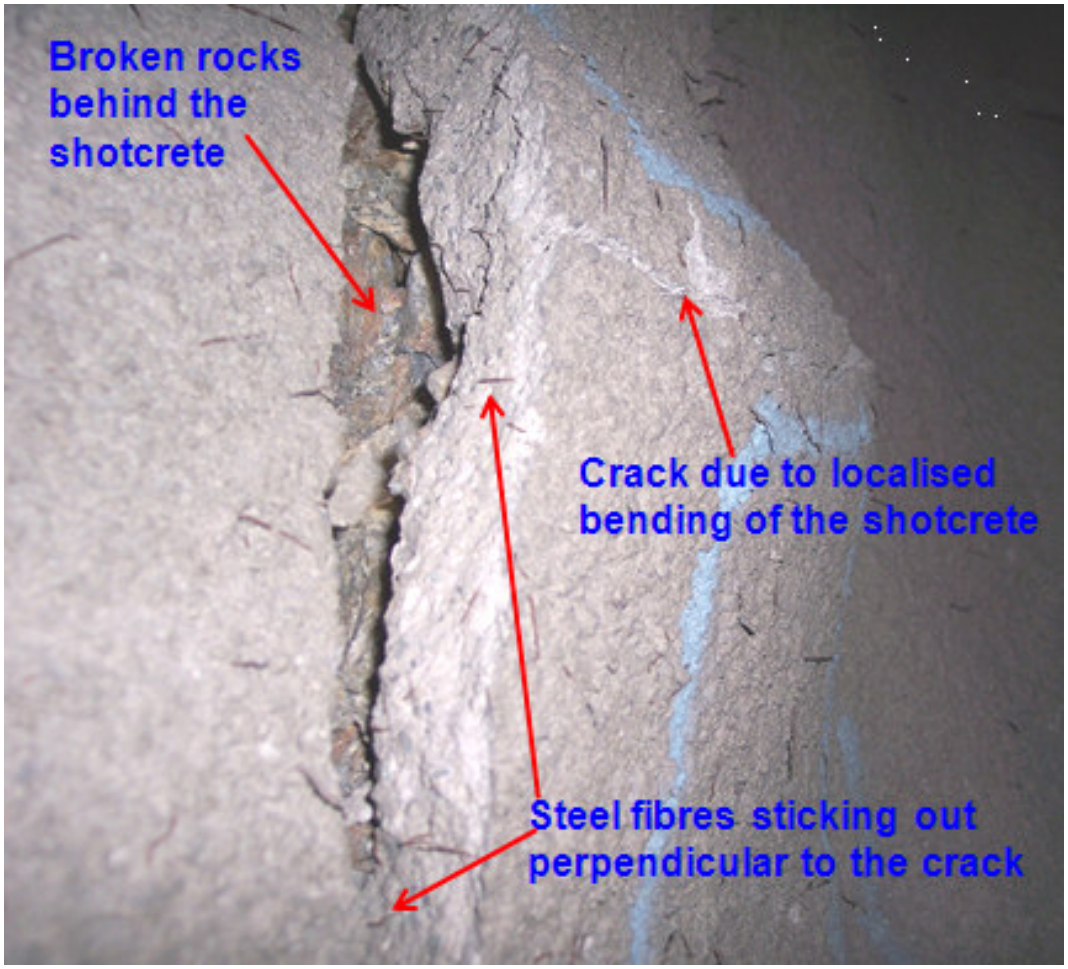


Figure 3.38b Photograph showing bending failure of shotcrete on Pillar B at South Deep Mine

3.7 Conclusion

Monitoring of the shotcreted pillars and tunnels have enhanced the understanding of the behaviour of shotcrete in situ as the pillars and tunnels deformed due to mining induced stresses. The pillars at South Deep Mine experienced the greatest mining induced stresses after the mining of benches surrounding the monitoring site commenced. Various modes of shotcrete failure were identified and possible causes for the failure were discussed. However, the challenge remaining is that the deformation of pillars is a slow process and therefore the actual

mechanism of shotcrete failure may be different from the observational conclusions. However, the monitoring exercise provided a step in the learning curve regarding the in situ behaviour of shotcrete. The next chapter describes the laboratory tests carried out to determine the influence of fibres on sprayed shotcrete as it supports the rock in mining excavations.

CHAPTER 4

LABORATORY TESTS

4.1 Introduction

Chapter 3 has provided in situ monitoring results using various in situ monitoring instruments. The previous chapter has also enabled the identification of shotcrete failure mechanisms as the pillars and tunnels at South Deep Mine site responded to mining induced stresses. The monitoring exercise has provided invaluable information in identifying the most likely failure modes of sprayed shotcrete in situ. This chapter presents laboratory tests carried out to improve the understanding of shotcrete behaviour due to fibre reinforcement. The laboratory testing of sprayed shotcrete samples was done using the EFNARC standards and the ASTM standards for panels and beams tested for their 28^{th} day strength. The chapter indicates the objectives of performing the laboratory tests, test suitability and the test programme followed. A review of the laboratory test methods was carried out. Results have been presented graphically showing load deflection, energy absorption, toughness, peak load, and residual strength trends. Also presented are the results for UCS and fibre content analysis on cores drilled from surface sprayed EFNARC panels.

4.2 Objectives of laboratory testing

Shotcrete laboratory tests were done to achieve the following objectives:

- To improve the understanding of the support capacity and mechanisms of support by fibre reinforced shotcrete (FRS).
- To determine the effect of fibre addition on fibre reinforced shotcrete performance.

4.3 Test suitability

The suitability of a test can be related to a number of issues (Bernard, 1999):

- A post crack test must produce results that are structurally relevant to the intended application for the material. Relevance here should relate to the shotcrete when it is sprayed underground.
- A toughness test must be based on specimens that are representative of the shotcrete used in the finished structure. This will enable correct evaluation of results for similar sprayed shotcrete underground.
- Results obtained from the test must be a reliable indication of the material performance. This entails following the test procedures as well as ensuring that all the specimens for a given test undergo similar conditions up to the testing stage.
- A test must be economical. Economy is determined by cost of procedure, production, transportation and reliability.

4.4 Test programme

The sprayed samples consisted of 40MPa shotcrete obtained from Concrete Lining Products (CLP).

Sprayed samples included the following batches:

- Eight batches using polypropylene fibre with fibre densities of 1kg/m^3 up to 8kg/m^3 and
- Three batches using steel fibre having fibre densities of 40kg/m^3, 55 kg/m^3 and 70kg/m^3.

Table 4.1 shows the spray set up per fibre density for the samples sprayed. A total of 220 samples were tested from the eight batches of polypropylene fibre reinforced shotcrete specimens and from the three batches of steel fibre shotcrete specimens. All specimens were sprayed and tested for 28 day strength.

Table 4.1 Test programme per fibre density batch

INDEX	**DIMENSIONS (mm)**				**Number of panels**	**Number of samples available**	**Number of samples tested**
	Length	**Width**	**Depth**	**Diameter**			
EFNARC Panels	600	600	100		4	4	4
*EFNARC Beams	600	125	75			4	3
RDPs			75	800	4	4	4
*ASTM Beams	450	100	100			4	3
*UCS Cores	100			100		3	3
*Fibre density cores	100			100		3	3
					Total	22	20

*Beams, Uniaxial Compressive Strength (UCS) cores and fibre density cores were cut or drilled out of the surface sprayed EFNARC Panels.

4.5 Fibre specifications

Steel fibres and polypropylene fibres were used in the tests.

4.5.1 Steel Fibres

The steel fibres used were hook end type as shown in the diagram in Figure 4.1. Table 4.2 shows the steel fibre dimensions and tensile strength.



Figure 4.1 Metalloy steel fibre dimensions

Where:
d: diameter in mm
L: fibre length in mm
l: the hook range in mm
h: the hook depth in mm

Table 4.2 Steel fibre specifications

Fibre type	D (mm)	L (mm)	l (mm)	H (mm)	σ_t (MPa)
0530/35	0.5	30	1-4	1-2	1100

4.5.2 Polypropylene fibres

This fibre is extruded from a natural Polypropylene homo polymer and formed into a flat profile with profiled surface in order to anchor it in a

cementitious matrix. The dimensions of the fibre are shown in Table 4.3 and Figure 4.2.

Table 4.3 Polypropylene fibre specifications

Length, L (mm)	Width, w (mm)	Thickness, t (mm)	Elongation at yield (%)	σ_t (MPa)	E (MPa)
50	1.8	0.13	24.4	100	1550

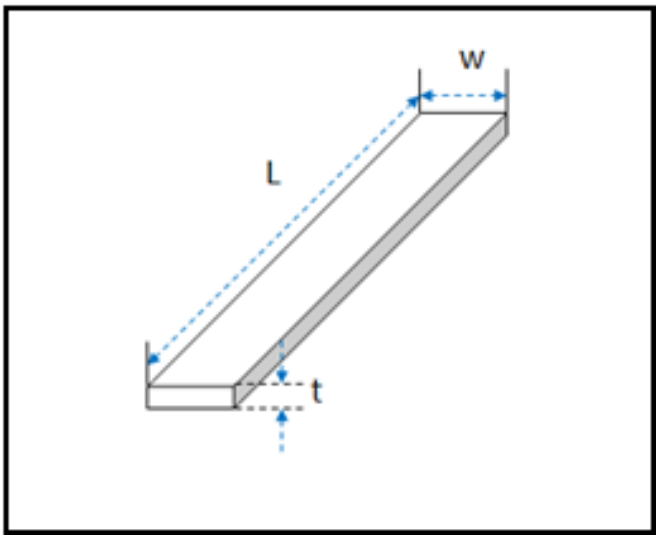


Figure 4.2 Polypropylene fibre dimensions

4.6 Control of consistency

Every attempt was made to produce specimens in a consistent manner using the 40 MPa shotcrete.

All the samples were cured in curing tanks under controlled temperature conditions at 20 +/- 2℃.

All the samples were tested to determine their strength on the 28th day after spraying.

4.7 Determination of shotcrete performance

The standards used for the determination of fibre reinforced shotcrete performance are summarised in Table 4.4.

Table 4.4 Summary of standard test methods for testing shotcrete beams and panels

Specimens	Standard test method
ASTM Beams	ASTM C1018 (1997)
EFNARC Beams	EFNARC Specifications for beams (1996)
EFNARC Panels	EFNARC Specifications for panels (1996)
RDPs	ASTM C 1550 (2005)

4.7.1 ASTM beams

Performance was measured in terms of:

a) Modulus of rupture (R): is defined as the maximum surface stress in a bent beam at the instant of failure (first crack stress) and is given by the following formula according the ASTM C1018 (1997) standard:

$$R = 3 P L / (2 b d^2)$$

Where:

R = modulus of rupture (N/mm^2)

b = average specimen width (mm)

P = peak load (N),

d = average specimen depth (mm) and

L = span length (mm)

(b) Toughness index: is defined as the ratio of the absorbed energy up to a given deflection to the absorbed energy up to first crack deflection. Toughness indices i.e. I_5, I_{10}, I_{20}, I_{30} and I_{50} are calculated as specified in the ASTM C1018 (1997) Standard where:

(i) Toughness index I_5 is the number obtained by dividing the area under the load-deflection curve up to at a deflection of 3.0 times the first-crack deflection by the area up to first crack.

(ii) Toughness index I_{10} is the number obtained by dividing the area under the load-deflection curve up to a deflection of 5.5 times the first-crack deflection by the area up to first crack.

(iii) Toughness index I_{20} is the number obtained by dividing the area under the load-deflection curve up to a deflection of 10.5 times the first-crack deflection by the area up to first crack.

(iv) Toughness index I_{30} is the number obtained by dividing the area under

the load-deflection curve up to a deflection of 15.5 times the first-crack deflection by the area up to first crack.

(iv) Toughness index I_{50} is the number obtained by dividing the area under the load-deflection curve up to a deflection of 25.5 times the first-crack deflection by the area up to first crack.

Figure 4.3 shows graphically how the toughness indices are estimated under the ASTM load-deflection curve.

From Figure 4.3, the toughness indices are obtained by doing the following calculations:

I_5 = OACD/OAB,
I_{10} = OACEF/OAB
I_{20} = OACEGH/OAB
I_{30} = OACEGIJ/ OAB
I_{50} = OACEGIKL/OAB

Therefore toughness index is a dimensionless quantity. For the idealised perfectly elasto-plastic material, the toughness indices have the following values:

I_5 = 5, I_{10} = 10, I_{20} = 20 and I_{30} = 30 and I_{50} = 50 (Papworth et al, 1996). However, for steel fibre reinforced shotcrete, Morgan (1988) performed several tests and based on the results obtained, suggested the following ratings shown in Table 4.5.

Table 4.5 Suggested toughness indices (After Morgan, 1988)

Category	**Rating**	**I_{10}**	**I_{30}**
I	Marginal	<4	<12
II	Fair	4	12
III	Good	6	18
IV	Excellent	8	24

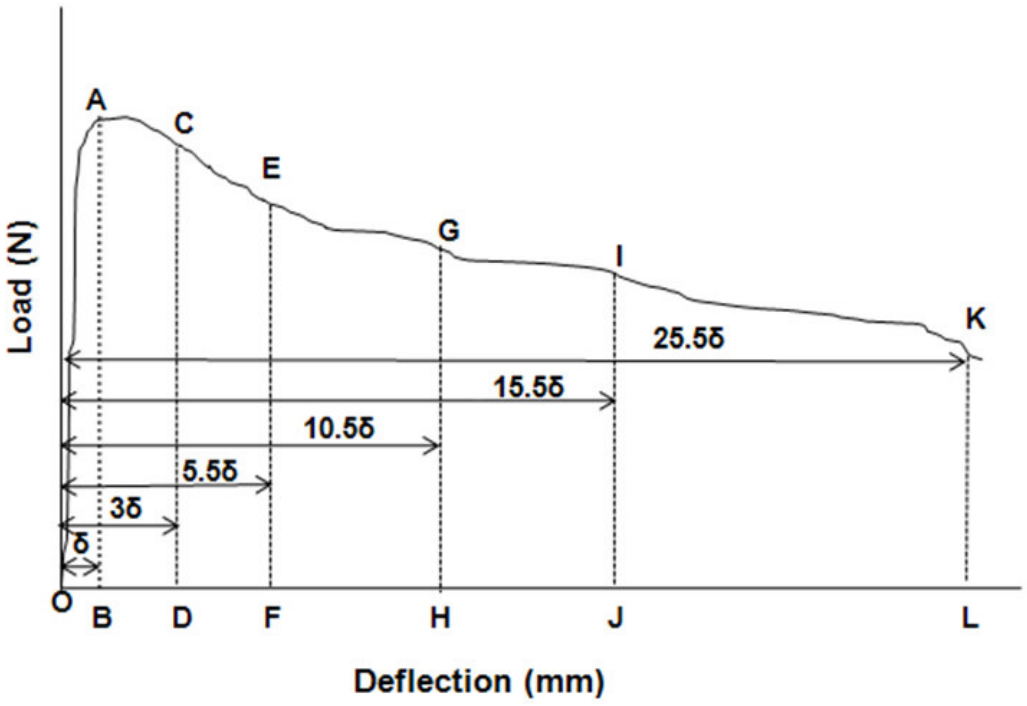


Figure 4.3 Determination of toughness indices (ASTM C1018, 1997)

4.7.2 EFNARC beams

Performance was measured in terms of:

(a) Flexural strength (FS)

Flexural strength is defined as the equivalent maximum elastic tensile stress at the peak load (EFNARC, 1996). Flexural strength for EFNARC beams is calculated as specified in the EFNARC (1996) Standard using the following equation:

$$FS = P_{0.1} \times L / (b\ d^2)$$

Where:

FS = Flexural strength (N/mm^2)

$P_{0.1}$ = peak load (N)

L = span length (mm)

b = actual beam width

d = actual beam depth

(b) Residual strength: The residual flexural strength (RS) was determined as specified in the EFNARC (1996) Standard at displacements of 0.5mm, 1.0mm, 2.0mm and 4.0mm using the equation below:

$$RS = P_x * L / (b\ d^2)$$

Where:

P_x = load at x =0.5; 1.0; 2.0; and 4.0mm respectively.

L = span length (mm)

b = actual beam width

d = actual beam depth

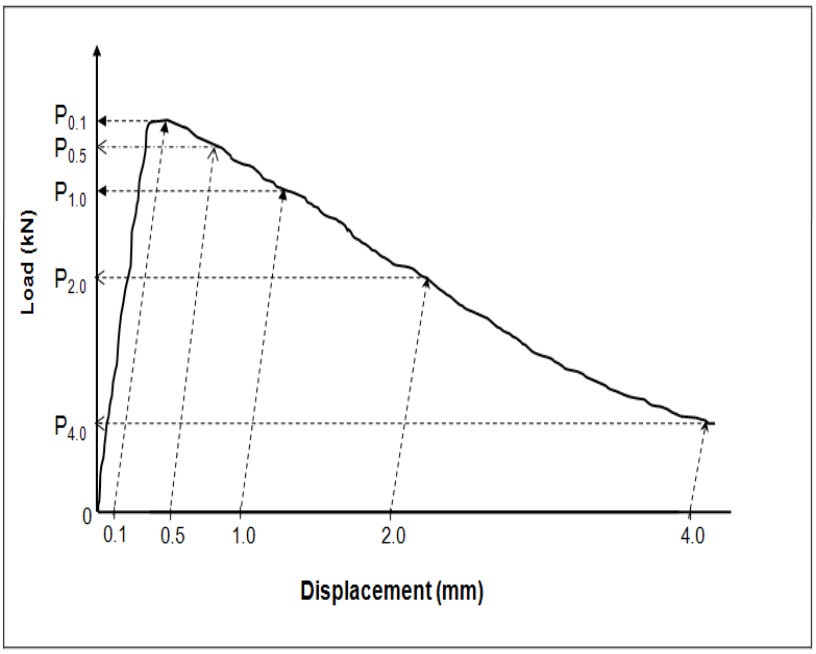


Figure 4.4 P values from the Load-Deflection graph for flexural and residual strengths (EFNARC, 1996)

4.7.3 EFNARC Panels

Performance was measured in terms of:

(a) Peak loads and

(b) Energy absorption

4.7.4 ASTM centrally loaded Round determinate Panels

Performance was measured in terms of:

(a) Peak loads and

(b) Energy absorption

4.7.5 Uniaxial Compressive Strength (UCS) tests

UCS testing cores were drilled out of EFNARC Panels. The cores had a diameter and a length of 100mm, giving a diameter to length ratio of 1.

4.7.6 Spraying losses of steel fibres

Fibre losses were only determined for steel fibres as the laboratory used did not have the capacity to determine the polypropylene fibre losses for polypropylene fibre reinforced shotcrete specimens.

4.8 Presentation and discussion of results

The results obtained from all the tests have been presented graphically in the form of load-deflection and energy absorption-deflection curves as shown in Appendix A. Also, the results for the performance parameters of

beams and panels have been summarised and tabulated in Appendix B. The following sub-sections present a discussion of the test results for all the fibre reinforced shotcrete tests for beams and panels.

4.8.1 ASTM beams modulus of rupture

The modulus of rupture results in Figure 4.5 and Figure 4.6 show that fibre incorporation has little effect on the modulus of rupture of the ASTM beams. The modulus of rupture for most of the polypropylene fibre reinforced shotcrete and steel fibre reinforced shotcrete ranges between 7 and 10MPa. However, the 2kg/m^3 polypropylene fibre reinforced shotcrete had a modulus of rupture less than 5MPa. This anomalous lower value could be a factor of cracking in the beam before testing. The 55kg/m^3 for the steel fibre reinforced shotcrete specimens show a lower value compared to the 40Kg/m^3 with a lower density. The lower modulus of rupture for the 55kg/m^3 may be attributed to pump problems experienced during the spraying of the 55kg/m^3 fibre reinforced shotcrete specimens.

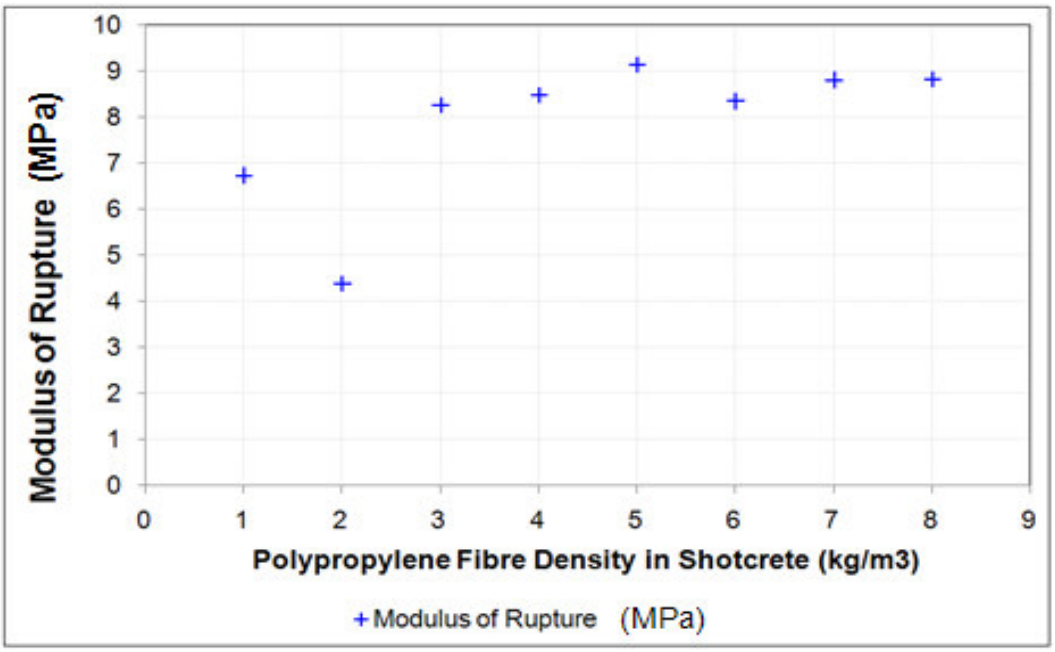


Figure 4.5 Modulus of rupture for the polypropylene fibre reinforced shotcrete ASTM beams

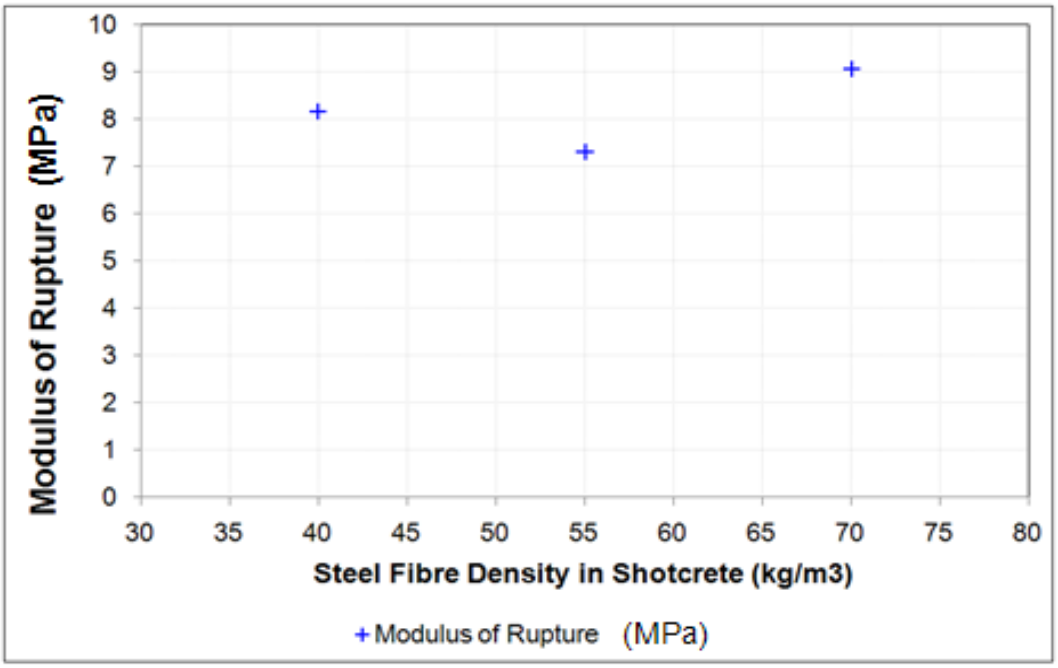


Figure 4.6 Modulus of rupture for the steel fibre reinforced ASTM shotcrete beams

4.8.2 ASTM beams toughness indices

The general trend of the toughness indices shown in Figure 4.7 and Figure 4.8 is that the toughness index value increases as the deflection increases from 3δ to 25.5δ (δ = deflection at first crack) per fibre density, for both steel and polypropylene fibre reinforced shotcrete ASTM beams. However, Figure 4.7 and Figure 4.8 show that I_5 and I_{10} toughness values do not increase significantly as the fibre density in shotcrete increases. Probably, this is because I_5 and I_{10} values are calculated at very low deflections when the fibres in the shotcrete are less effective. Also, this could be a result of the scatter in the load-deflection results (shown in Appendix A), reflecting lack of repeatability of the test method in giving consistent results; or the challenge in determining the first crack, which greatly influences the toughness value calculation when using the ASTM standard test method.

I_{20} to I_{50} toughness values for steel fibre reinforced shotcrete specimens are higher than those of polypropylene fibre reinforced shotcrete specimens. The higher toughness values for the steel fibre reinforced shotcrete specimens is likely to be due to the higher tensile strength of steel fibres which is about 1100MPa compared to the 100MPa of polypropylene fibres, as indicated in Table 4.2 and Table 4.3 in section 4.52 and section 4.53 respectively.

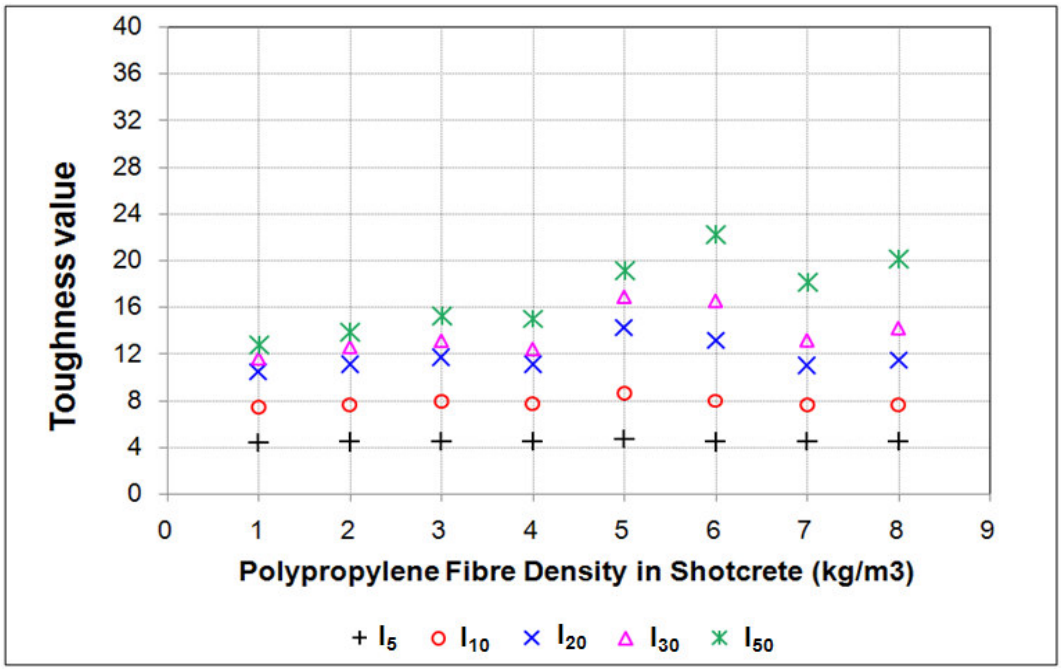


Figure 4.7 Toughness indices for the polypropylene fibre reinforced shotcrete ASTM beams

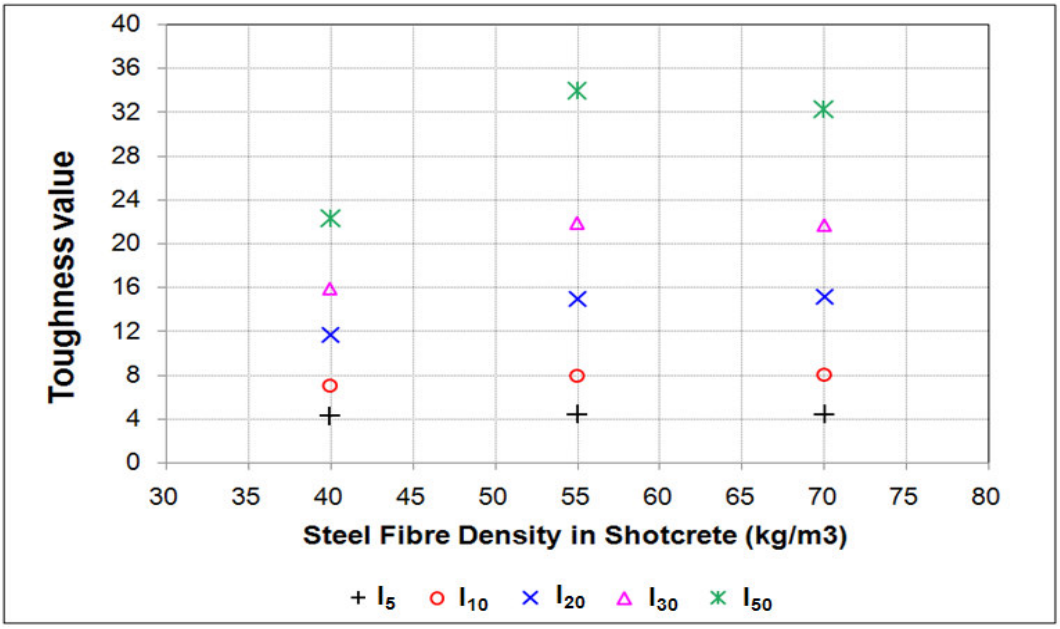


Figure 4.8 Toughness indices for the steel fibre reinforced shotcrete ASTM beams

4.8.3 EFNARC beams flexural strength

Flexural strength gives an indication of the resistance to bending. The flexural strength results obtained are shown in Figure 4.9 and Figure 4.10. The polypropylene fibre reinforced shotcrete specimens with densities ranging from 1kg/m^3 to 5kg/m^3 have been omitted from the discussion since they were mistakenly tested on a span length of 300mm instead of the standard 450mm for the EFNARC beams. Only the 6kg/m^3 to 8kg/m^3 polypropylene fibre reinforced shotcrete specimens and the steel fibre reinforced shotcrete specimens, which were tested on the correct span length of 450mm, have been incorporated in this discussion.

Figure 4.9 and Figure 4.10 show that steel fibre reinforced shotcrete has slightly higher flexural strength than polypropylene fibre reinforced shotcrete. The higher flexural strength for the steel fibre reinforced shotcrete may be attributed to the superior tensile strength of steel fibres compared to that of polypropylene fibres, as shown in Table 4.2 and Table 4.3. Also, steel fibres have a much higher modulus of elasticity of about 200GPa compared to the 1.6GPa of the polypropylene fibres used in the experiment. However, the density of fibres, whether steel or polypropylene, has a negligible effect on the shotcrete flexural strength. This is due to the fact that the flexural strength is estimated using the peak loads at very low deflections when the shotcrete matrix itself has more influence than the fibres incorporated in the shotcrete. The fibres become more “engaged” after the shotcrete experiences the first crack.

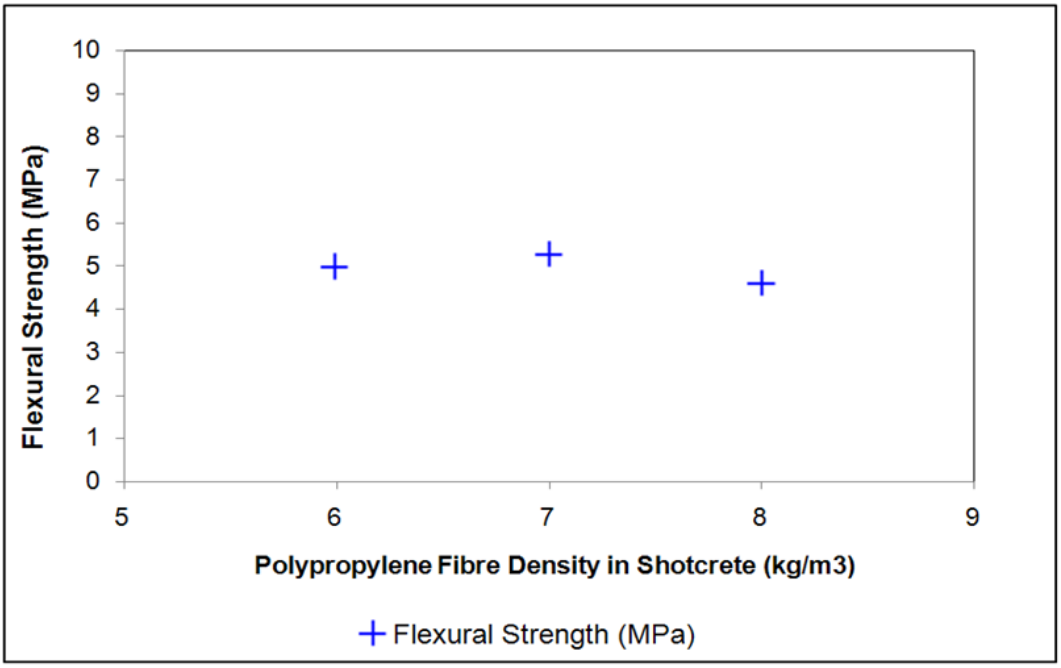


Figure 4.9 Flexural strength for the polypropylene fibre reinforced EFNARC beams

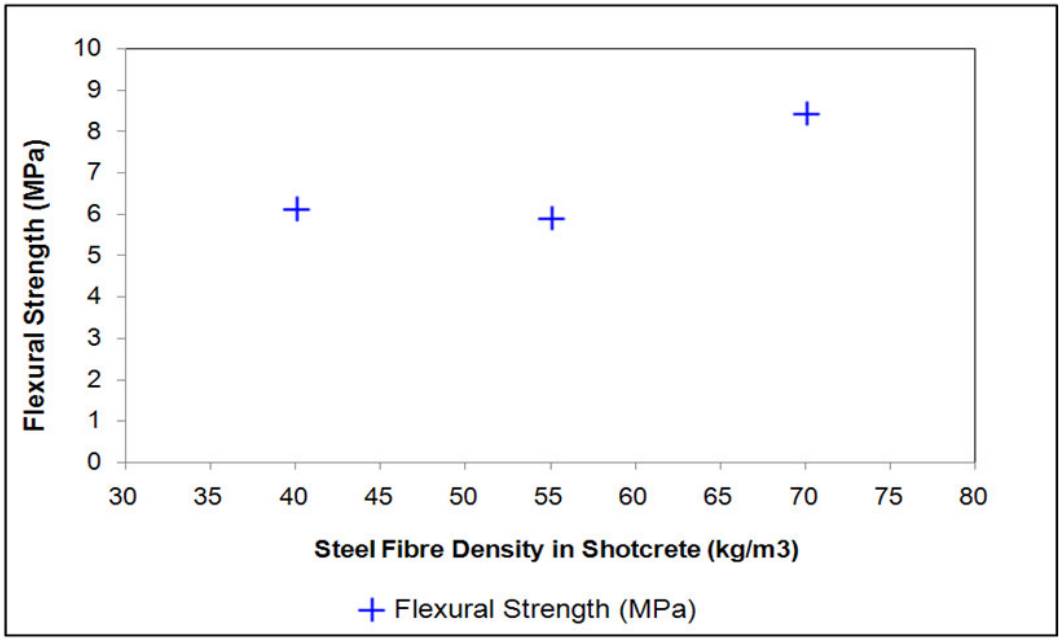


Figure 4.10 Flexural strength for the steel fibre reinforced shotcrete EFNARC beams

4.8.4 EFNARC Beams residual strength

The residual strength gives an indication of the post peak performance of the fibre reinforced shotcrete. Figure 4.11 and Figure 4.12 show the residual strength results obtained for both steel and polypropylene fibre reinforced shotcrete EFNARC beams. The polypropylene fibre reinforced shotcrete beams which were tested on a shorter span length of 300mm rather than the standard 450mm have been omitted from this discussion for consistency purposes when using the standard test method.

Figure 4.11 and Figure 4.12 show that the steel fibre reinforced beams have a higher residual strength than the polypropylene fibre reinforced beams. The higher residual strength of steel fibre reinforced shotcrete beams may also be attributed to the higher tensile strength of steel fibres, which is about 1100MPa compared to that of polypropylene fibres of about 100MPa.

The polypropylene fibre reinforced shotcrete beams in Figure 4.11 display effectively a constant residual strength as the deflection increases from 0.5mm to 4.0mm per fibre density. This may be attributed to their ability to elongate about 24%, which result in an almost constant load capacity as deflection increases (Appendix A).

The residual strengths for steel fibre reinforced beams shown in Figure 4.12 display a much clearer linear trend which shows, as could be expected, an increase in residual strength as the fibre density increases. The magnitude of the residual strength decreases as the deflection increases from 0.5mm to 4.0mm per fibre density. Probably, it was due to the steel fibres yielding, pulling out of the shotcrete, or breaking as the deflection increases thereby causing the beam capacity to decrease.

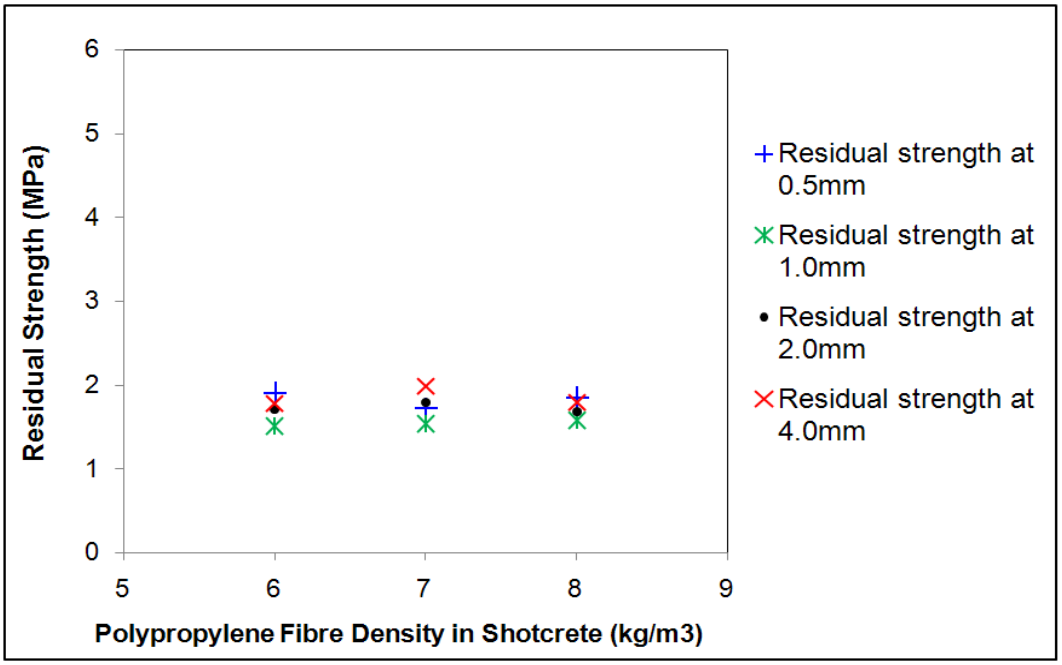


Figure 4.11 Residual strength for the polypropylene fibre reinforced shotcrete EFNARC beams

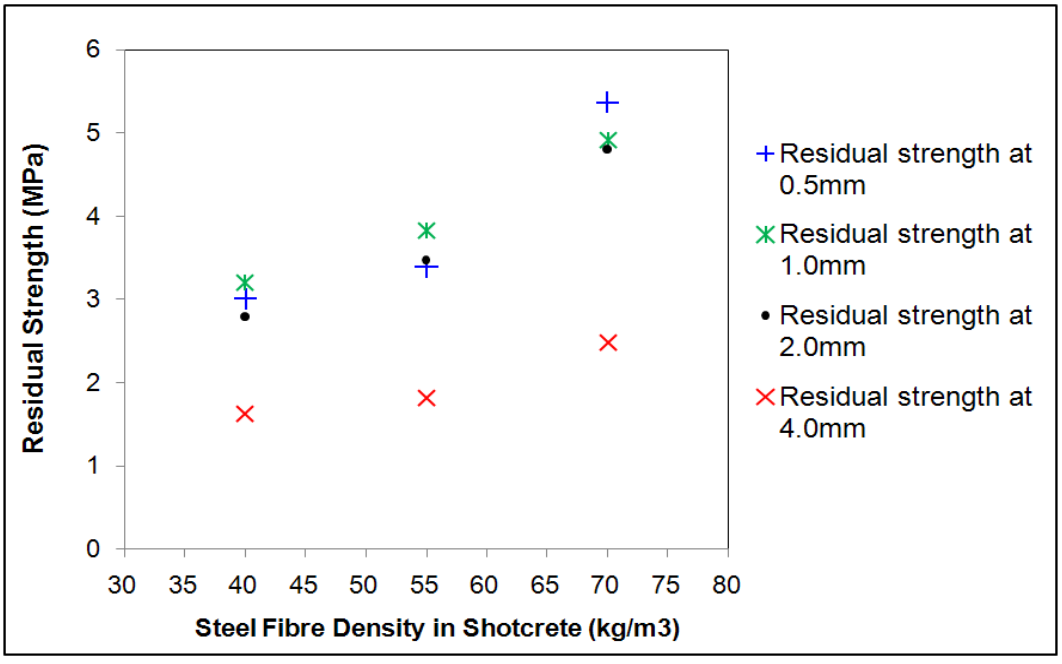


Figure 4.12 Residual strength for the steel fibre reinforced shotcrete EFNARC beams

4.8.5 EFNARC panels peak load results

The EFNARC panels peak load capacity results are shown in Figure 4.13 and Figure 4.14. The polypropylene fibre reinforced shotcrete panels peak loads range from 35 kN to 71 kN whereas those of steel fibre reinforced shotcrete panels range from 75 kN to about 100 kN. The higher tensile strength and much greater modulus of elasticity of the steel fibres compared with the polypropylene fibres again probably contributed to the higher peak strength of the steel fibre reinforced shotcrete panels.

The irregularity in the shape of the graph in Figure 4.13 may be attributed to a number of reasons. Firstly, the testing laboratory did not have the capacity to measure the true fibre content of the polypropylene specimens. Figure 4.13 reflects the fibre densities specified in the mix rather than the measured. It is possible that during the spraying process, the percentage of fibre losses may have been inconsistent resulting in lower actual fibre densities in some specimens than in others. Further explanations may include differences in panel thicknesses, as it is impossible to produce perfect standard sizes when cutting the specimens; hair line cracks formed during curing that were noticed in some of the specimens may have also contributed to the irregularity in the trend in Figure 4.13; lastly, some of the specimens could not be placed perfectly flat on the testing machine stand due to the slightly irregular shape produced from the cutting process.

Although there are only three results, the steel fibre reinforced shotcrete EFNARC panels in Figure 4.14 show the expected linear trend as the peak load capacity increases with the increase in fibre density.

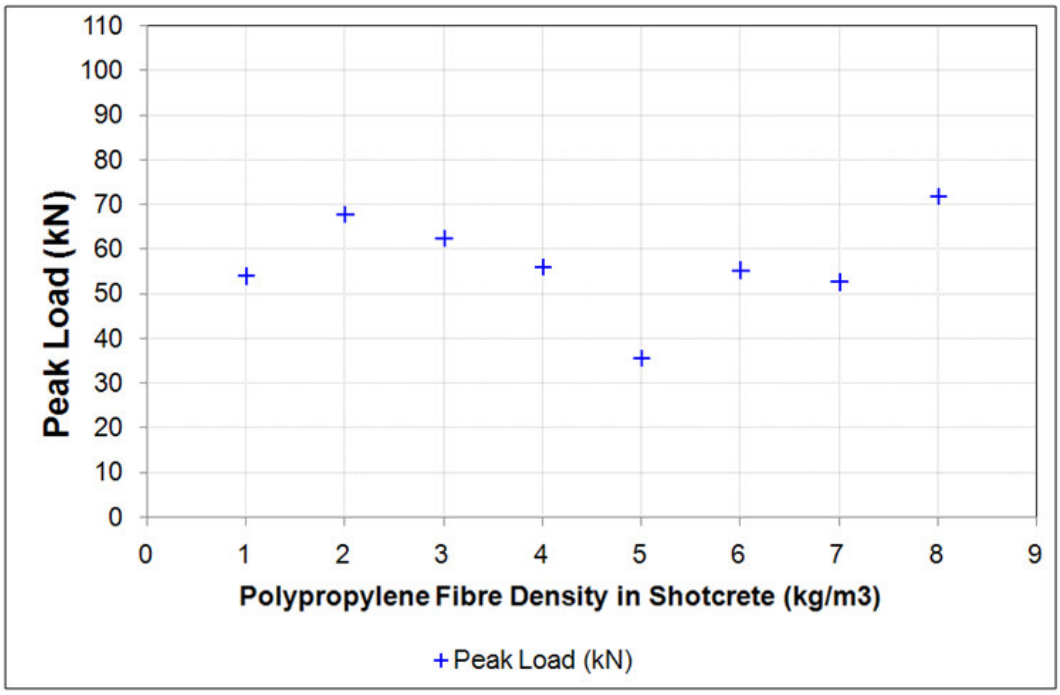


Figure 4.13 Peak loads for the polypropylene fibre reinforced shotcrete EFNARC panels

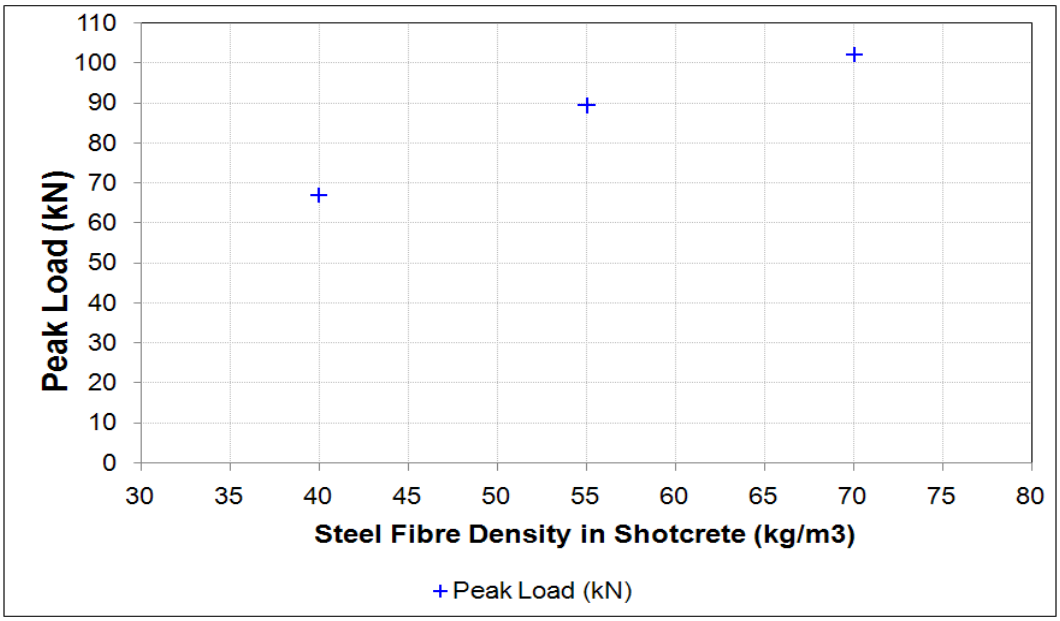


Figure 4.14 Peak loads for the steel fibre reinforced shotcrete EFNARC panels

4.8.6 EFNARC panels energy absorption

The energy absorption results for the EFNARC panels are shown in Figure 4.15 for the polypropylene fibre reinforced shotcrete panels and in Figure 4.16 for the steel fibre reinforced shotcrete panels. Generally, both steel and polypropylene fibre reinforced shotcrete specimens show a linear variation as the energy absorption increases due to an increase in fibre content. Therefore the more the fibres added to the shotcrete, the greater the energy absorption capability of the fibre reinforced shotcrete.

Energy absorption results in Figure 4.15 show that the 5kg/m^3 density and the 7kg/m^3 show some irregularity in the shape of the graph. As explained above, no actual fibre density measurements were done for the polypropylene fibre reinforced panels, and inconsistent fibre contents may have been a cause of the irregularity. Also, the shapes of the load deflection graphs for the 7kg/m^3 polypropylene fibre reinforced shotcrete specimens in Appendix A display clearer single peak loads except for only one of the specimens compared to other specimens. The flatness of the 7kg/m^3 panels is likely to have influenced the shape of the load deflection graphs and the energy absorption graphs in Appendix A, relative to the other specimens.

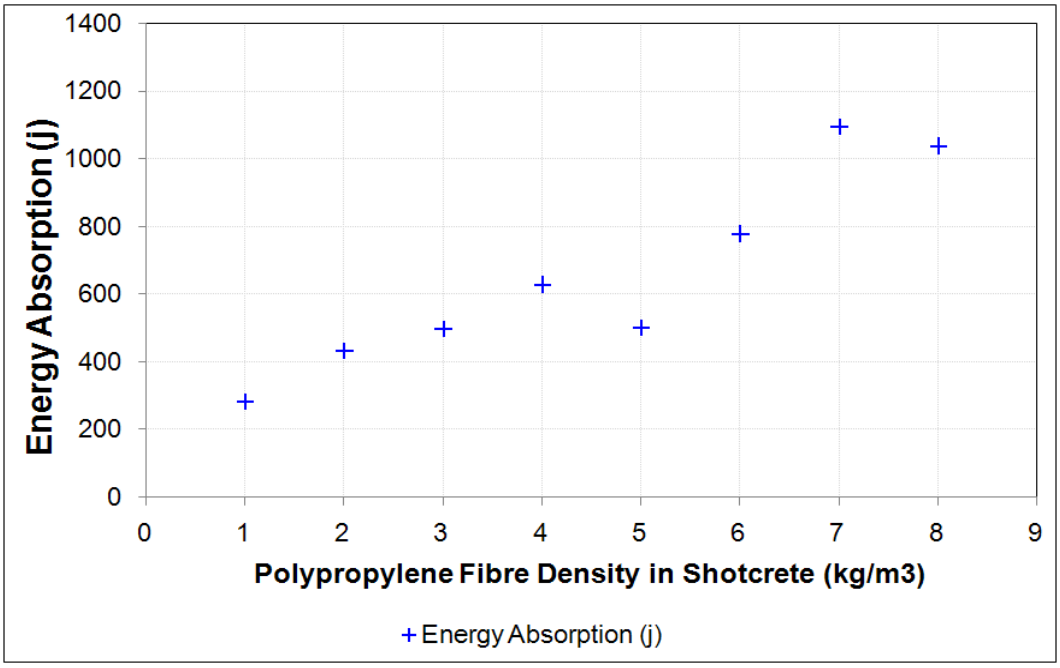


Figure 4.15 Energy absorption for the polypropylene fibre reinforced shotcrete EFNARC panels

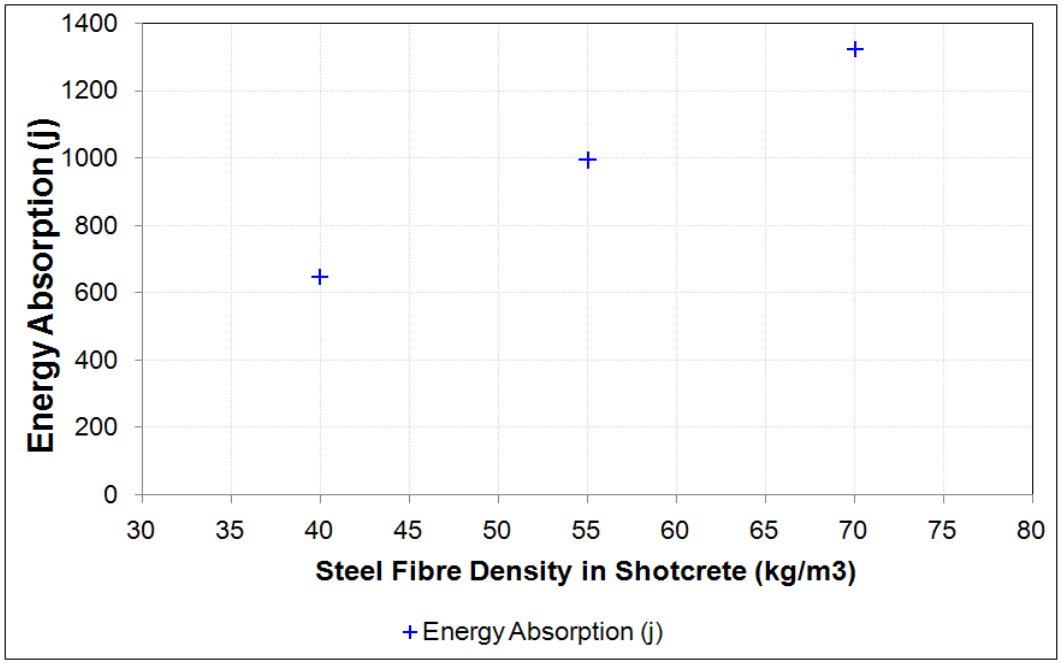


Figure 4.16 Energy absorption for the steel fibre reinforced shotcrete EFNARC panels

4.8.7 ASTM Round determinate panels peak loads

The peak load results for the Round Determinate Panels (RDPs) are shown in Figure 4.17 and Figure 4.18. Figure 4.17, showing the polypropylene fibre reinforced shotcrete panels peak loads, displays a downward trend in the peak loads graph as the fibre content increases from 1 kg/m^3 to 8 kg/m^3. The downward trend may be attributed to the irregularities in the shapes and measured thicknesses of the panels causing a reduction in the peak load capacity as the specified fibre density in the shotcrete mix increases. The expected trend would have been a flat graph since the peak load is reached at low deflections when the fibres are not "engaged". Since the fibres are not engaged at low deflections, the peak load capacity of the shotcrete is largely dependent on the shotcrete matrix strength as mentioned by Stacey (2004).

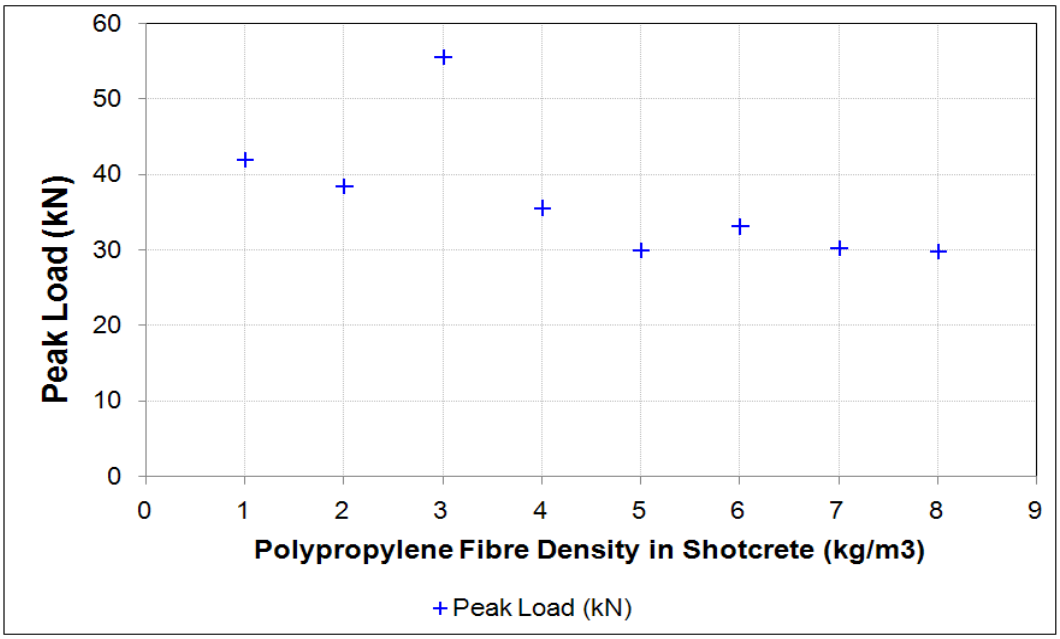


Figure 4.17 Peak loads for the polypropylene fibre reinforced shotcrete round determinate panels

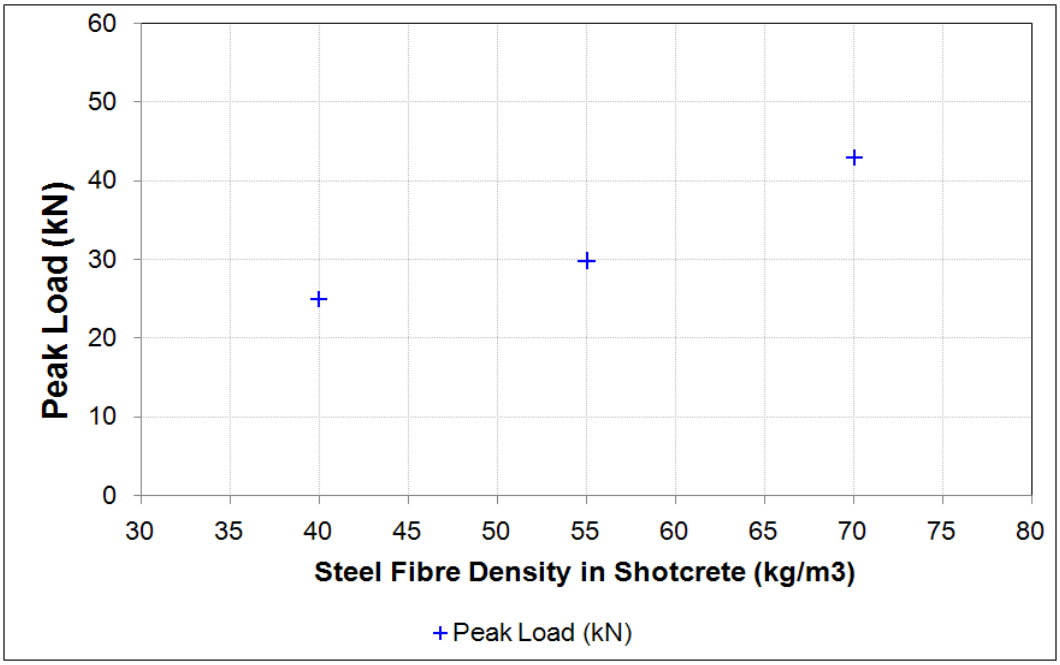


Figure 4.18 Peak loads for the steel fibre reinforced shotcrete round determinate panels

4.8.8 ASTM Round Determinate Panels (RDPs) Energy Absorption

The average energy absorption results for the RDPs are shown in Figure 4.19 and Figure 4.20 for the polypropylene and the steel fibre reinforced shotcrete panels. Results for both the steel and polypropylene round determinate shotcrete panels show a positive linear trend. Since energy absorption has an effect on the residual carrying capacity of shotcrete, it has been found worthwhile to present the average RDP load-deflection results for both the polypropylene and steel fibre reinforced shotcrete specimens as shown in Figure 4.21 and Figure 4.22. Of major interest is the shape of the graphs post the peak load.

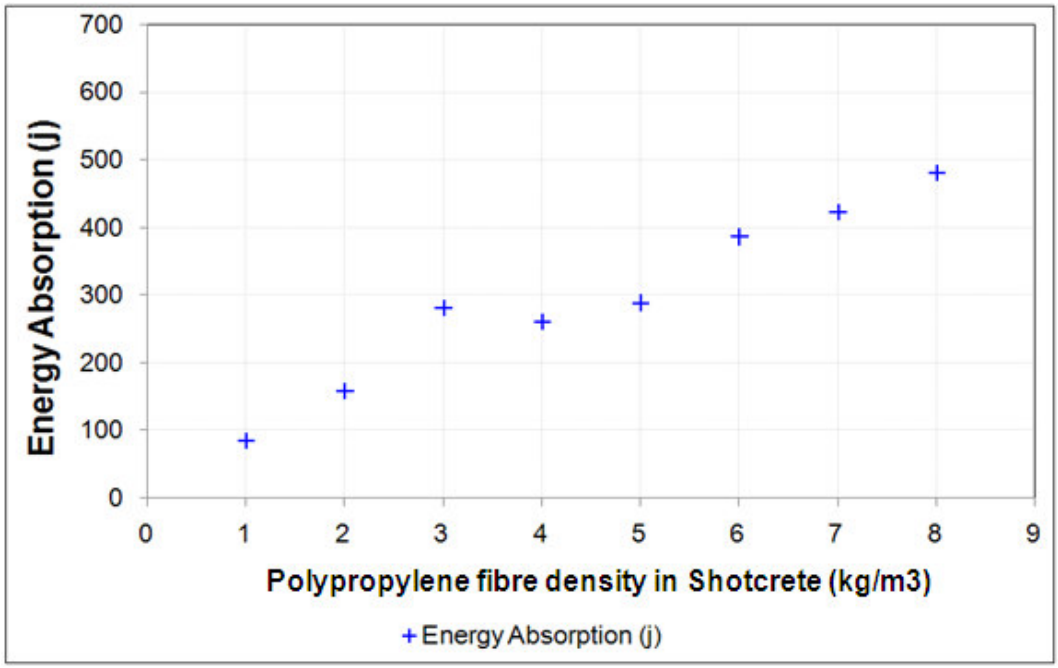


Figure 4.19 Energy absorption for the polypropylene fibre reinforced round determinate panels

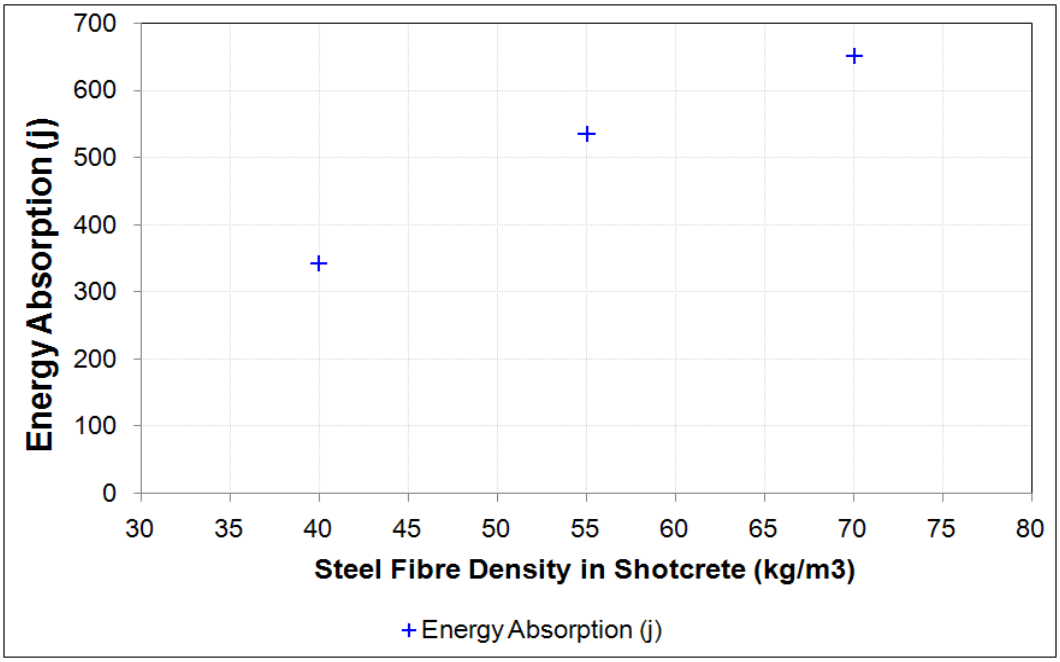


Figure 4.20 Energy absorption results for the steel fibre reinforced round determinate panels

Figure 4.21 shows that after the peak load, there is a sharp drop in the load-deflection graphs to the point when crack arrest by the polypropylene fibres comes into effect. After the sharp drop, the load deflection graphs display an almost flat trend in the residual load capacities which drop slightly as deflection increases to 40mm deflection. The ability of polypropylene fibres to elongate to about 24% their original length may have enabled them to maintain this residual load capacity with increase in deflection.

The steel fibre reinforced RDP shotcrete panels in Figure 4.22 display a gradual decrease in the load capacity, after reaching the peak load as the deflection increases. The trend displayed by the steel fibre reinforced shotcrete RDPs could be attributed to the tensile properties of the steel fibres in the shotcrete which influence the load-deflection behaviour in the shotcrete.

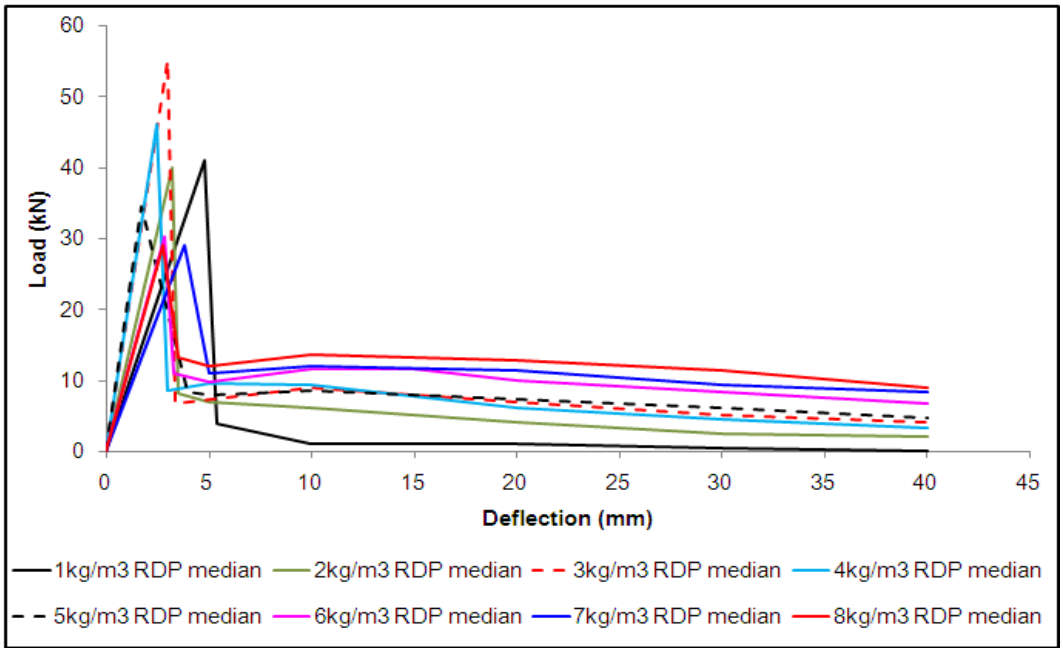


Figure 4.21 Load-deflection results for the polypropylene fibre reinforced shotcrete round determinate shotcrete panels

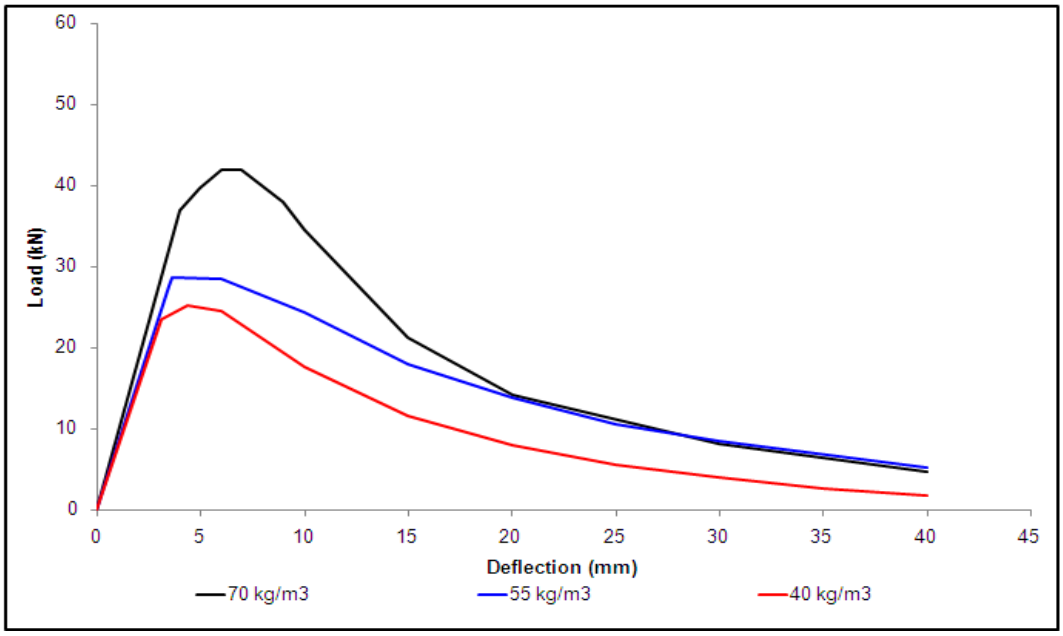


Figure 4.22 Load-deflection results for the steel fibre reinforced shotcrete round determinate shotcrete panels

4.8.9 Uniaxial compressive strength

The uniaxial compressive strength (UCS) test results are presented in Figure 4.23 and Figure 4.24 for the polypropylene and steel fibre reinforced shotcrete specimens respectively.

Figure 4.23 shows that the UCS of the steel fibre reinforced shotcrete specimens ranges between 50 MPa and 65 MPa. From Figure 4.23, the density of steel fibre has a negligible effect on the UCS of shotcrete. During the spraying of 55 kg/m^3 steel fibre density shotcrete, clogging problems were encountered due to pump failure. These clogging problems encountered appear to have slightly affected the UCS of one of the 55kg/m^3 steel fibre density shotcrete specimens.

From Figure 4.24, the UCS results for polypropylene fibre reinforced shotcrete specimens range between 40 MPa and 60 MPa. The increase in

polypropylene fibre density has a negligible effect on UCS as displayed in Figure 4.24.

The UCS results show that steel fibre reinforced shotcrete specimens have a slightly higher UCS compared to the polypropylene fibre reinforced shotcrete specimens.

These UCS results may not be comparable to the UCS results obtained from field tests shown in Table 3.3 and Table 3.4 in section 3.53, because the latter were tested at different ages – a year after curing for the field specimens, while the specimens in this chapter were tested on the 28th day after spraying. The age factor may play a major role in the performance capacity of the shotcrete specimens.

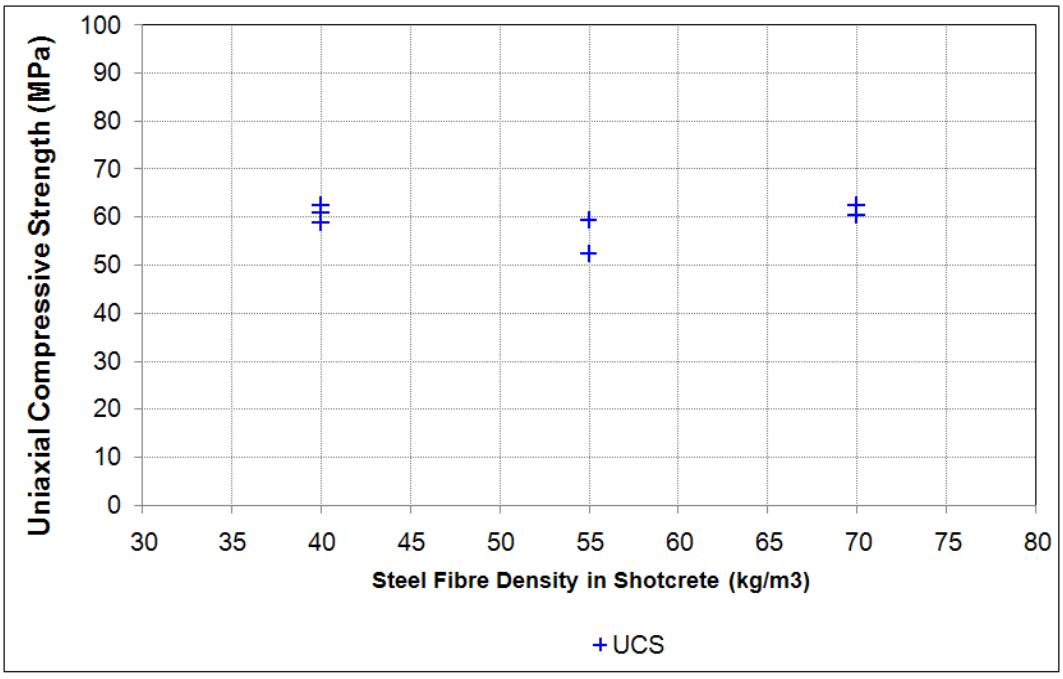


Figure 4.23 Uniaxial compressive strength test results for the steel fibre reinforced shotcrete cores

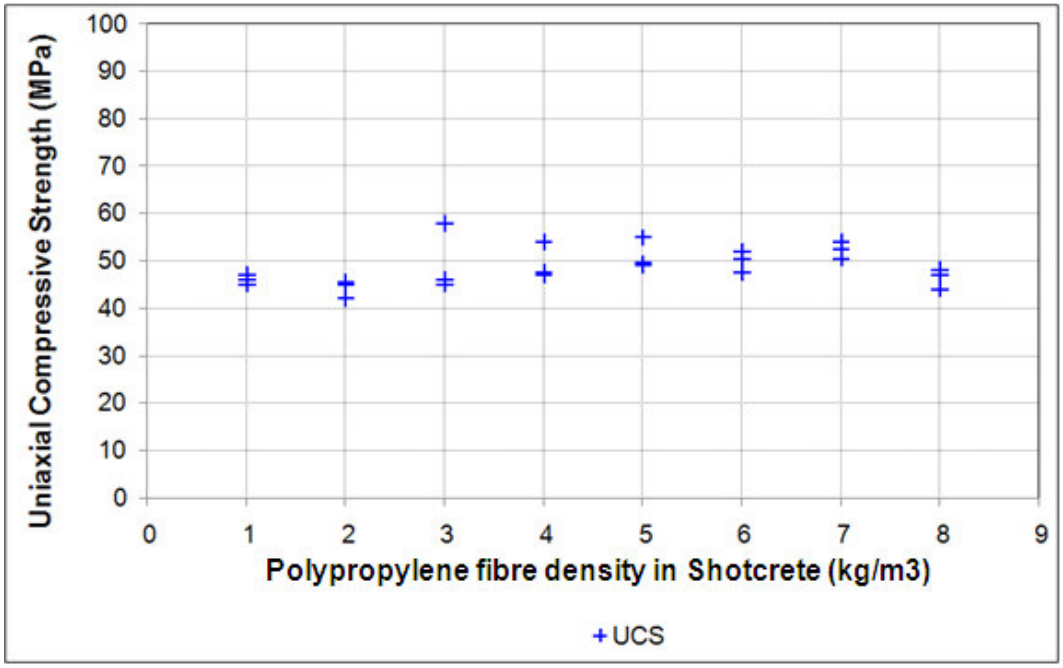


Figure 4.24 Uniaxial compressive strength test results for the polypropylene fibre reinforced shotcrete cores

4.8.10 Steel fibre spraying losses

The determination of the actual density of fibres in the final shotcrete product was carried out to give an estimate of the fibre rebound losses due to spraying. Due to the limitation in fibre determination by the testing laboratory used in the laboratory tests, only the steel fibre densities were determined for the final fibre reinforced shotcrete product and the results are shown in Figure 4.25. The measured results showed variation between 15 % and 30 % fibre rebound losses for the 40kg/m^3 and the 70kg/m^3 shotcrete specimens (see Figure 4.25). The average fibre rebound loss for the 40kg/m^3 and the 70kg/m^3 shotcrete specimens was 22%. Clogging problems caused by pump failure while spraying the 55kg/m^3 specimens are likely to be the cause for their increased fibre losses which ranges between 20 – 45%. However, the steel fibre rebound losses for the 40kg/m^3 and the 70kg/m^3 densities in the laboratory tests are higher than those reported by Banthia et al (1994), which were

indicated to range between 12 – 18%. The difference in fibre losses may be due to the difference in operator skills or differences in the efficiencies of the mixing and spraying equipment used.

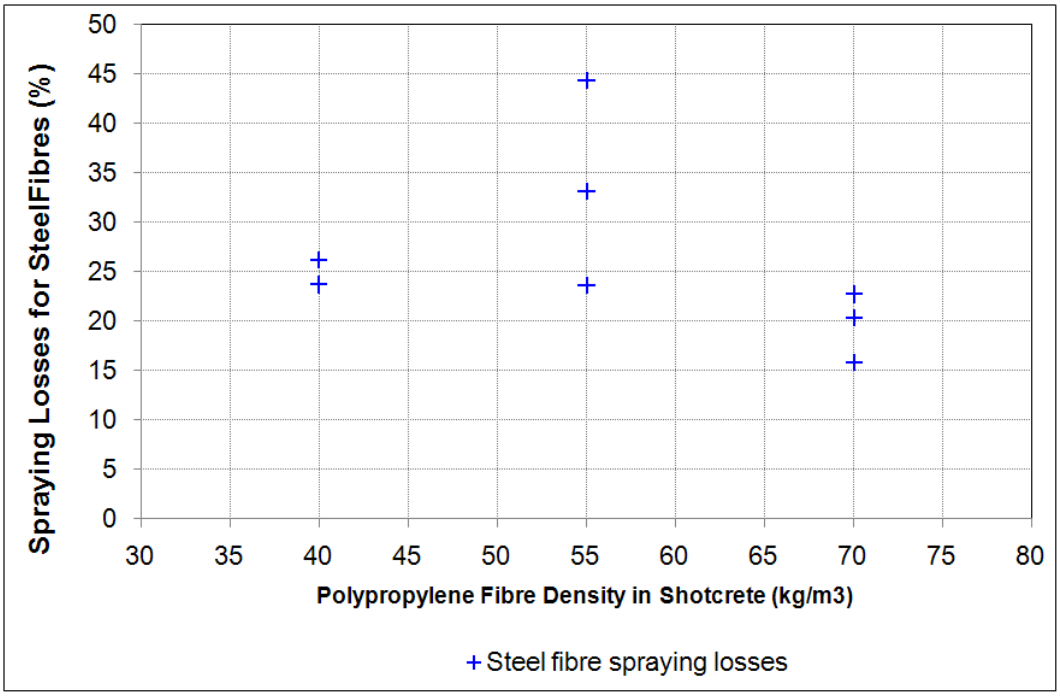


Figure 4.25 Steel fibre spraying rebound loss results for the steel fibre reinforced shotcrete specimens

Fibre spraying losses for the specimens obtained from the field in section 3.53 have been summarised in Table 4.6 together with the fibre losses for the surface sprayed shotcrete specimens reported in this section. Table 4.6 shows that the average fibre losses for the cores drilled from pillars are higher than those of cores drilled from the EFNARC panel sprayed in the field and the EFNARC panels sprayed on surface. The higher fibre losses for the cores drilled from field pillars may be due to the fact that the EFNARC tray sides may have slightly influenced the lower fibre losses during spraying in the EFNARC trays compared to spraying on the rock. The maximum and minimum fibre losses help in indicating the range of fibre losses for each set of specimens tested. The cores drilled from the

pillars have the highest range of 23% which may be a good indication of poor distribution of the actual fibres in the sprayed shotcrete due to spraying losses.

Table 4.6 Fibre content losses for shotcrete specimens sprayed underground and on surface

	Fibre losses (%)		
	Maximum	Minimum	Average
Cores drilled from a field sprayed EFNARC panel	36	23	30
Cores drilled from pillars in the field	59	16	48
Cores drilled from a surface sprayed EFNARC panel	44	16	26

4.9 Comments on laboratory testing results

The post peak load behaviour of shotcrete was displayed through toughness for the ASTM beams, residual strength for the EFNARC beams and energy absorption for RDPs and EFNARC panels.

The Round Determinate Panels (RDP) displayed less scattered load-deflection results compared to the EFNARC panels. Therefore the RDP testing method appears to produce better results in terms of repeatability of the test method and may be the best method for use in the post-peak load bearing capacity assessment of shotcrete during design. The design of shotcrete could be based on the post peak load bearing capacity, which has a direct influence on the energy absorption of shotcrete.

The toughness indices results obtained from the ASTM beam tests have shown that the increase in fibre density in shotcrete has a negligible effect

on the toughness of shotcrete. Probably, this is because the ASTM beam testing method has a very low deflection range of up to 2mm and the range may not give a clear picture on the influence of fibres. This may require the use of a testing machine that loads the beam to complete failure. For the current ASTM test method, the toughness indices results may be used to check whether the shotcrete meets set standards, for example, the toughness category ratings by Morgan (1988) reproduced in Table 4.4 in Section 4.7.

The residual strength values obtained from the polypropylene fibre reinforced EFNARC beams show no linear trend as the fibre density increases. This may also be attributed to the deflection of the beams which was done up to 4mm according to the test method. At low deflections, the increase in fibre density may not be easily noticeable hence the need to load the beam to destruction during testing.

4.10 Conclusions

Various properties of fibre reinforced shotcrete were assessed in this chapter. The laboratory test results have revealed that the incorporation of fibres in shotcrete has little effect on the modulus of rupture and the uniaxial compressive strength of shotcrete. However, the incorporation of fibres improves the post peak performance of shotcrete by offering it residual strength and energy absorption capacities. The shape of the specimens has an effect on the performance of shotcrete. This is especially the case with EFNARC panels due to the nature of the testing method, which requires the panel base to be flush with the stand on which the panel is placed during testing. It has been noted that the performance of fibre reinforced shotcrete depends on the types of fibres used in the shotcrete. The next chapter provides an investigation into the mechanisms of rock support provided by sprayed liners, based on field observations.

CHAPTER 5

INVESTIGATIONS INTO THE MECHANISMS OF ROCK SUPPORT PROVIDED BY SPRAYED LINERS BASED ON FIELD OBSERVATIONS

5.1 Introduction

The previous chapter dealt with the laboratory testing of shotcrete reinforced with steel or polypropylene fibres. The laboratory testing exercise has shown the benefits in shotcrete performance obtained from the incorporation of fibres. The laboratory testing results, together with field observations made during the monitoring of shotcreted pillars and tunnels in Chapter 3, will be used to investigate the possible mechanisms of rock support provided by shotcrete as a sprayed liner. Most of the mechanisms identified in Chapter 2 have been useful in the discussion of the possible mechanisms that were observed in the field as the shotcrete responded to loading by the pillars and tunnels due to mining induced stresses.

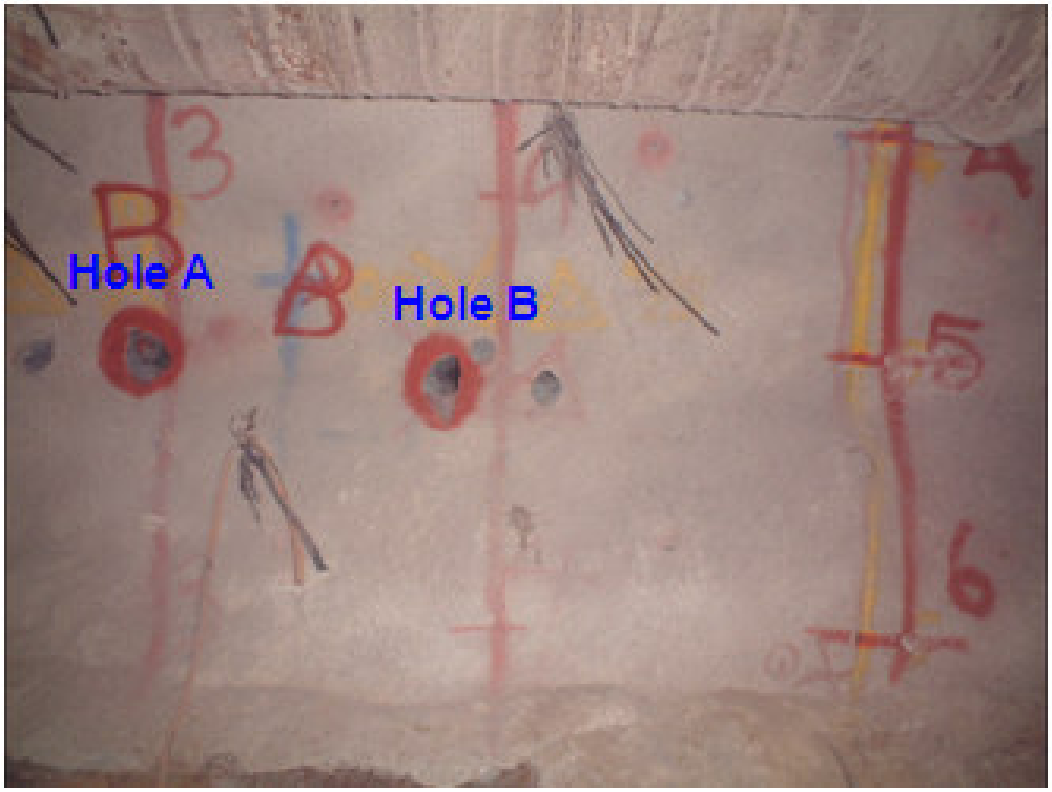
5.2 Mechanisms of rock support provided by sprayed liners based on field observations

5.2.1 Promotion of block interlock through bonding

Stacey (2001) indicated that block interlock is promoted by the bonding of the thin sprayed liners to the rock. During the research, bond strength

tests carried out at the South Deep Mine monitoring site have shown that the bond strength between the shotcrete and rock interface ranged from 0.2 MPa to 2.0 MPa. At Mponeng Mine, there was evidence of block interlock where the rock was observed to be broken, but still held in position by the shotcrete.

Borehole observations, as shown in Figure 5.1a at Mponeng 109 Level, show that the depth of loosened rock blocks was up to about 0.5m behind the shotcrete. Figure 5.1b shows the loose rock blocks held back by the wire mesh and lace support adjacent to the intact shotcreted section. Figure 5.1c shows a broken section of the mesh and lacing which is 10m away from the shotcreted section at Mponeng Mine Level 109. Also shown in Figure 5.1c is the depth of loosened rock blocks which is approximately 0.5m. The shotcrete played a major role in keeping the loosened rocks in place, thereby maintaining the integrity of the tunnel.



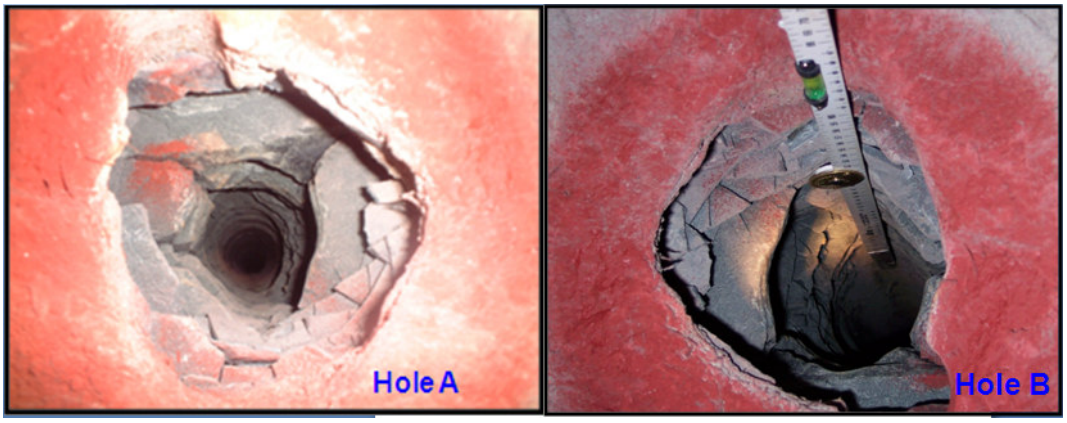


Figure 5.1a Borehole A and Borehole B in Mponeng Level 109 showing broken rock (about 0.5m) but interlocked in place by the shotcrete

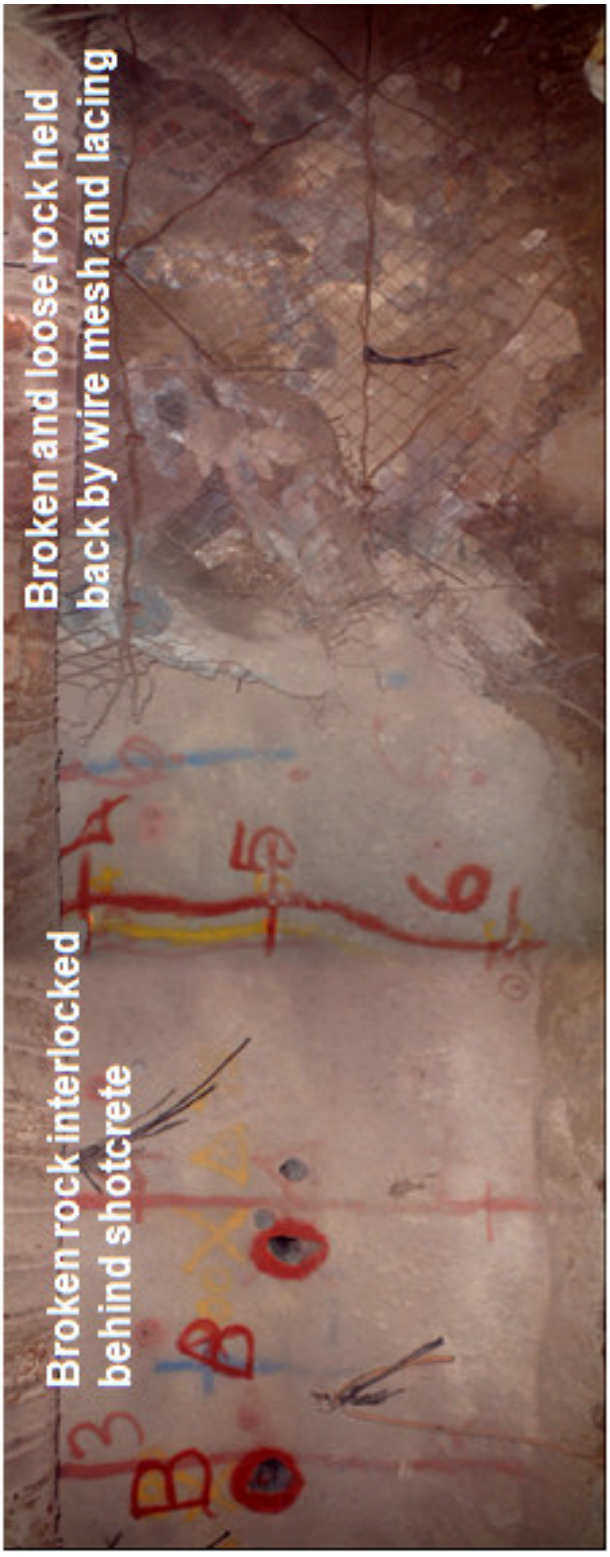


Figure 5.1b Broken and loose rock held back by wire mesh and rope lacing and broken rock interlocked behind shotcrete at Mponeng Mine Level 109



Figure 5.1c Side view of the loosened blocks (about 0.5m depth) held back by the mesh and lacing a few metres from the intact shotcreted section shown in Figure 5.1a and Figure 5.1b

5.2.2 Tensile strength of liner

Unreinforced shotcrete has low tensile strength properties and low strain capacity at fracture. However, the incorporation of fibres into the shotcrete improves the strain capacity of shotcrete as fibre addition improves the ductility of the shotcrete. As a result, the gradual nature in which the fibres pull out from the shotcrete imparts post crack ductility properties to the shotcrete that would otherwise fail in a brittle manner. Shotcrete laboratory testing results have shown that an improvement in ductility depends on the density of fibres and the type of fibres added to the shotcrete. Laboratory

test results in Chapter 4 have shown that the compressive strength of steel fibre reinforced shotcrete is slightly higher than that of polypropylene fibre reinforced shotcrete. For shotcrete, it follows that high compressive strength means high elastic modulus (Grov and Blindheim, 1997 and Melbye, 1994). Hook ended fibres provide improved anchorage thereby increasing the resistance to pullout compared to straight fibres.

Underground observations noted that steel fibres sticking out between cracks were perpendicular to the crack as indicated in Figure 5.2. There are various explanations related to the sticking out of fibres. Firstly, the fibres may have failed in tension as they offered resistance to the tensile stresses in the shotcrete as illustrated in Figure 5.3a. Alternatively, the fibres could be sticking out due to fibre pull out as the bond between the shotcrete and the fibre fails when the shotcrete responds to loading by the rock as illustrated in Figure 5.3b.

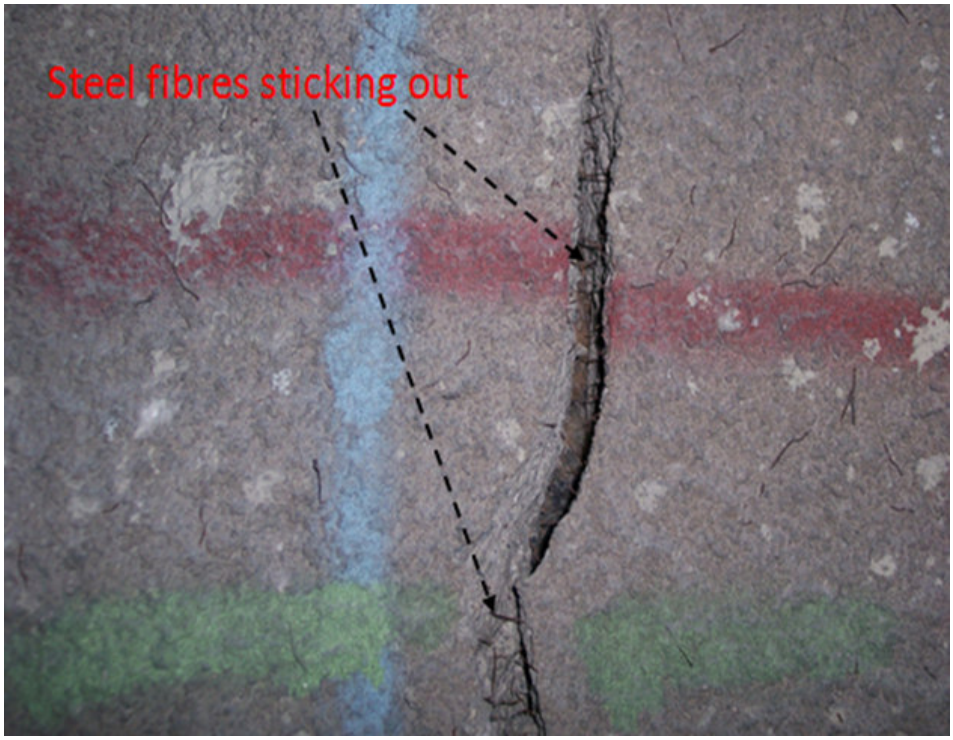


Figure 5.2 **Fibres sticking out due to tensile stresses on a shotcrete crack at South Deep Mine**

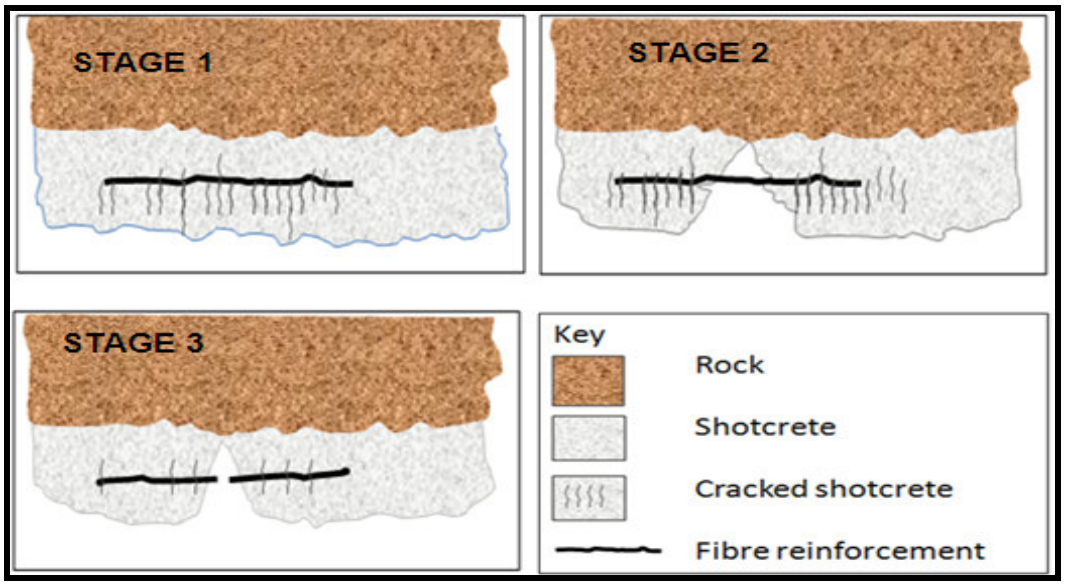


Figure 5.3a **Diagram illustrating the tensile failure of fibres in fibre reinforced shotcrete**

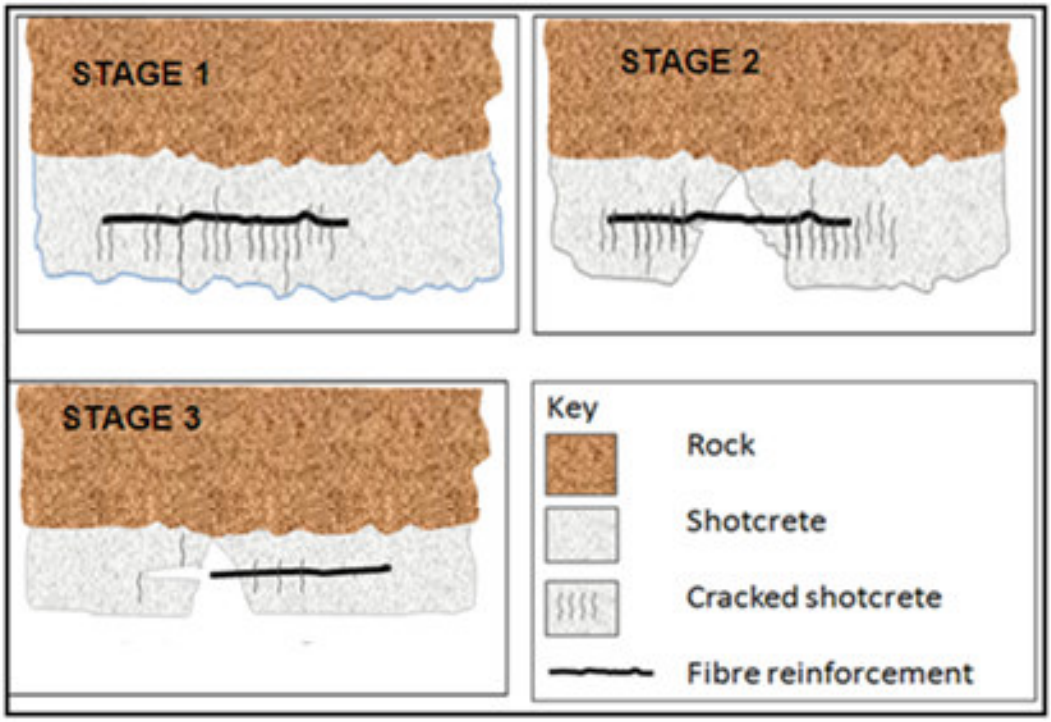


Figure 5.3b Diagram illustrating the pullout (failure) of fibres in fibre reinforced shotcrete

5.2.3 Basket mechanism

Stacey (2001) pointed out that when the sprayed liners support the rock in the form of a basket, the sprayed liner will be acting mainly in tension. Stacey (2001) also indicated the importance of ductility when the sprayed liner supports the rock through this mechanism. The load-deformation results in Chapter 4 have shown that the incorporation of fibres in the shotcrete helps improve the post peak load bearing capacity of shotcrete by offering it some ductility. The improvement in the post peak load performance was also illustrated through the energy absorption which improved with an increase in fibre density for both the steel fibre and polypropylene fibre reinforced round determinate panels. Therefore the ductility which is necessary for the basket mechanism to be effective has been demonstrated in the laboratory testing of fibre reinforced shotcrete specimens. The importance of ductility in the basket mechanism is

illustrated in Figure 5.4 where the fibre reinforced shotcrete was used together with mesh and lacing. Figure 5.4 shows that the shotcrete tensile strength has been exceeded, but that the shotcrete is being assisted by the mesh and lacing to hold back the loosened rock behind.

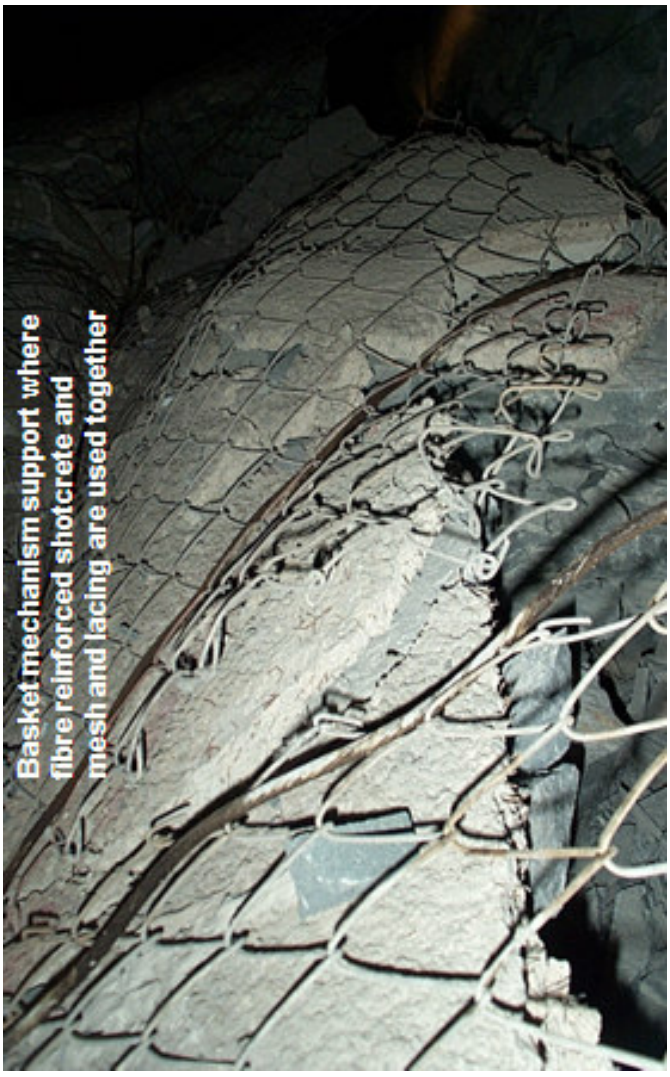


Figure 5.4 Basket mechanism where shotcrete has been applied together with rock bolts; mesh and lacing support (Mponeng Mine Level 116)

5.2.4 Shotcrete structural support mechanism

Structural support mechanism provided by shotcrete can be in the form of structural beam, structural arch or rock slab enhancement.

When shotcrete supports the excavation as a structural arch, it would be acting mainly in compression as it offers resistance to rock loads. The structural arch is illustrated in the tunnel in Figure 5.5a. The tunnel displays an arch shape in the roof and in adjacent sections there is evidence of loosened rock supported by mesh and lace as illustrated in Figure 5.5b. The excavation arch shape is therefore likely to have influenced the structural arch support mechanism offered to the rock by the shotcrete in the tunnel, preventing loosening of the rock. The rock blocks are also small such that the shotcrete provide sufficient structural support to keep them in place.

The structural beam support mechanism was evident in the roof sections of a tunnel that were found to be almost flat as illustrated in Figure 5.5c. The beam theory can be applicable to the flat sections of the tunnel roof. When shotcrete acts as a beam, it causes the formation of a stronger and more resistant to bending rock-shotcrete composite beam, thereby enhancing the stability of the tunnel.



Figure 5.5a **Demarcation between shotcrete, mesh and lacing support on Level 109 at Mponeng Mine. Shotcreted section shows no signs of loosening whereas the mesh and lacing section show signs of rock loosening.**

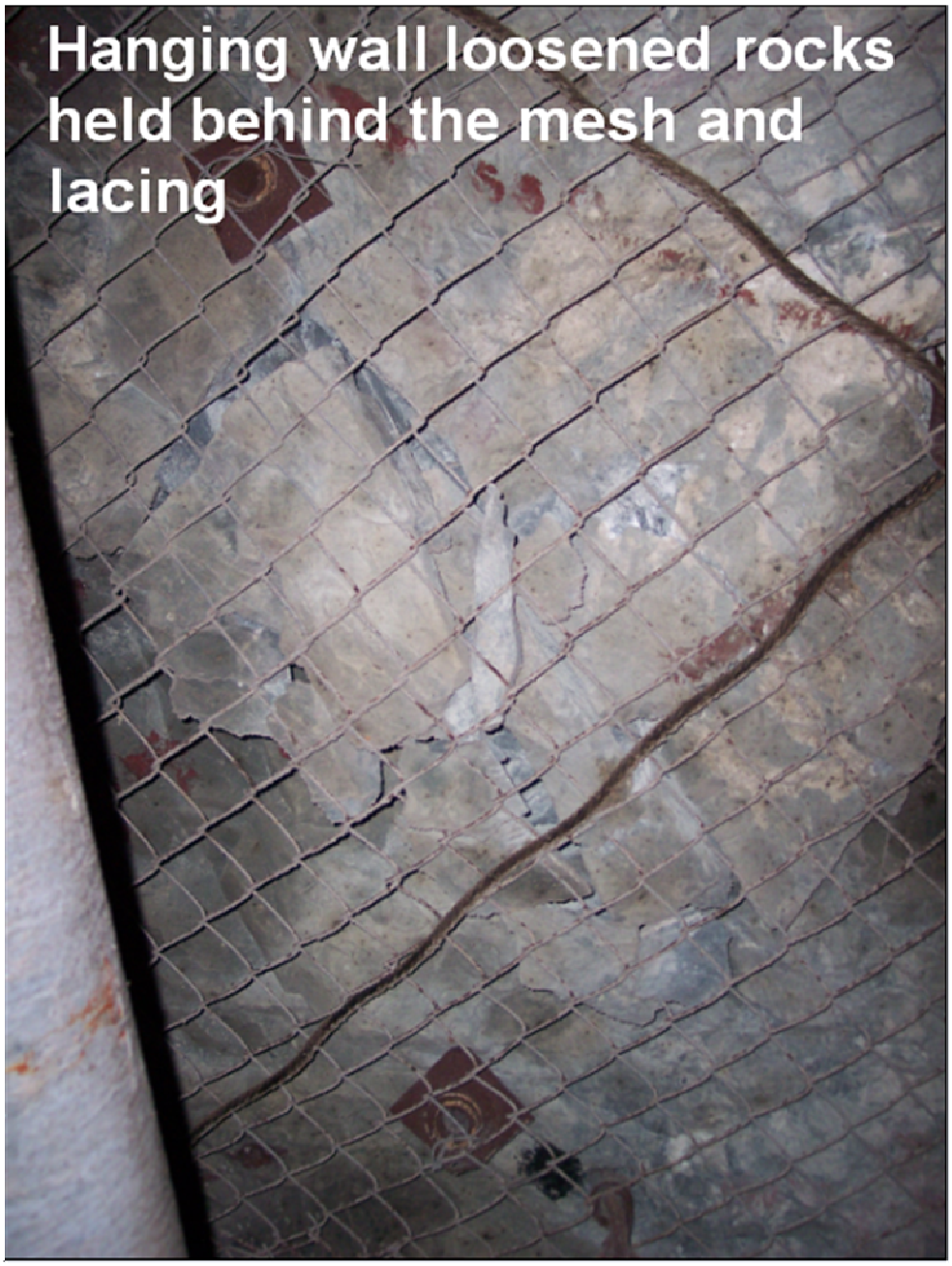


Figure 5.5b Close view of Mponeng Mine Level 109 mesh and lacing section (mesh and lace section in Figure 5.5a) showing loosened rock held back by mesh and lacing support



Figure 5.5c Close view of Mponeng Mine Level 109 shotcreted roof section (shotcreted roof section in Figure 5.5a) still intact and showing no signs of failure in the shotcrete as the shotcrete provides support through the beam support mechanism

Observations made in two boreholes at Impala Platinum Mine revealed that the rock was cracked a few centimetres behind the shotcrete as illustrated in Figure 5.6. The shotcrete bonded to the rock has helped maintain stability by enhancing the slab bending resistance due to the formation of a strong rock-shotcrete composite beam.

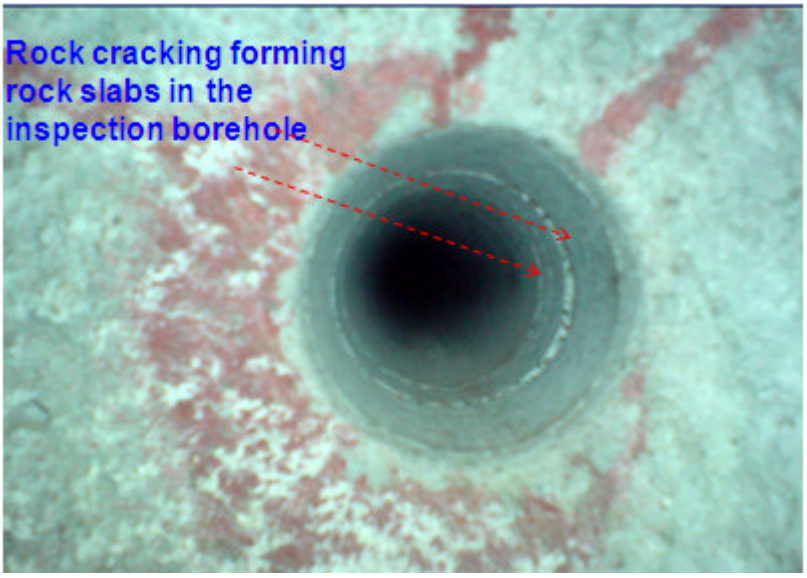


Figure 5.6 Cracks observed in a borehole showing a possibility of rock slabs forming in the tunnel walls due to mining induced stresses at Impala Platinum Mine

5.2.5 Extended faceplate

Stacey (2001) mentioned that all surface support will increase the area of influence of face plates attached to rock bolts or cable bolts. The face plate extension mechanism is achieved when face plates are installed as illustrated in Figure 5.7, where the tensioned cable bolt face plates were installed on top of the shotcrete. Tensioning of the cable bolts improved the direct contact between the shotcrete and the face plates which is necessary for the face plate mechanism to be valid. However, there was no photographic evidence showing partial failure of shotcrete to illustrate the extended face plate during the period of this research.

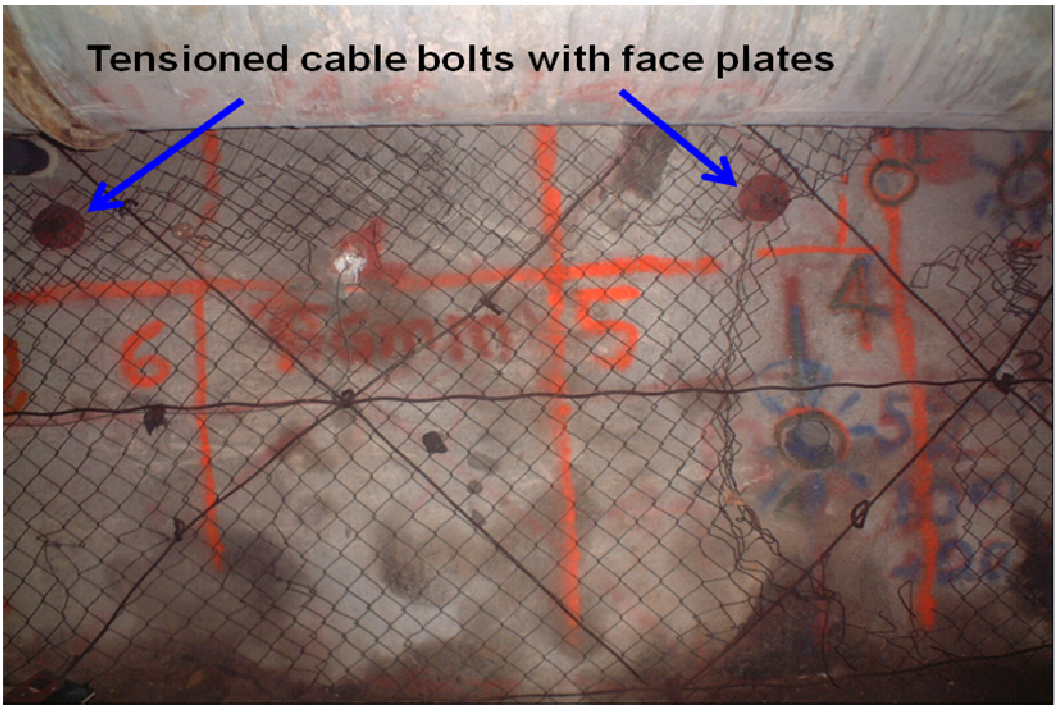


Figure 5.7 Tensioned cable bolting with face plates on the surface of shotcrete at Mponeng Mine Level 116

5.2.6 Mechanical protection

Stacey (2001) pointed out the importance of mechanical protection offered by sprayed liners to the rock. Mechanical protection is offered to the rock by the sprayed liner mainly where heavy underground machinery is being used for production and other underground purposes. As the equipment moves from one place to another, it can come into direct contact with the walls of an excavation. The extent of damage to shotcreted excavations would be lower relative to those that are not shotcreted. Figure 5.8 shows an illustration of the protection offered to one of the pillars at South Deep Mine where a loosened slab of shotcrete was observed after underground heavy equipment in motion came into contact with the pillar. An unprotected pillar would have experienced the damage itself rather than the shotcrete support as shown in Figure 5.8.

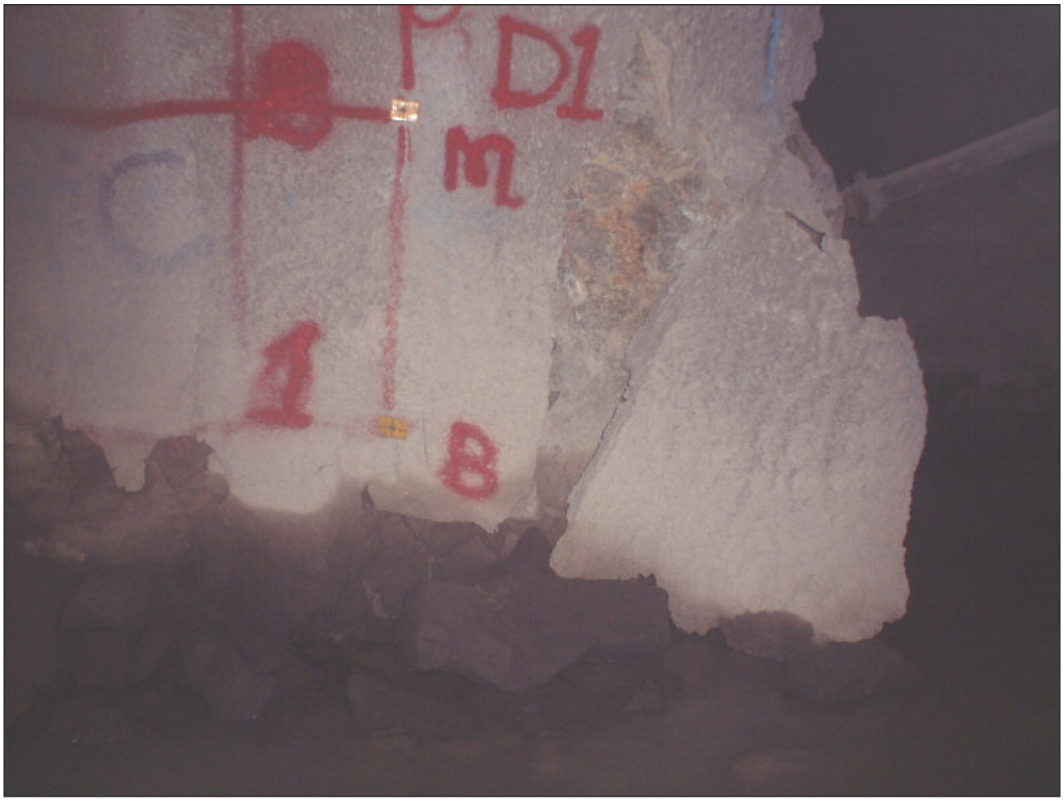


Figure 5.8 Damaged corner of one of the pillars that were monitored at South Deep Mine

5.2.7 Durability enhancement

Stacey (2001) pointed out that some rocks deteriorate on exposure and when subjected to wetting and drying. Sprayed liners help protect the rocks from deteriorating by providing a protective layer to weathering. It is mainly the water flowing through openings like joints in the rock that the sprayed liner will not be able to protect the rock against. Unfortunately, there was no photographic evidence to support the durability enhancement in the monitored sites. However, Bartlett and Borejszo (2002) evidence of durability enhancement in Kimberlite environments.

5.3 Conclusion

The field monitoring exercise afforded the opportunity to observe practically some of the mechanisms of rock support provided by the sprayed liners. These include promotion of block interlock, structural arch support and the basket mechanisms. Not all mechanisms found in the literature review in Chapter 2 could be identified in the three underground monitoring sites assessed during this study. However, the observed mechanisms provided a step in improving the understanding of the mechanisms of rock support provided by sprayed liners in the field.

CHAPTER 6

CONCLUSIONS AND RECOMMENDATIONS

The research described in this dissertation has been able to identify, practically, some of the mechanisms of rock support provided by sprayed liners through field monitoring, field tests and laboratory tests. Based on the study, the following conclusions can be drawn regarding the mechanisms of rock support provided by the sprayed liners:

- Sprayed liners can offer structural support to loosened rock blocks in an excavation provided that the excavation is not exposed to high mining induced stresses, and provided that the block sizes are small such that the dead weight of an individual block does not exceed the capacity of the sprayed liner. Structural support mechanisms offered to the rock by sprayed liners have been found to be in the form of rock slab enhancement, beam enhancement and structural arch support. It has also been noted that the shape of the excavation plays a crucial role in determining the form of the structural support mechanism offered by shotcrete.

- The Mponeng Mine site afforded the opportunity to understand the promotion of key block interlock since there was a shotcreted section in the tunnel monitored, and adjacent to this shotcreted section the tunnel was supported by wire mesh and lacing. Small blocks of loosened rock could be seen in the wire mesh and lace supported section, and in the shotcreted section loose blocks were identified behind the shotcrete via the boreholes. The fractured blocks in the shotcreted section were held back by the shotcrete.

This was possible because the tunnel was in a destressed state as the stope above had progressed past the tunnel and no further mining induced stresses affected the stability of the excavation.

- Other mechanisms of rock support provided by sprayed liners identified in the field were the basket mechanism and mechanical protection offered to the rock by shotcrete.

- The instruments used during the field monitoring exercise at the three underground mine sites helped identify the period in which displacement of the pillars and tunnels took place at increased rates. Signs of shotcrete cracking could be seen during this period and when further displacement was recorded, failure of the shotcrete at the South Deep Mine site could be identified. The monitoring exercise was useful in identifying some of the failure modes of shotcrete in situ. The modes of shotcrete failure identified in the field include tensile failure, adhesion failure, punching failure, shear failure and bending failure.

- Laboratory tests showed that the addition of fibres to shotcrete increases its ductility. The ductility rendered to the shotcrete improves its energy absorption, toughness and residual strength capacity. Also, it was noticed that the fibre content and fibre types have a direct influence on the shotcrete properties, which in turn play an important role in the mechanisms of rock support provided by the sprayed liners.

In order to improve on the understanding of the mechanisms of rock support provided by sprayed liners, the following recommendations are made for further study:

- More field monitoring exercises of shotcreted pillars need to be carried out at various mine sites to see how the shotcrete behaves in different environments.

- This research work focussed on shotcrete only as a sprayed liner. More field monitoring should be carried out on thin spray-on liners (TSL) to improve the understanding of the mechanisms by which they support the rock.

- The laboratory work carried out during the course of this research did not include plain shotcrete specimens. Therefore the tests should be repeated for both plain and fibre reinforced shotcrete for comparison purposes.

- During the field monitoring exercise, no stress measurements were taken to give an indication of the actual stress changes in the pillars and tunnels. Stress measurement in the pillars and tunnels should be included for further study to enable the observed rock deformations and shotcrete failures to be related to the stress changes in the supported rock. The correlation may help to improve the understanding of shotcrete behaviour in those mining environments.

- When further field monitoring of sprayed liners is carried out, systematic photographs of the sites need to be taken routinely and stored in a database such that the observed condition of the sprayed liner can be correlated with results from the displacement, stress and strain results.

- Strain measurements during the monitoring exercise were carried out in the rock and not in the shotcrete. Inside the rock, strain changes may be lower compared to those on the excavation periphery. Therefore further study should include strain

measurements in the shotcrete so that the strain in the shotcrete is known for use in the analyses of shotcrete behaviour.

REFERENCES

Aagaard, B., Grov, E., and Blindheim, O,T.,(1997), Sprayed concrete as part of rock support systems for adverse rock mass conditions. Proceedings of the International Symposium on Rock Support – Applied Solutions for Underground Structures, Lillehammer, Norway, pp. 13 – 24.

Alberts, C., and Backstrom, S., (1971), Instant shotcrete support in rock tunnels. Tunnels and Tunnelling, Unknown source.

ASTM C1018-97, (1997), Standard test method for flexural toughness and first-crack strength of fibre-reinforced concrete (Using beam with third point loading).

ASTM C1550-05, (2005), Standard test method for flexural toughness of fibre reinforced concrete (Using centrally loaded round panel).

Banthia, N., Trottier, J.F., Baupre, D., and Wood, D., (1994), Influence of fibre geometry in steel fibre reinforced wet mix shotcrete. Concrete International, Vol. 16, pp. 27 – 32.

Banton, C., Diederichs, M.S., Hutchinson, D.J., and Espley S., (2004), Mechanisms of shotcrete roof support. Proceedings of the 2nd International Conference on Engineering Developments in Shotcrete, Cairns, Queensland, Australia, pp. 39 – 45.

Barrett, S.V.L., and McCreath, D.R., (1995), Shotcrete support design in blocky ground: Towards a deterministic approach. Tunneling and Underground Space Technology, Vol. 10, No. 1, pp. 79 – 89.

Bartlett, P., and Borejszo, R., (2002), Tunnelguard in the mining industry. SAIMM 2nd International Seminar on Surface Support Liners: Thin Sprayed Liners, Shotcrete, Mesh, Sandton, South Africa.

Bartlett, P., and Nesbitt, K., (2000), Durability of Kimberlite and its effect on drilling and support in tunnels, Proc. AITES-ITA 2000 World Tunnel Congress, Tunnels Under Pressure, ed. T.R. Stacey, South African Institute of Mining and Metallurgy, pp. 37–40.

Barton, N., Lien, R., and Lunde, J., (1974), Engineering classification of rock masses for the design of tunnel support. Rock Mechanics, Vol. 6, No. 4, pp. 189 – 236.

Barton, N., (2002), Some new Q-value correlations to assist in site characterisation and tunnel design. International Journal of Rock Mechanics and Mining Sciences, Vol. 39, pp. 185 – 216.

Bernard, E.S., (1999), Correlations in the performance of fibre reinforced shotcrete beams and panels, Engineering Report CE9, School of Civil Engineering and Environment, University of Western Sydney, Nepean Kingswood, Australia.

Bieniawski, Z.T., (1989), Engineering rock mass classifications. John Wiley and Sons, New York.

Brady, B.H.G., and Brown, E.T., (1993), Rock Mechanics for Underground Mining. 2nd Edition, Allen and Unwin, London.

Brown, E.T., and Bray, J., (1987), Analytical and computational methods in engineering rock mechanics. London; Boston, Allen & Unwin.

Chen, L., Mindess, S., and Morgan, D.R., (1994), Specimen geometry and toughness of steel fibre reinforced concrete. Journal of Materials in Civil Engineering, Vol. 6, No. 4, pp. 529 – 541.

Douglas, T.H., and Arthur, L.J., (1983), A guide to the use of rock reinforcement in underground excavations. London, CIRIA Research Report 101.

EFNARC, (1996), European specification for sprayed concrete, www.efnarc.org

Egger, H.R., (1981), The role of shotcrete in underground construction. Symposium on Modern Techniques in Underground Construction and Tunnelling Works, Bangkok, Thailand, pp. 76 – 97.

Fernandez-Delgado, G., Mahar, J.W., Parker, H.W., (1976), Structural behaviour of thin shotcrete liners obtained from large scale tests. Proceedings of the Engineering Foundation Conference, Shotcrete for Ground Support, Easton, Maryland, USA, American Concrete Institute SP-54, pp. 399 – 442.

Fernandez-Delgado, G., Cording, E.J., Mahar, J.W., and Van Sint Jan, M.L., (1981), Thin shotcrete linings in loosening rock. The Atlanta Research Chamber: Applied Research for Tunnels, US Department of Transportation Report: UMTA-GA-06-0007-81-1, Monograph 21.

Finn, D.J., Teasedale, P., and Windsor, C.R., (1999), In situ trials and field testing of two polymer restraint membranes. Proceedings of Rock Support and Reinforcement Practice in Mining, E. Villaescusa, C.R. Windsor, and A.G. Thompson (ed.), Kalgoorlie , Australia, A.A. Balkema, pp. 139 – 153.

Fredriksson, A., and Stille, H., (1992), Bergforstarkningsprinciper for olika typfall i svenska gruvor. Gruvteknik 2000, report no. 92:07 (in Swedish).

Grov, E., and Blindheim, O.T., (1997), Selecting properties of sprayed concrete for different rock support applications. Proceedings of the International Symposium on Rock Support – Applied Solutions for Underground Structures, Lillehammer, Norway, pp. 68 – 82.

Hahn, T., and Holmgren, J., (1979), Adhesion of shotcrete to various types of rock surfaces. Proceedings of the 4th International Congress on Rock Mechanics, Rotterdam: Balkema, pp. 431 – 439.

Henderson, N.B., and Lewis, B.P., (2001), Mondi Rock-hold, development and application of a structural membrane support system. Journal of The South African Institute of Mining and Metallurgy, Vol. 101, No. 7, pp. 343 – 351.

Hoek, E., and Wood, D.W.F., (1987), Rock support in underground mines. In Underground Support Systems, ed. J.E. Udd, Montreal: Canadian Inst. Min. Metall. 35, pp. 1 – 6.

Hoek, E., Kaiser, P.K., and Bawden, W.F., (1995), Support of underground excavations in hard rock, AA Balkema.

Hoek, E., Kaiser, P.K., and Bawden, W.F., (2000), Support of underground excavations in hard rock. Balkema, Rotterdam.

Holmgren, J., (1983), Tunnel linings of steel fibre reinforced shotcrete. Proc. 5th International Congress on Rock Mechanics, pp. D311 – D314, Rotterdam: Balkema.

Holmgren, J., (1987), Bolt anchored steel reinforced shotcrete linings. Tunnelling and Underground Space Technology, Vol. 2, pp. 319 – 333.

Hudson, J.A., and Harrison, J.P., (1997), Engineering rock mechanics: An introduction to the principles. Oxford, Pergamon.

Humphries,W.R., and Funkhouser, M.R., (1993), The use of shotcrete on recent tunnel projects in the South and East, USA. Proceedings of Shotcrete for Underground Support VI, American Society for Civil Engineers, pp. 138 - 149.

Johansen, K.W., (1962), Yield line theory. London, Cement and Concrete Association.

Kaiser, P.K. and McCreath, D.R., eds., (1992), Proceedings of the International Symposium on Rock Support: Rock support in mining and underground construction. Rotterdam, NE: Balkema.

Kaiser, P.K., and Tannant, D.D., (1997), Use of shotcrete to control rock mass failure. International Symposium on Rock Support – Applied Solutions for Underground Structures, Lillehammer, Norway, pp. 580 – 595.

Kennedy, G., Goodchild, C.H., (2004), Practical yield line design. The Concrete Centre. www.concretecentre.com.

Kuchta, M.E., (2001), The use of high-pressure water for scaling of loose rocks in mine openings. 32nd Annual Conference, Institute on Mining Health, Safety & Research, August 5-7, Salt Lake City, Utah.

Kuchta, M.E., (2002), Quantifying the increase in adhesion strength of shotcrete applied to surfaces treated with high pressure water. Society for Mining, Metallurgy, and Exploration (SME) Annual Meeting, Phoenix Arizona.

Kuchta, M.E., Hustrulid, W.A., and Lorig, L.J., (2004), The importance of rock surface preparation in shotcreting operations. Surface Support in Mining, ed. Y. Potvin, D. Stacey and J. Hadjigeorgiou. Australian Centre for Geomechanics, Western Australia, pp. 283 – 290.

Kuijpers, J.S., and Toper, Z., (2002), Towards a better understanding of the support function of thin sprayed liners. SAIMM 2nd International Seminar on Surface Support Liners: Thin Sprayed Liners, Shotcrete, Mesh and Lace, Sandton, South Africa.

Kumar, D., Behera, P.K., and Singh, U.K., (2002), Shotcrete adhesion strength, EJGE Paper, http://www.ejge.com/2002/Ppr0203/Ppr0203.htm

Lang, T.A., (1961), Theory and practice of rock bolting. Transaction of the American Institute of Mining, Metallurgy and Petroleum Engineers, Transaction Vol. 220, pp. 333 – 348.

Langille, C., Espley, S., and McCreath, D., (1995), Innovative liner support trials in underground hard rock mines, CIM Bulletin Vol. 88 No. 992, pp. 66 – 74.

Langille, C., (2001), Shotcreting, In Advanced Rock Mechanics Practice for Underground Mines, Australian Center for Geomechanics Short Course.

Laubscher, D.H., (1990), A geomechanics classification system for the rating of rock mass in mine design. Journal of the South African Institute of Mining and Metallurgy, Vol. 90(10), pp. 257 – 273.

Leach, A.R., (1998), Specifications of shotcrete for deep gold mine conditions (beam and slab tests), ITASCA Internal Report.

Leach, A.R., (2002), Comparison of support requirement performance characteristics of sprayed cementitious coatings. SAIMM 2nd International Seminar on Surface Support Liners: Thin Sprayed Liners, Shotcrete, Mesh, Sandton, South Africa.

MacKay, J., and Trottier, J.F., (2004), Post-crack creep behaviour of steel and synthetic fibre reinforced concrete under flexural loading. Shotcrete: More Engineering Developments, Proceedings of the 2nd International Conference on Engineering Developments in Shotcrete, ed. E.S. Bernard, Taylor and Francis Group, London, pp. 183 – 192.

Malmgren, L., and Svensson, T., (1999), Investigation of important parameters for unreinforced shotcrete as rock support in the Kiirunavaara

Mine, Sweden, Proceedings of the 37th U.S. Rock Mechanics Symposium, Vail, Colorado, USA, pp. 629 – 635.

Malmgren, L., (2001), Shotcrete rock support exposed to varying load conditions, Licentiate Thesis, Department of Civil and Mining Engineering, Lulea University of Technology.

Malmgren, L., Nordlund, E., and Rolund, S., (2004), Adhesion strength and shrinkage of shotcrete, LKAB R&D and Division of Rock Mechanics, Lulea University of Technology, Sweden (LKAB, S-981 86 Kiruna, Sweden), Division of Rock Mechanics, Lulea University of Technology, S-971 87 Lulea , Sweden.

Malmgren, L., (2005), Interaction between shotcrete and rock - experimental and numerical study. Lulea University of Technology, Department of Civil and Environmental Engineering, Division of Mining and Geotechnical Engineering - Rock Mechanics and Rock Engineering, Sweden.

Melbye, T.A., (1994), Shotcrete for rock support. MBT Europe (MAC spa), 2nd Edition.

Melbye, T., Opsahl, O.A., Holtmon, J., (1995), Shotcrete for rock support. In. Austin, S.A., Robins, P.J., Sprayed Concrete: Properties, design and application. McGraw-Hill, Inc. UK, 1995. pp. 317-356.

Morgan, D.R., and Mowatt, D.N., (1984), A comparative evaluation of plain, mesh and steel fibre reinforced shotcrete. Proceedings of the International Symposium on Fibre Reinforced Concrete, American Concrete Institute SP-81, Detroit, pp. 307 – 324.

Morgan, D.R., (1988), Recent Developments in Shotcrete Technology - A Materials Engineering Perspective. The World of Concrete, Nevada (Las Vegas).

Morgan, D. R., Chen, L., and Beaupré, D., (1995), Toughness of fibre reinforced shotcrete. ASCE Shotcrete for Underground Support VII, Telfs, Austria, pp. 66-87.

Morrison, J. A., Madsen, P. H., and Carayol, S., (1999), Ground control program for the Río Piedras Project, Tren Urbano, San Juan, Puerto Rico, Proc. Rapid Excavation and Tunneling Conference, Orlando, SME, pp. 415 – 435.

Obert, L., and Duvall, W.I., (1967), Rock mechanics and the design of structures in rock, John Wiley, New York.

Ortlepp, W.D., Stacey, T.R., and Kirsten, H.A.D., (1999), Containment support for large static and dynamic deformations in mines. Rock Support and Reinforcement Practice in Mining, Karlgoorlie, Western Australia, ed. Villaescusa, E., Windsor, C.R., and Thompson, A.G., A.A Balkema/Rotterdam/Brookfield, pp. 359 - 364.

Papworth, F., Ratcliffe, R., and Grant, B., (1996), Design of steel fibre reinforced concrete slabs on ground and shotcrete linings. The New Zealand Concrete Society, Making Innovations Happen Conference, Taupo, New Zealand.

Pells, P.J.N., (2008), What happened to the mechanics in rock mechanics and geology in engineering geology? The Journal of The Southern African Institute of Mining and Metallurgy, Vol. 108, pp. 309 – 323.

Player, J.R., (2004), Field performance of cone bolts at Big Bell mine. Proceedings of the 5th International Symposium on Ground Support in Mining and Underground Construction, Perth, Western Australia, ed. Villaescusa, E., and Potvin, Y., A.A. Balkema Publishers, Taylor and Francis Group, London.

Ratcliffe, R., (1999), The important properties of steel fibre reinforced shotcrete (SFRC) used in mining. Rock Support and Reinforcement Practice in Mining, Proc. Int. Symp. on Ground Support, ed. E. Villaescusa, C.R. Windsor, and A.G. Thompson. Karlgoorlie, Western Australia, Balkema, Rotterdam, Brookfield, pp. 209 – 218.

Ray, J., (1997), Shotcrete performance assessment. 3rd National Shotcrete Workshops, Kalgoorlie, Brisbane and Sydney, Unknown Source.

Rose, D., (1985), Steel fibre reinforced shotcrete for tunnel linings: The state of the art. In Proceedings of the Rapid Excavation and Tunnelling Conference, New York, Vol. 1, pp. 319 – 412.

Saiang, D., Malmgren, L., and Nordlund, E., (2004), Strength and stiffness of shotcrete-rock interface – a laboratory study. Proceedings of the Fifth International Symposium on Ground Support in Mining and Underground Construction, Perth, Western Australia, ed. E. Villaescusa, and Y. Potvin. Balkema, pp. 555 – 565.

Shi, G.H., and Goodman, R.E., (1981), A new concept for support of underground and surface excavations in discontinuous rocks based on the keystone principle, In Rock mechanics from Research to Applications, Proc. 22nd U.S. Symp. for Rock Mechanics, Massachusetts Institute for Technology, Cambridge, pp. 290 – 296.

Spearing, A.J.S., and Hague, I., (2003), The application of underground support liners reaches maturity, ISRM, Technology Roadmap for Rock Mechanics, South African Institute of Mining and Metallurgy, pp. 1127 – 1132.

Speers, C.R., (1998), Shallow excavation requirements. School: Shotcrete and its Application, The South African Institute of Mining and Metallurgy, Mintek, Randburg.

SRK Consulting Company, SIMRAC Internal Report, (2008), Shotcrete project.

Stacey, T.R., and Ortlepp, W.D., (1999), Retainment support for dynamic events in mines. Proceedings of the International Symposium on Ground Support, Kalgoorlie, Western Australia, pp. 329- 333.

Stacey, T.R., (2001), Review of membrane support mechanisms, loading mechanisms, desired membrane performance, and appropriate test methods. Journal of The South African Institute of Mining and Metallurgy, Vol. 101, No. 7, pp. 343 – 351.

Stacey, T.R., (2003), Presidential Address: Rock engineering – Good design or good judgement? Journal of the South African Institute of Mining and Metallurgy, Vol. 103, pp. 411 – 421.

Stacey, T.R., and Yu, X., (2004), Investigations into the mechanisms of rock support provided by sprayed liners. Ground Support in Mining and Underground Construction, ed. E. Villaescusa, and Y. Potvin. Taylor and Francis Group, London, pp. 565 – 569.

Stacey, T.R., (2004), Shotcrete in mines: State-of-the-art in South Africa. Surface Support in Mining, ed. Y. Potvin, D. Stacey and J. Hadjigeorgiou. Australian Centre for Geomechanics, Western Australia, pp. 247 – 253.

Stille, H., and Franzen, T., (1990), Design of shotcrete support from a rock mechanical point of view. Shotcrete for Underground Support. Proc. Eng. Found. Conf. Uppsala, pp. 1 – 9.

Sutcliffe, H., and McClure, C.R., (1969), Large aggregate shotcrete challenges steel ribs as a tunnel support. American Society for Civil Engineering Publication.

Swan, G. and Henderson, A., (2001). Water-based spray-on liner implementation at Falconbridge Limited. Proceedings of the 15th Mine

Operators' Conference, Sudbury (Ontario), The Canadian Institute of Mining, Metallurgy and Petroleum (CIM), CIM Editor/Publisher.

Tannant, D.D., Swan, G., Espley, S., and Graham, C., (1999), Laboratory test procedures for validating the use of thin spray-on liners for mesh replacement. Canadian Institute of Mining and Metallurgy Annual General Meeting, Calgary, published on CD ROM.

Tannant, D.D., (2001), Thin spray-on liners for underground rock support. 17th Int. Mining Congress and Exhibition of Turkey. IMCET 2001, ed. Unal, E., Unver, B., and Tercan, E., Ankara, Turkey, pp. 57–65.

Tannant, D.D., (2002), Thin spray-on liners for underground rock support-testing and design issues. Surface Support in Mining, ed. Potvin, Y., Stacey, D., and Hadjigeorgiou, J. pp. 51 – 59.

Vandewalle, M., (1992), Dramix tunneling the world (2nd edition), An N.V. Bekeart SA publication, Zwevegem, Belgium.

Vandewalle, M., (1998), The use of steel fibre reinforced shotcrete for the support of mine openings. School: Shotcrete and its Application, South African Institute of Mining and Metallurgy, Randburg, South Africa.

Whittaker, B.N., and Frith, R.C., (1990), Tunnelling design, stability and construction. The Institution of Mining and Metallurgy, London.

BIBLIOGRAPHY

ASTM 506R-C90, (1990), Guide to shotcrete.

ASTM A820-90, (1990), Standard specification for steel fibres for reinforced concrete.

ASTM C1140 - 89, (1989) Standard specification for preparing and testing specimens from shotcrete prepared panels.

ASTM C31 Practice for Making and Curing Concrete Test Specimens in the field; and

ASTM C42 – 91, (1991), Standard test method for obtaining and testing drilled cores and sawed beams of concrete

www.efnarc.org

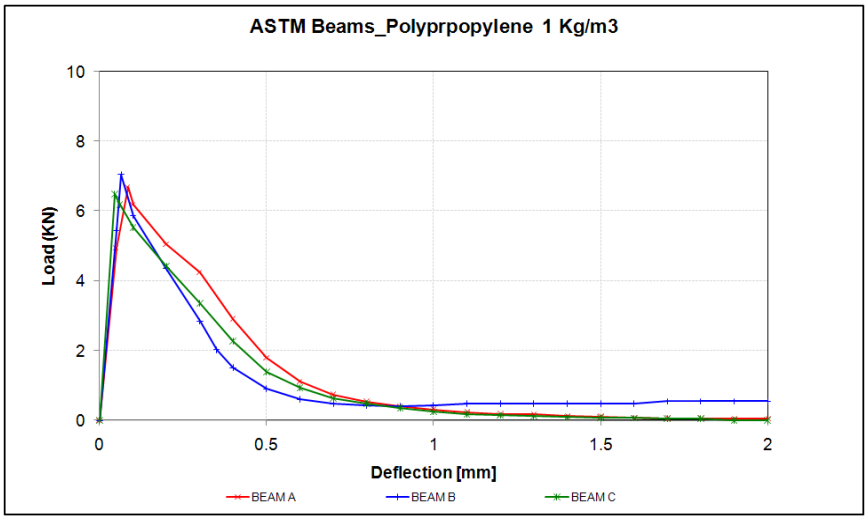
www.yieldpoint.com

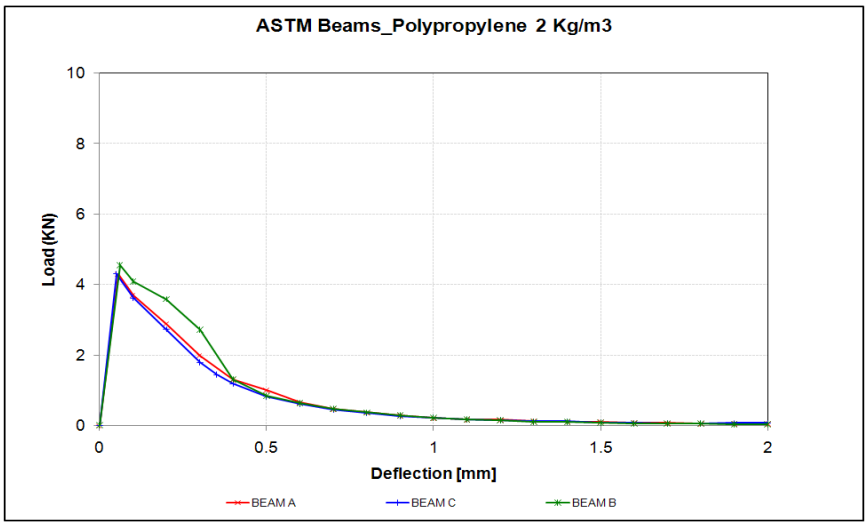
ASTM 1550 – 05, (2005), Standard test method for flexural toughness of fibre reinforced concrete (Using centrally loaded round panel)

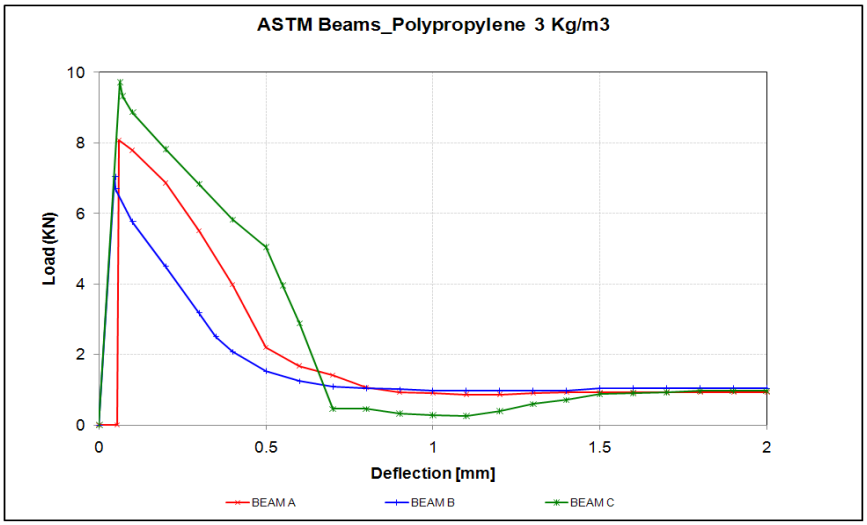
APPENDIX A: Load deflection graphs for ASTM beams, ASTM RDPs, EFNARC panels and EFNARC beams

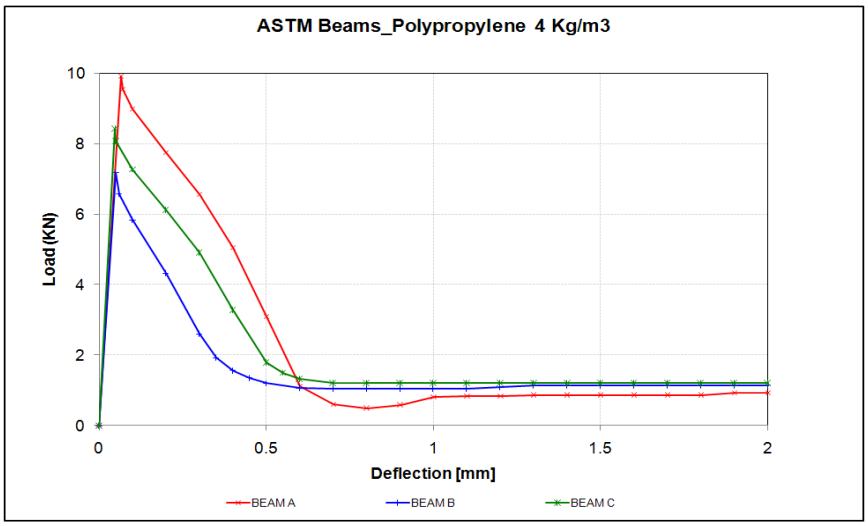


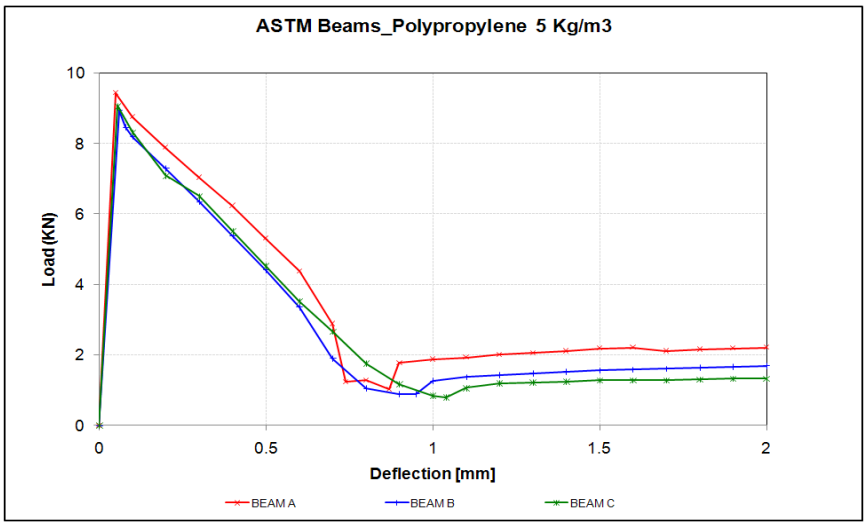
ASTM BEAMS

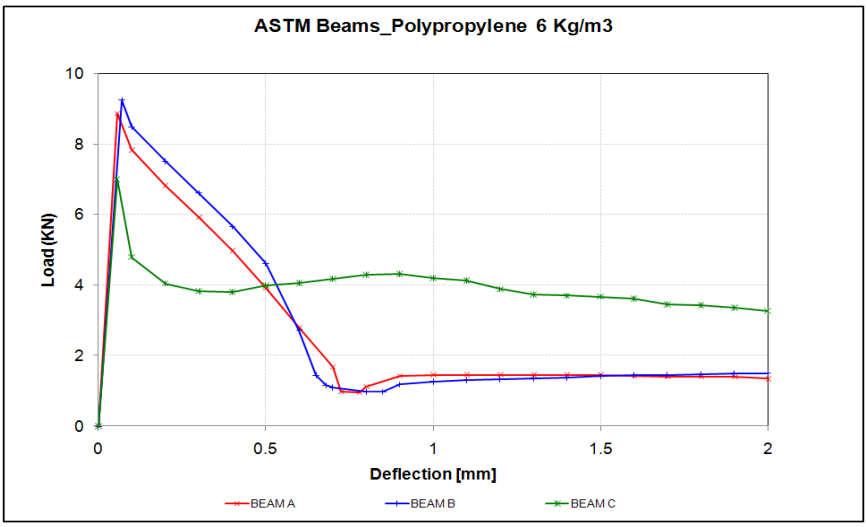

ASTM Beams_Polyprpopylene 1 Kg/m3
Load (KN)
Deflection [mm]
BEAM A
BEAM B
BEAM C

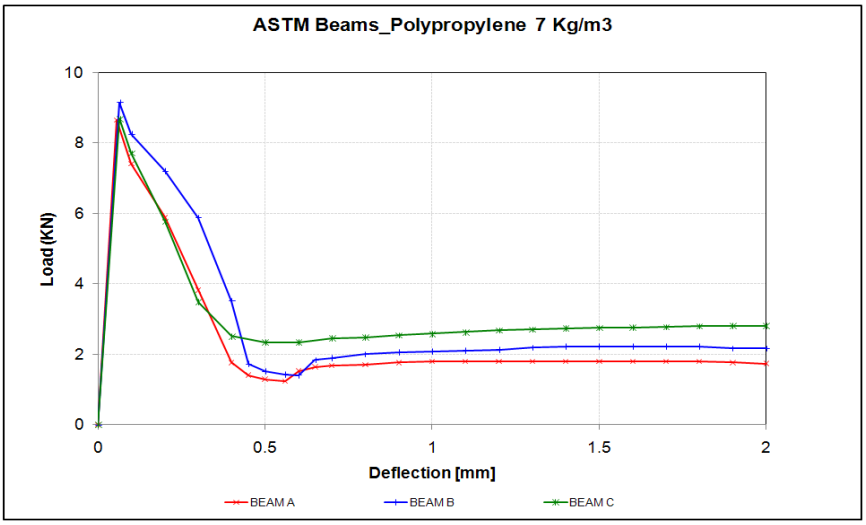

ASTM Beams_Polypropylene 2 Kg/m3
Load (KN)
Deflection [mm]
BEAM A
BEAM C
BEAM B

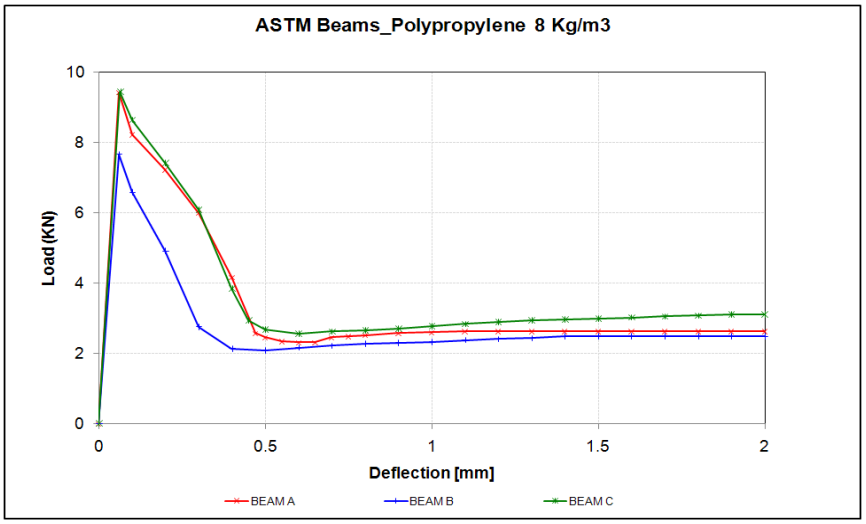

ASTM Beams_Polypropylene 3 Kg/m3
Load (KN)
Deflection [mm]
BEAM A
BEAM B
BEAM C

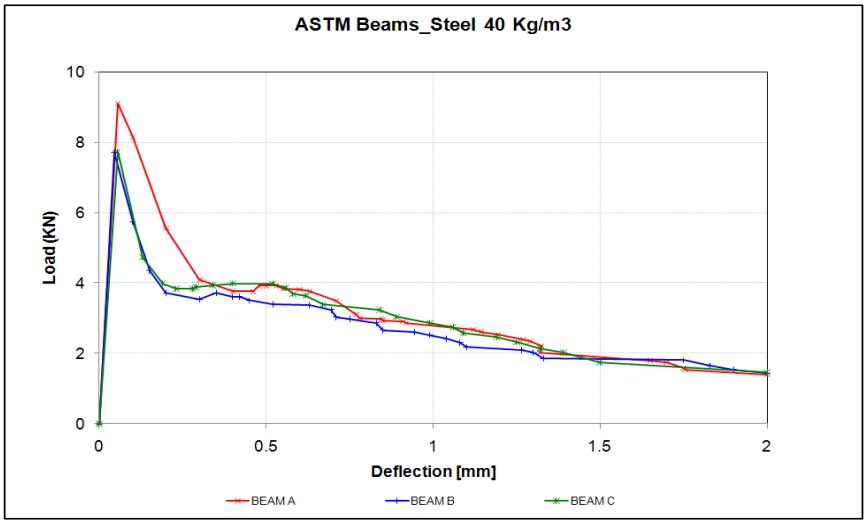

ASTM Beams_Polypropylene 4 Kg/m3
Load (KN)
Deflection [mm]
BEAM A
BEAM B
BEAM C

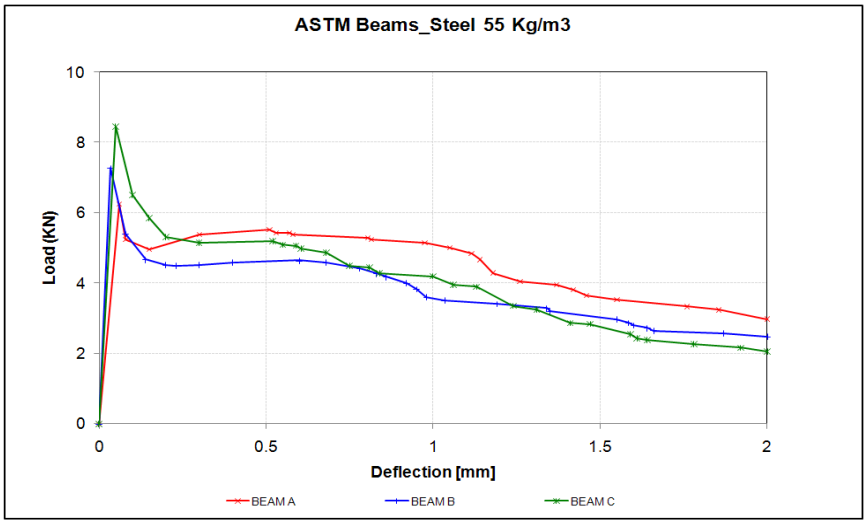

ASTM Beams_Polypropylene 5 Kg/m3
Load (KN)
Deflection [mm]
BEAM A
BEAM B
BEAM C

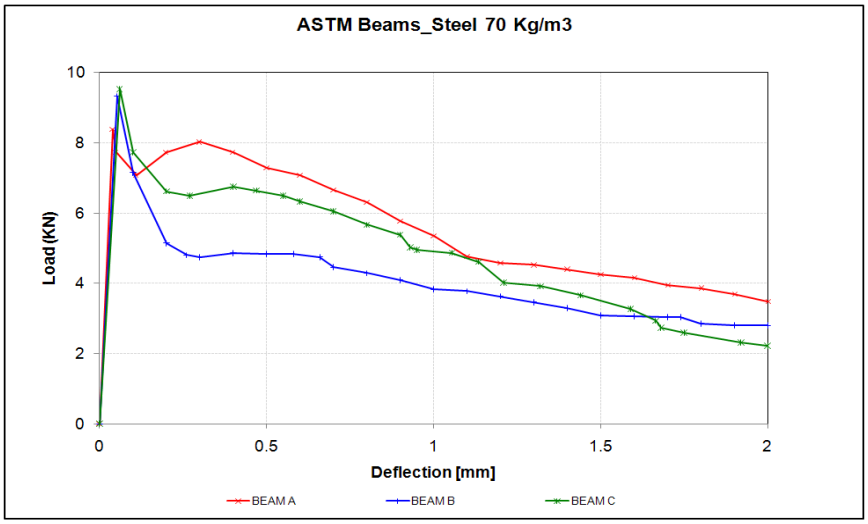

ASTM Beams_Polypropylene 6 Kg/m3
Load (KN)
Deflection [mm]
BEAM A
BEAM B
BEAM C


ASTM Beams_Polypropylene 7 Kg/m3
Load (KN)
Deflection [mm]
BEAM A
BEAM B
BEAM C

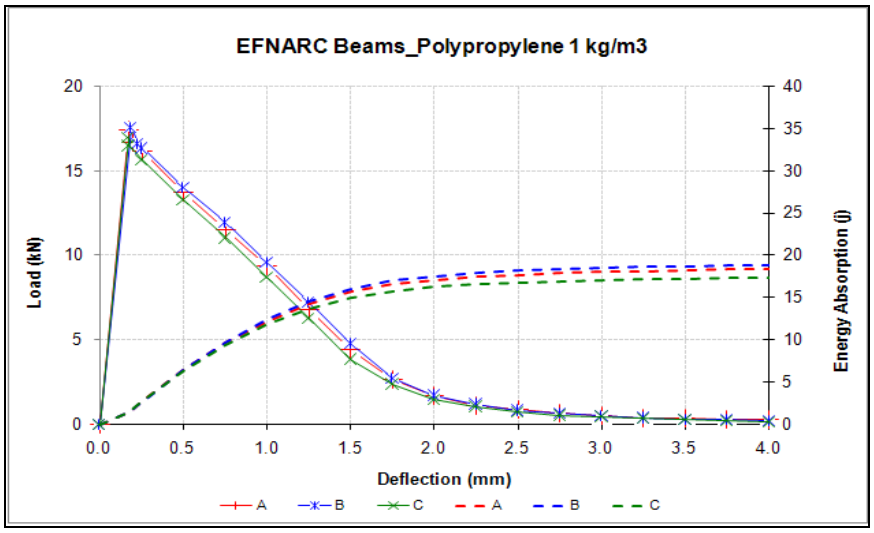

ASTM Beams_Polypropylene 8 Kg/m3
Load (KN)
Deflection [mm]
BEAM A
BEAM B
BEAM C

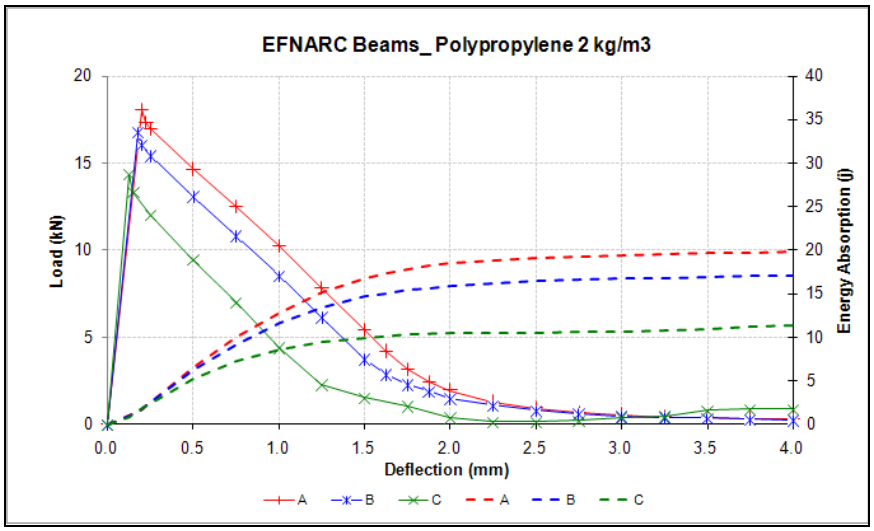

ASTM Beams_Steel 40 Kg/m3
Load (KN)
Deflection [mm]
BEAM A
BEAM B
BEAM C

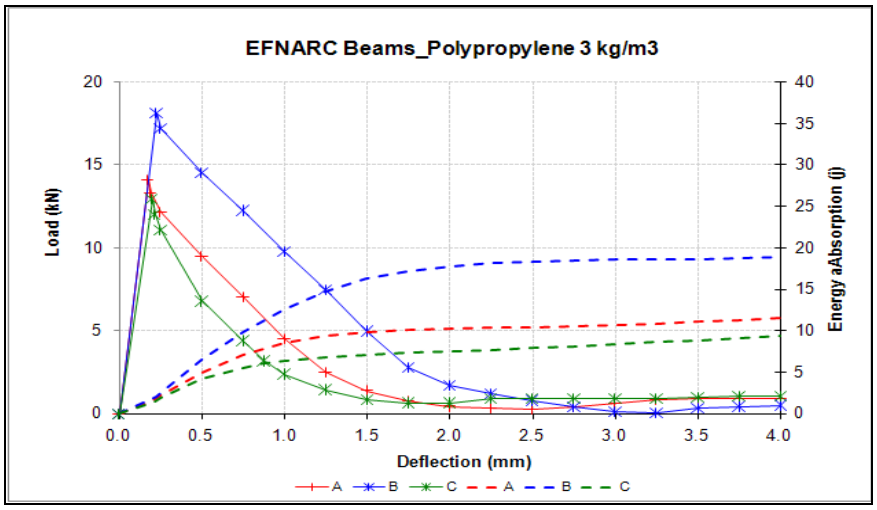

ASTM Beams_Steel 55 Kg/m3
Load (KN)
Deflection [mm]
BEAM A
BEAM B
BEAM C

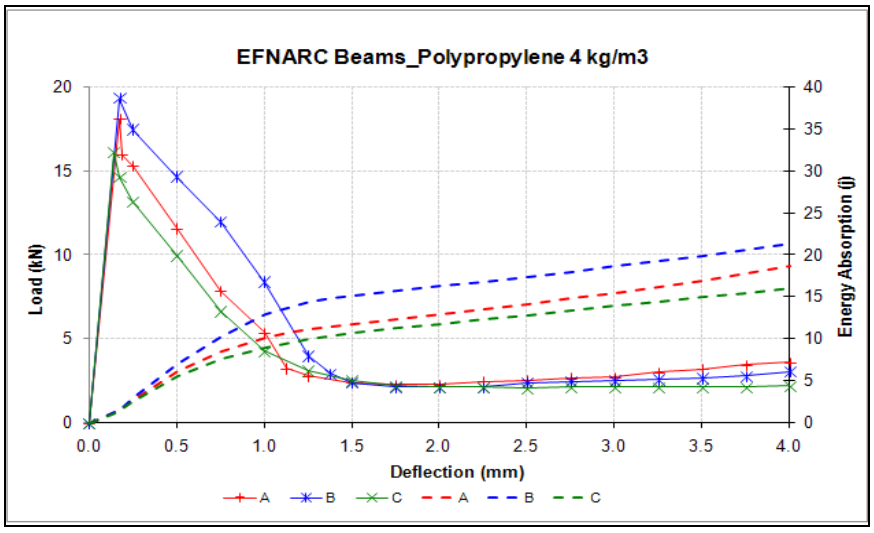

ASTM Beams_Steel 70 Kg/m3
Load (KN)
Deflection [mm]
BEAM A
BEAM B
BEAM C

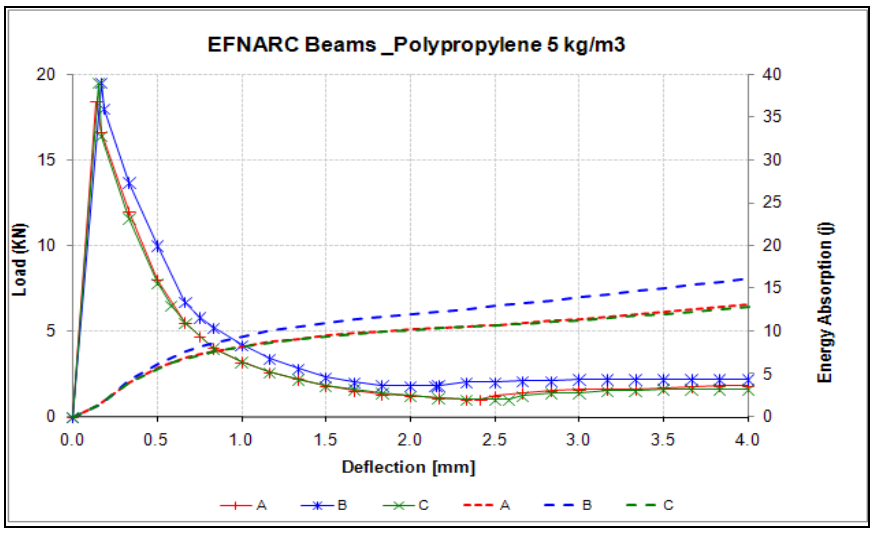
EFNARC BEAM TEST RESULTS

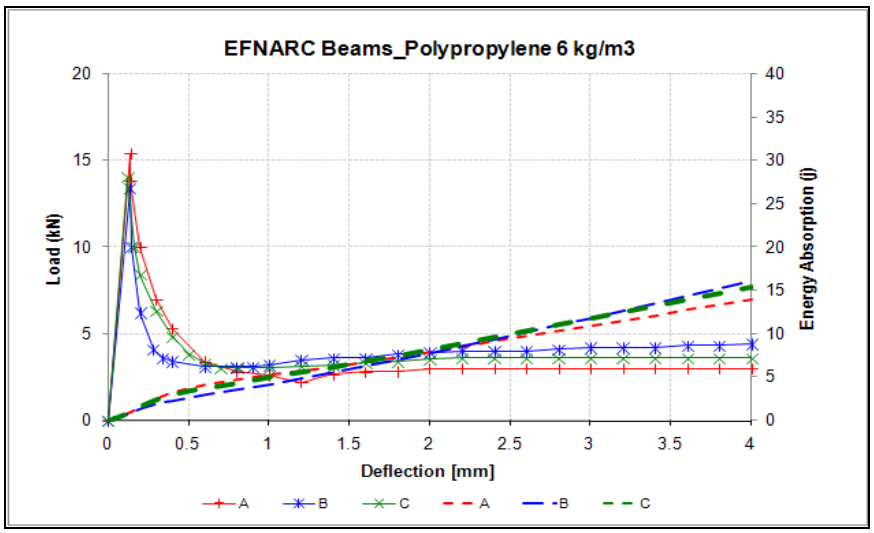


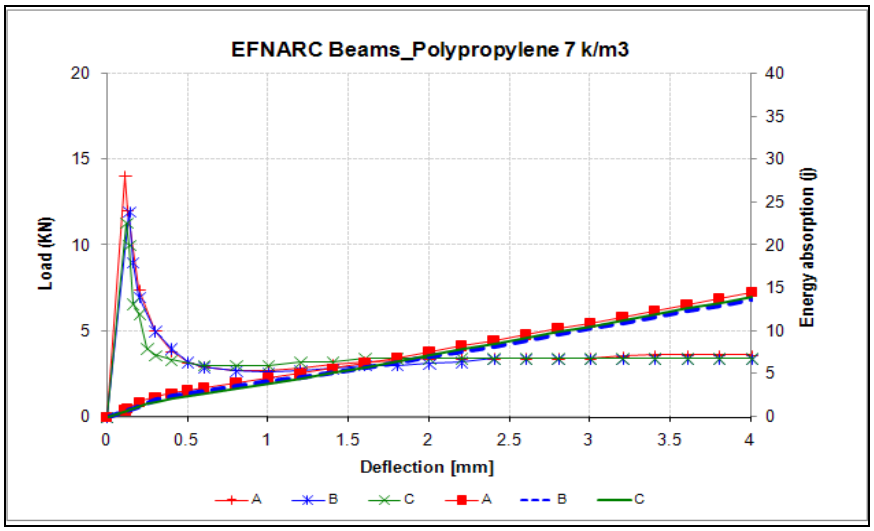


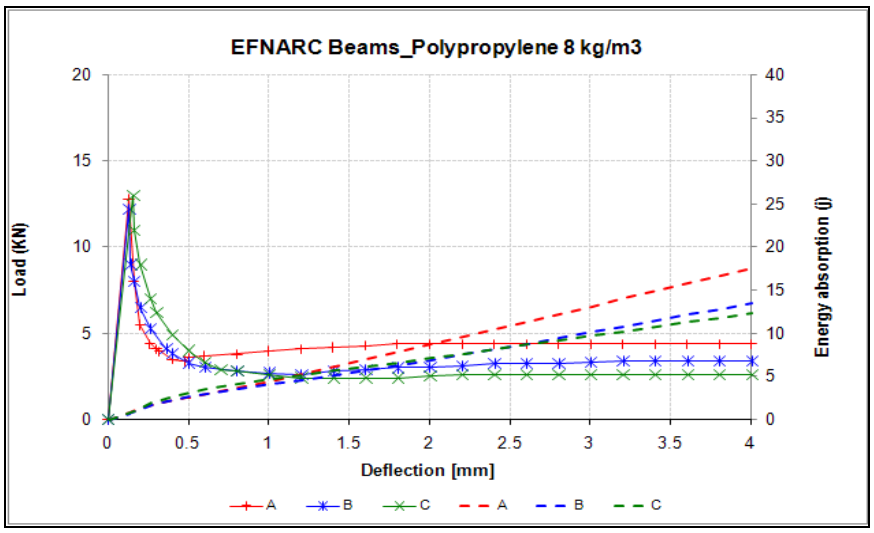


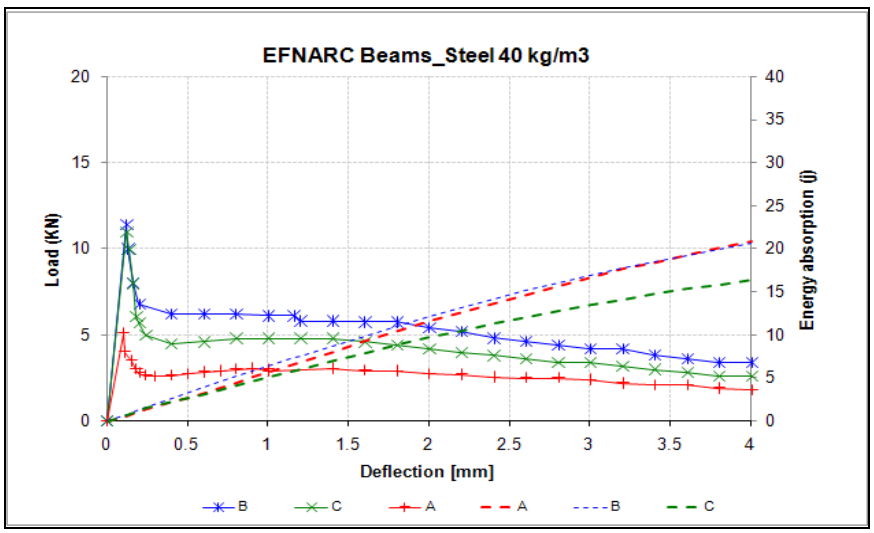

EFNARC Beams_Polypropylene 4 kg/m3
Load (kN)
Energy Absorption (j)
Deflection (mm)
A B C A B C

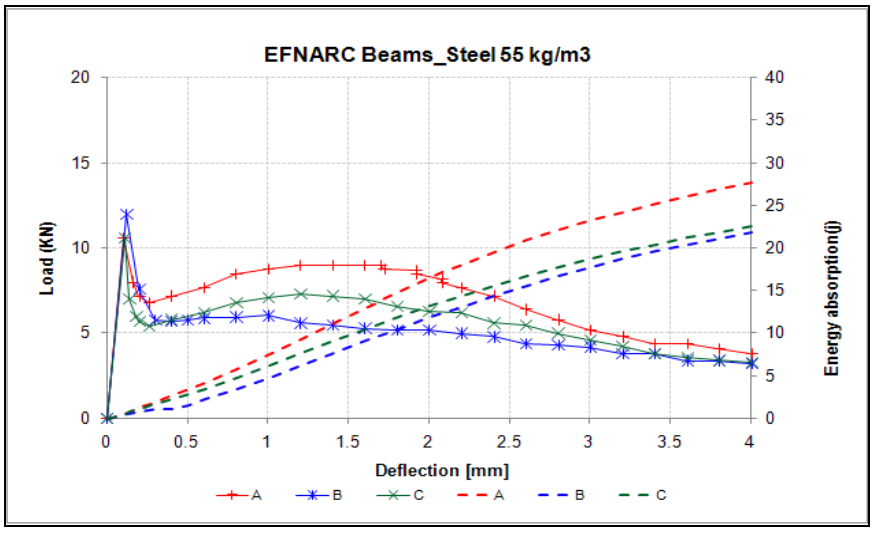

EFNARC Beams _Polypropylene 5 kg/m3
Load (KN)
Energy Absorption (j)
Deflection [mm]
A B C A B C

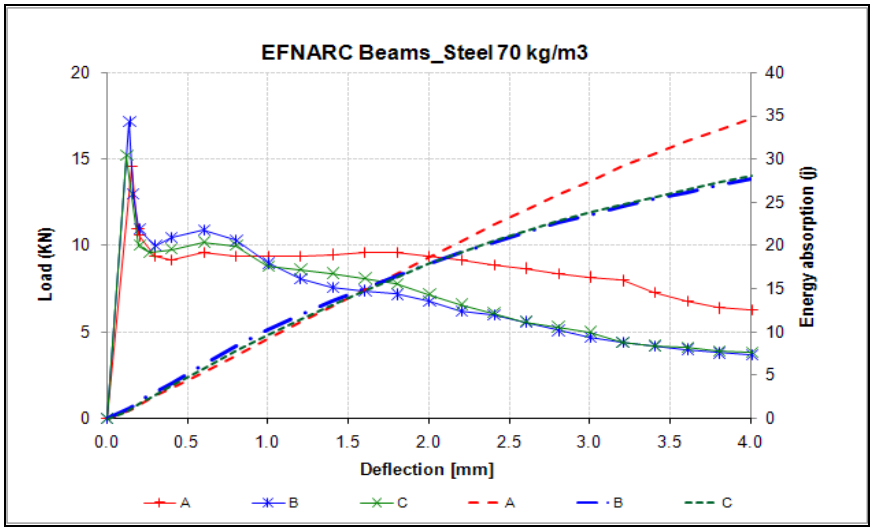

EFNARC Beams_Polypropylene 6 kg/m3
Load (kN)
Energy Absorption (j)
Deflection [mm]
A B C A B C


EFNARC Beams_Polypropylene 7 k/m3
Load (KN)
Energy absorption (j)
Deflection [mm]
A
B
C
A
B
C

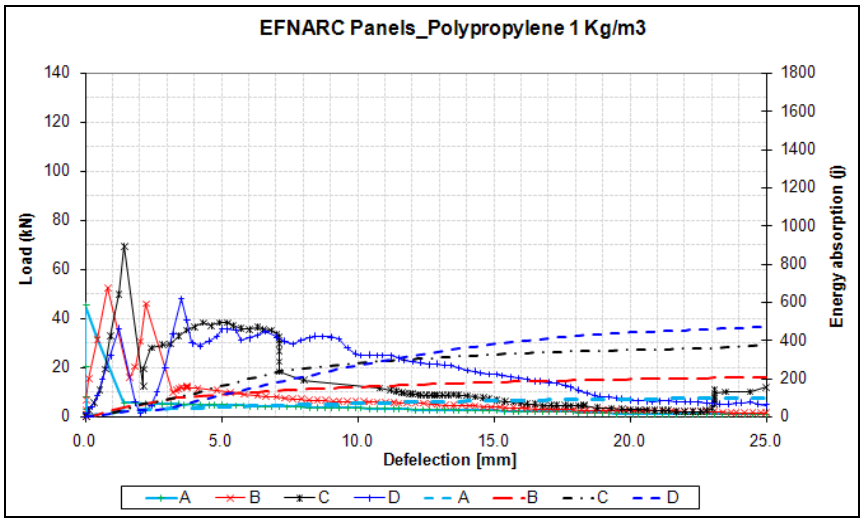

EFNARC Beams_Polypropylene 8 kg/m3
Load (KN)
Energy absorption (j)
Deflection [mm]
A
B
C
A
B
C

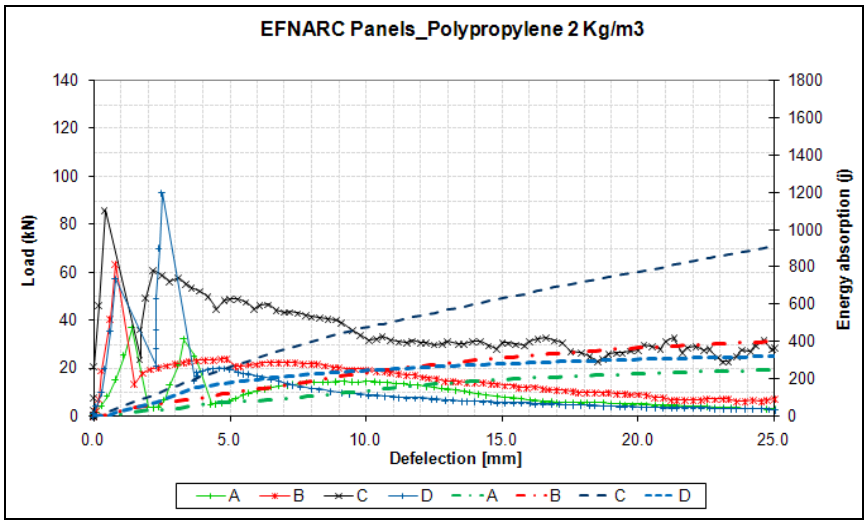

EFNARC Beams_Steel 40 kg/m3
Load (KN)
Energy absorption (j)
Deflection [mm]
B
C
A
A
B
C

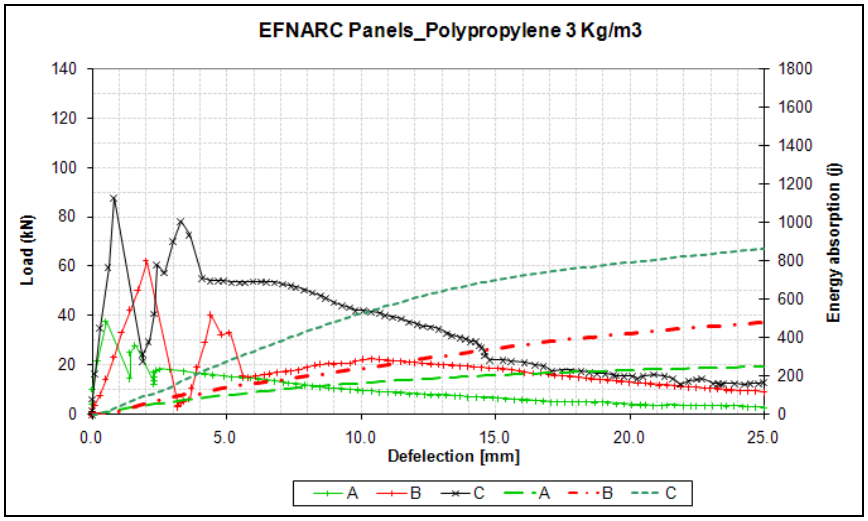

EFNARC Beams_Steel 55 kg/m3
Load (KN)
Energy absorption(j)
Deflection [mm]
A
B
C
A
B
C

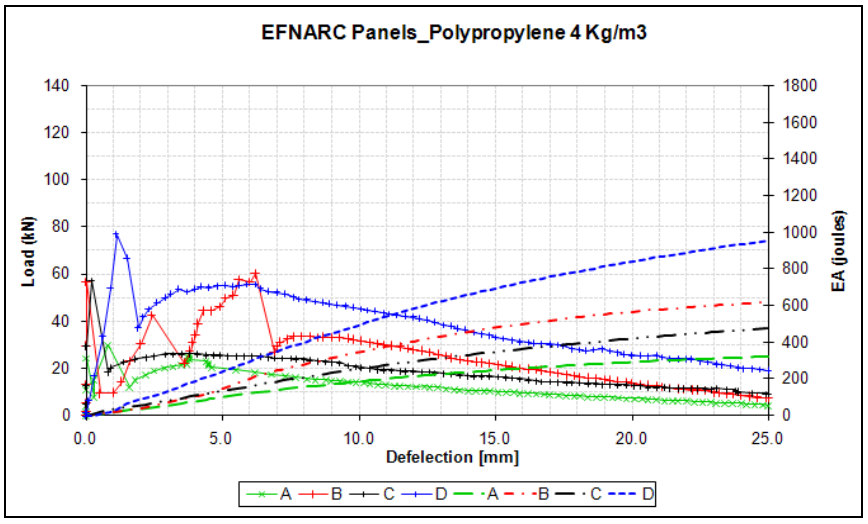

EFNARC Beams_Steel 70 kg/m3
Load (KN)
Energy absorption (j)
Deflection [mm]
A
B
C
A
B
C

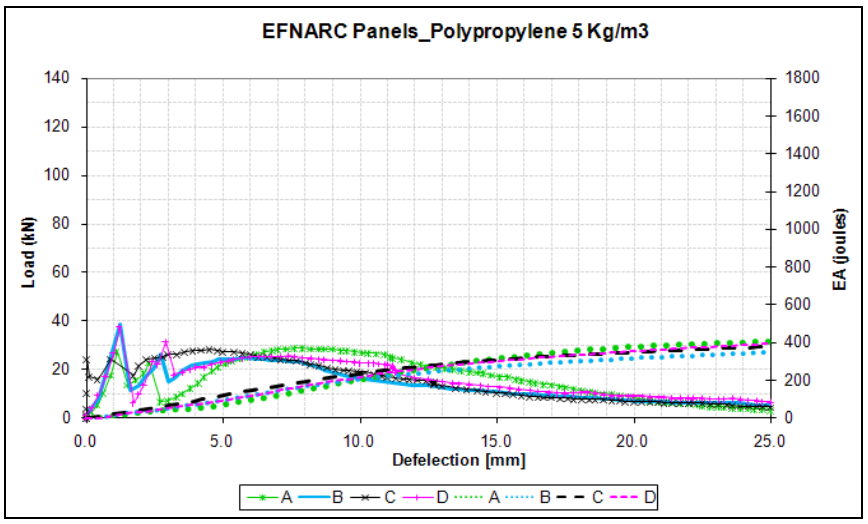
EFNARC PANEL TEST RESULTS

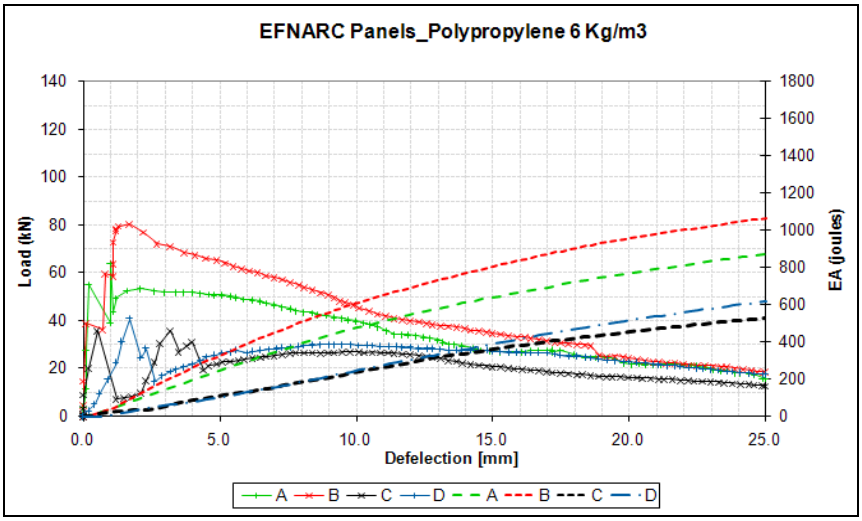


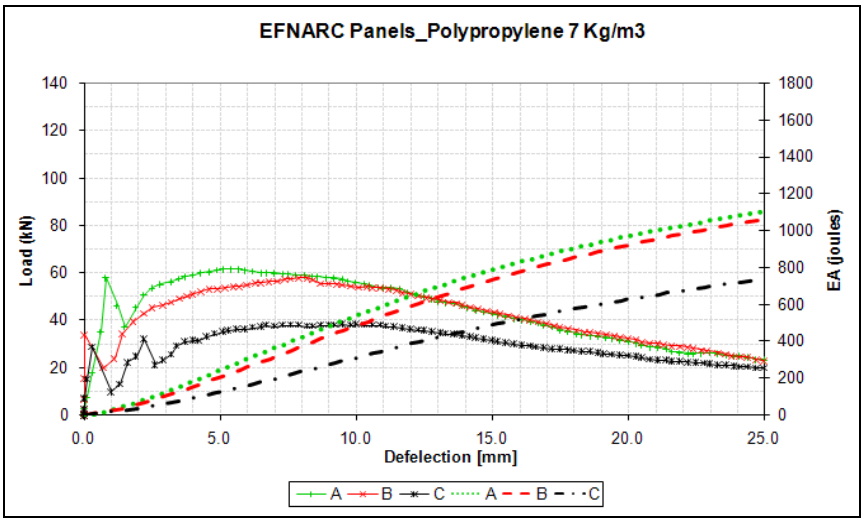


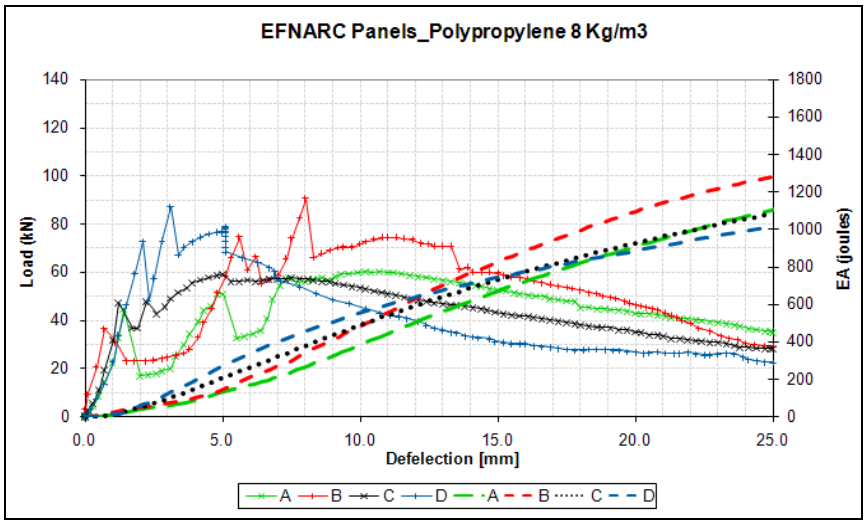


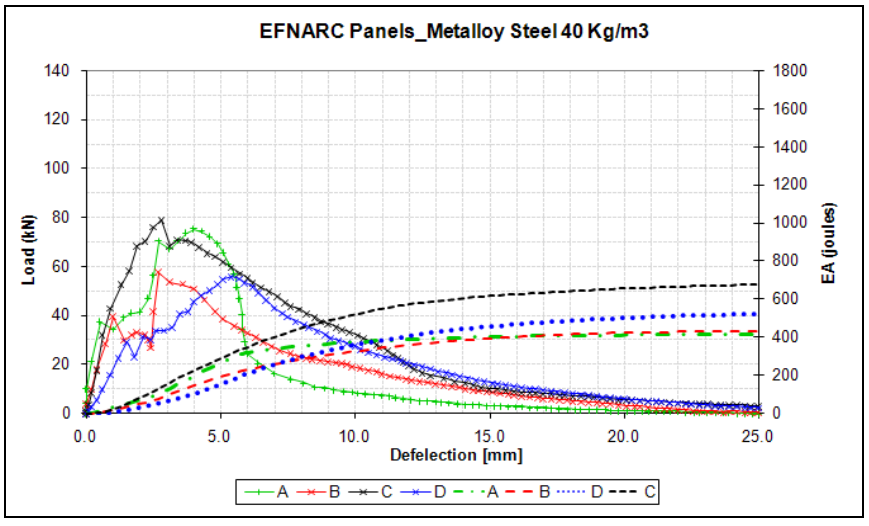

EFNARC Panels_Polypropylene 4 Kg/m3
Load (kN)
EA (joules)
Defelection [mm]
A B C D A B C D

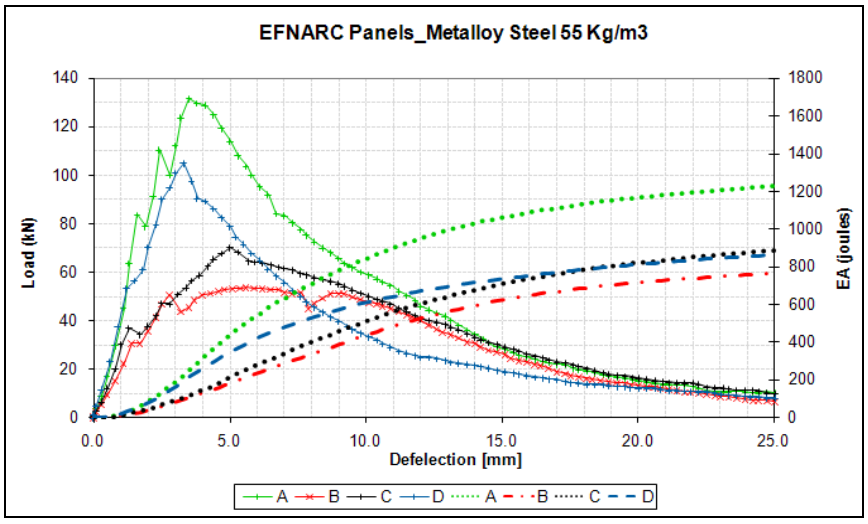

EFNARC Panels_Polypropylene 5 Kg/m3
Load (kN)
EA (joules)
Defelection [mm]
A B C D A B C D

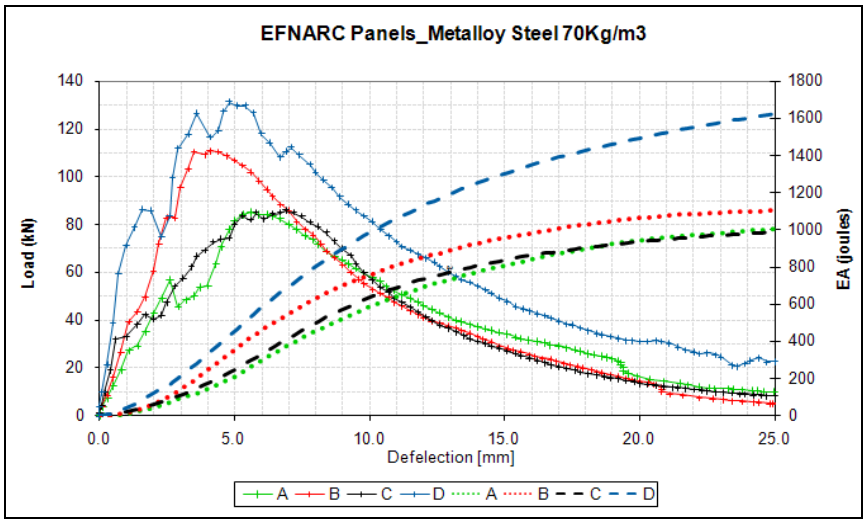

EFNARC Panels_Polypropylene 6 Kg/m3
Load (kN)
EA (joules)
Defelection [mm]
A B C D A B C D


EFNARC Panels_Polypropylene 7 Kg/m3
Load (kN)
EA (joules)
Defelection [mm]
A B C A B C

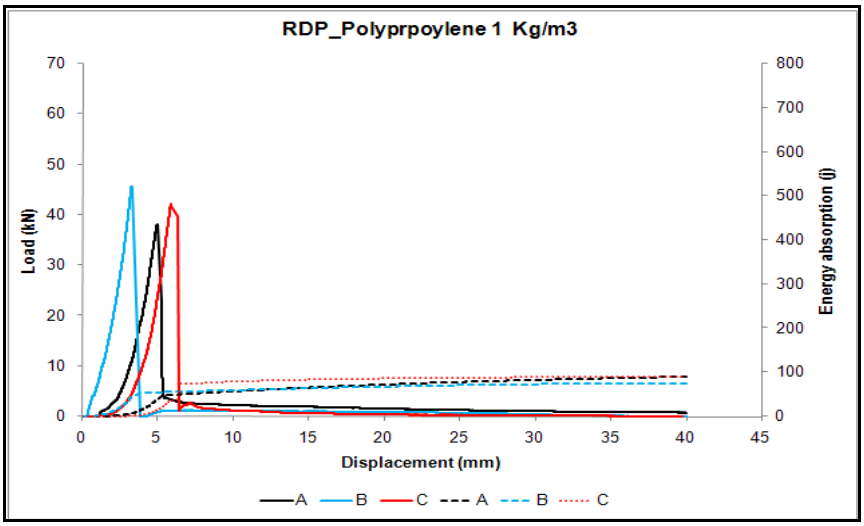

EFNARC Panels_Polypropylene 8 Kg/m3
Load (kN)
EA (joules)
Defelection [mm]
A B C D A B C D

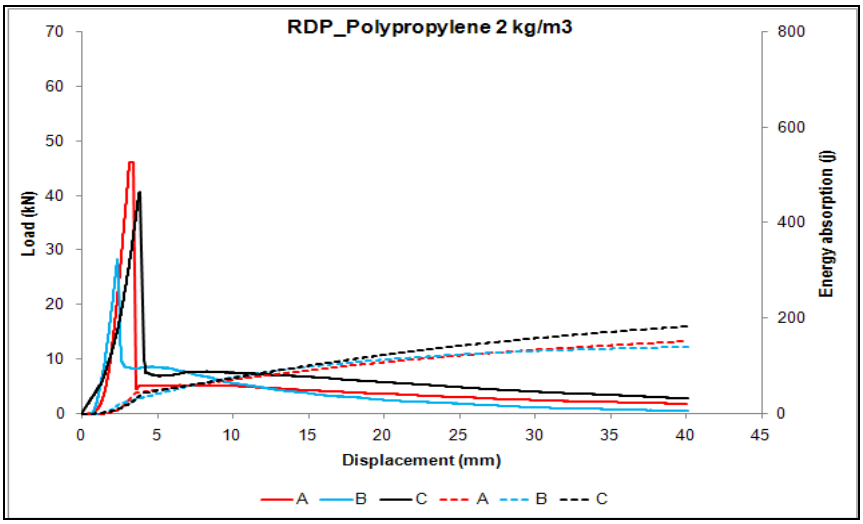

EFNARC Panels_Metalloy Steel 40 Kg/m3
Load (kN)
EA (joules)
Defelection [mm]
A B C D A B D C

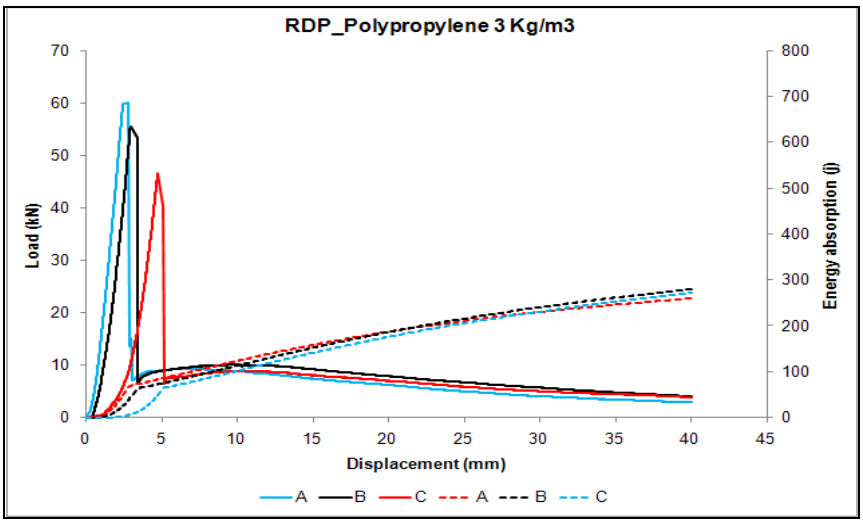

EFNARC Panels_Metalloy Steel 55 Kg/m3
Load (kN)
EA (joules)
Defelection [mm]
A B C D A B C D

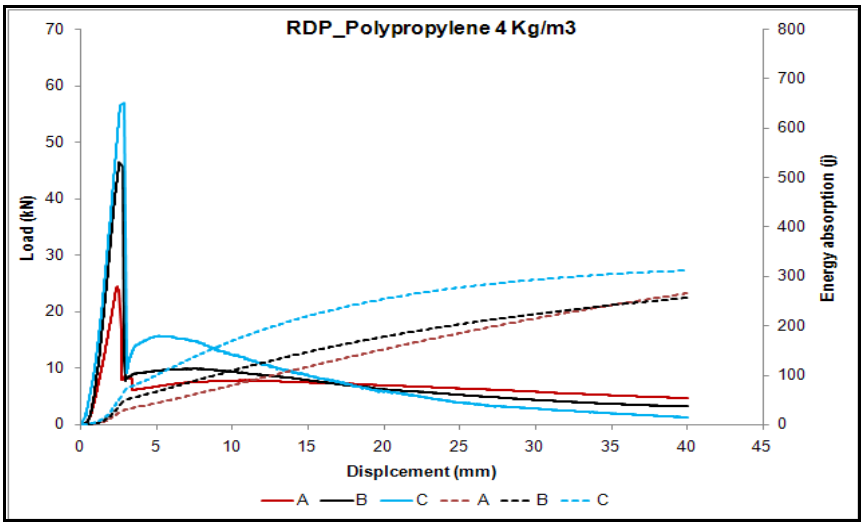

EFNARC Panels_Metalloy Steel 70Kg/m3
Load (kN)
EA (joules)
Defelection [mm]
A B C D A B C D

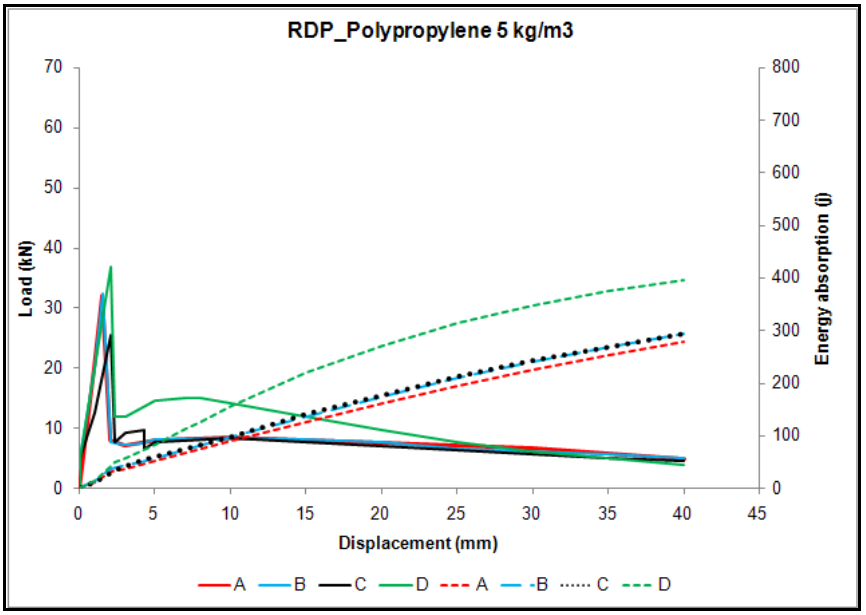
ROUND DETERMINATE PANELS

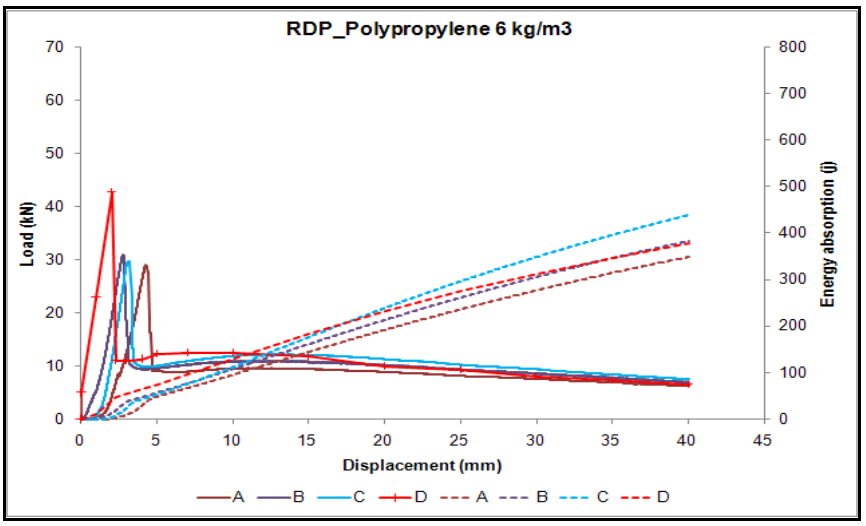


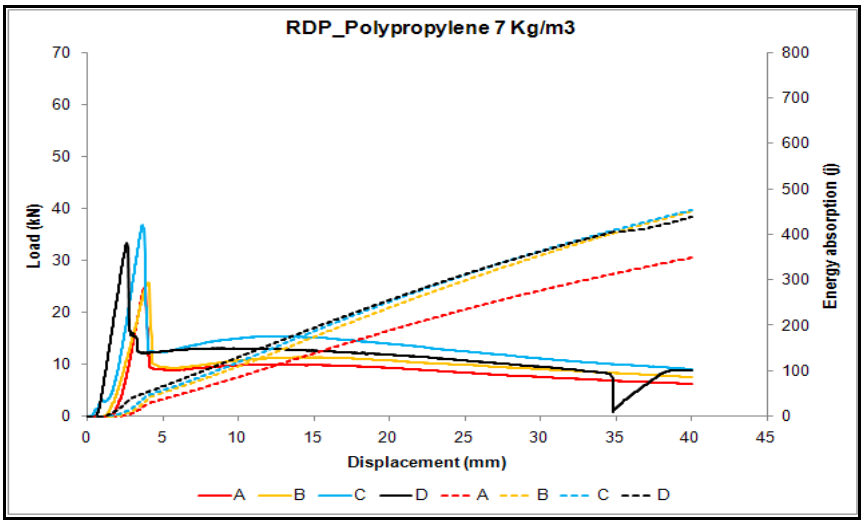


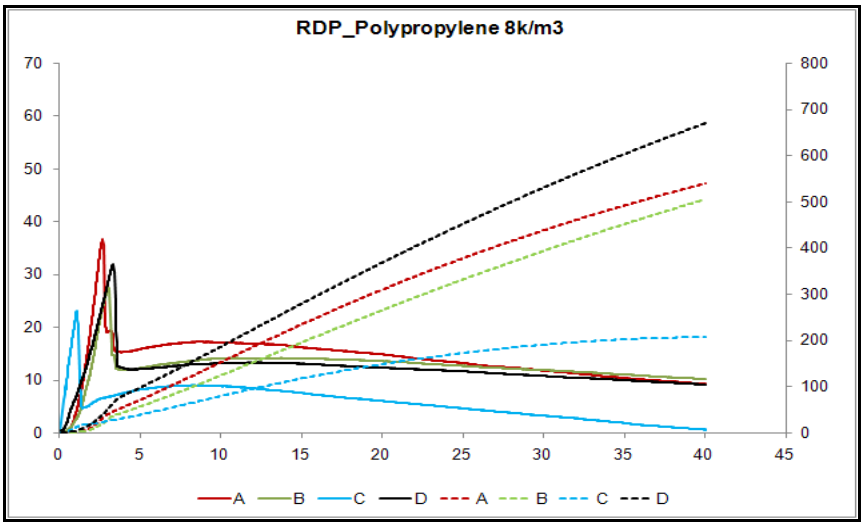


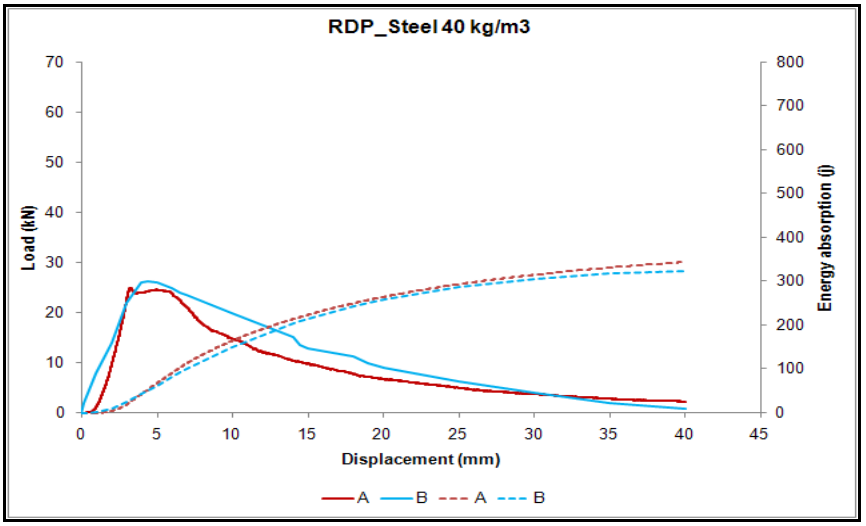

RDP_Polypropylene 4 Kg/m3
Load (kN)
Energy absorption (j)
Displcement (mm)
A B C A B C

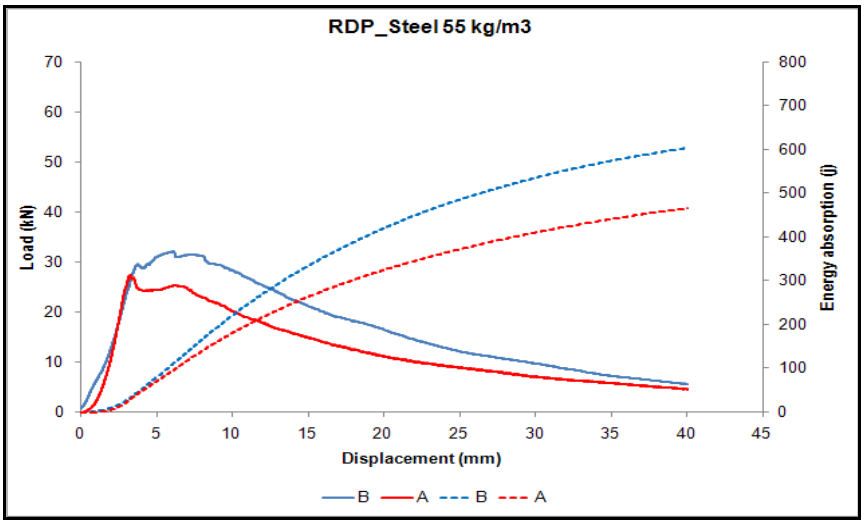

RDP_Polypropylene 5 kg/m3
Load (kN)
Energy absorption (j)
Displacement (mm)
A B C D A B C D

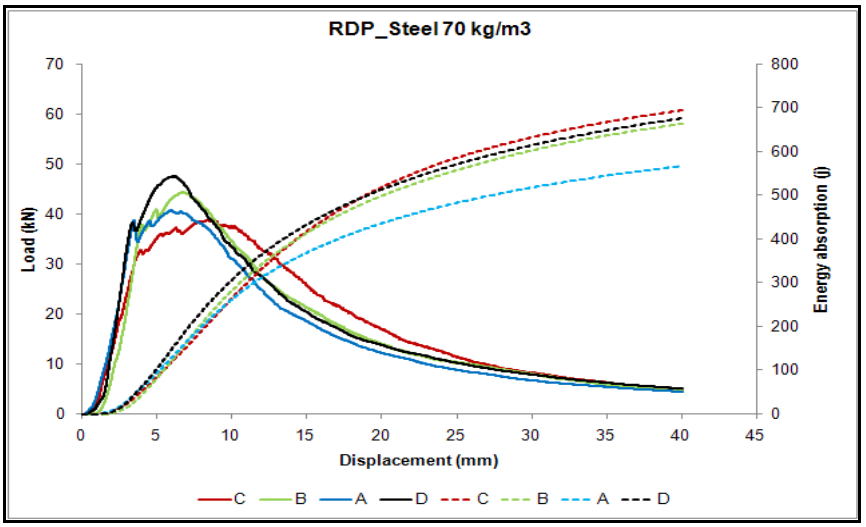

RDP_Polypropylene 6 kg/m3
Load (kN)
Energy absorption (j)
Displacement (mm)
A B C D A B C D


RDP_Polypropylene 7 Kg/m3
Load (kN)
Energy absorption (j)
Displacement (mm)
A B C D A B C D


RDP_Polypropylene 8k/m3
A B C D A B C D


RDP_Steel 40 kg/m3
Load (kN)
Energy absorption (j)
Displacement (mm)
A B A B


RDP_Steel 55 kg/m3
Load (kN)
Energy absorption (j)
Displacement (mm)
B A B A


RDP_Steel 70 kg/m3
Load (kN)
Energy absorption (j)
Displacement (mm)
C B A D C B A D

APPENDIX B: Table showing the strength, peak load, residual strength and energy absorption results for the laboratory tested shotcrete specimens

				EFNARC BEAMS						ASTM BEAMS							EFNARC PANELS		RDP	
Fibre Type	Fibre density	Fibre content	UCS	Flexural strength	Residual strength (N/mm²)				Energy absorption	Modulus of rupture	Toughness indices					Energy absorption	Peak Load	Energy absorption	Peak Load	Energy absorption
	(Kg/m³)	(Kg/m³)	(Mpa)	(N/mm²)	0.5mm	1.0mm	2.0mm	4.0mm	(joules)	(N/mm²)	I_5	I_{10}	I_{20}	I_{30}	I_{50}	(joules)	(KN)	(joules)	(KN)	(joules)
	1	-	45.00	8.86	5.18	1.57	0.20	0.07	18.74	6.69	4.39	7.05	9.27	9.78	10.15	8.25	46.00	94.00	42.30	90.00
	1	-	47.00	9.50	6.19	1.87	0.22	0.07	19.21	7.04	4.32	6.82	8.91	9.59	10.88	8.00	53.00	188.00	45.60	75.00
Polypropylene	1	-	46.00	9.16	5.55	1.44	0.14	0.07	17.66	6.49	4.64	8.34	13.20	15.44	17.12	7.40	70.00	401.00	38.10	90.00
	1																47.00	452.00		
	2	-	45.50	9.81	6.40	2.03	0.22	0.07	20.26	4.30	4.65	8.32	12.95	15.15	17.10	14.31	37.00	262.00	46.20	153.00
	2	-	45.00	8.71	5.30	1.39	0.21	0.07	17.40	4.55	4.38	7.08	9.67	10.59	11.28	15.69	64.00	320.00		
Polypropylene	2	-	42.00	7.97	3.50	0.30	0.45	0.45	13.19	4.29	4.46	7.45	10.68	12.02	13.12	13.40	83.00	926.00	28.50	139.00
	2																87.00	227.00	40.70	182.00
	3	-	45.00	9.92	4.44	0.85	0.66	0.76	13.59	8.07	4.54	7.83	11.33	12.69	14.97	35.04	37.00	318.00	60.10	260.00
	3	-	58.00	10.73	6.79	1.97	0.08	0.47	20.42	7.04	4.46	7.53	11.06	12.82	15.69	29.51	62.00	464.00	60.10	310.00
Polypropylene	3	-	46.00	9.07	2.55	0.47	0.66	0.94	11.86	9.72	4.65	8.40	12.73	13.84	15.02	42.40	88.00	711.00	55.50	280.00
	3	-																	46.60	274.00
	4	-	47.50	9.41	3.49	1.18	1.60	1.81	25.94	9.91	4.54	7.80	10.77	11.49	13.24	36.58	30.00	326.00		
	4	-	54.00	9.94	5.69	1.10	1.37	1.85	28.31	7.17	4.43	7.31	10.31	11.84	14.83	32.10	60.00	717.00	46.60	256.00
Polypropylene	4	-	47.00	8.17	2.90	1.15	1.08	1.35	20.88	8.42	4.59	8.13	12.21	13.89	16.83	37.62	57.00	579.00	24.50	265.00
	4	-															77.00	893.00		
	5	-	49.00	9.07	3.94	1.58	0.59	0.89	13.19	9.44	4.77	8.92	15.48	18.73	22.02	67.19	28.00	559.00	32.00	279.00
Polypropylene	5	-	49.50	9.72	5.01	2.11	0.90	1.10	16.20	8.94	4.66	8.43	13.46	15.59	16.37	53.67	49.00	450.00	32.40	294.00
	5	-	55.00	9.01	4.00	1.60	0.60	0.07	12.87	9.07	4.69	8.55	13.87	16.31	18.90	52.52	28.00	447.00	25.40	294.00
	5	-															37.50	548.00		
	6	-	52.00	7.01	1.90	1.50	1.70	2.10	13.94	8.85	4.63	8.38	13.92	16.58	19.30	19.12	64.00	825.00	42.70	377.00
Polypropylene	6	-	50.50	7.25	1.73	1.73	1.95	1.84	16.10	9.23	4.65	8.42	12.76	14.35	17.23	19.01	80.00	858.00	29.00	348.00
	6	-	47.50	7.57	2.09	1.30	1.49	1.40	15.63	7.00	4.22	7.12	12.73	18.65	30.10	29.42	36.00	687.00	30.90	383.00
	6	-															41.00	746.00	29.80	439.00
	7	-	52.50	6.98	1.60	1.40	1.70	1.80	14.52	8.65	4.52	7.76	11.12	12.82	16.84	16.25	62.00	1238.00	36.90	455.00
Polypropylene	7	-	50.50	6.94	1.88	1.53	1.77	2.12	13.77	9.14	4.62	8.09	11.75	13.65	18.35	21.50	58.00	1246.00	25.80	451.00
	7	-	54.00	6.28	1.68	1.68	1.91	2.02	14.00	8.68	4.42	7.05	10.14	13.01	19.13	21.75	38.00	799.00	33.30	440.00
	7	-																	24.90	349.00
	8	-	47.00	6.50	1.83	2.03	2.24	2.24	17.54	9.42	4.58	7.98	12.08	14.65	20.17	23.63	60.00	1019.00	23.10	209.00
Polypropylene	8	-	44.00	6.49	1.70	1.38	1.60	1.81	13.56	7.65	4.34	6.80	9.80	12.72	18.92	20.35	85.00	1153.00	27.40	506.00
	8	-	48.00	6.58	2.03	1.32	1.22	1.32	12.33	9.44	4.63	8.13	12.42	15.22	21.27	27.01	59.00	1195.00	31.90	670.00
	8	-															83.00	788.00	36.80	540.00
	40	29.54	61.00	5.89	3.12	3.47	3.12	2.08	20.92	9.09	4.46	7.46	11.95	15.75	21.68	22.93	75.00	538.00	25.00	343.00
steel fibres	40	30.50	59.00	6.60	3.41	3.53	2.96	1.71	20.68	7.71	4.30	7.09	11.75	16.27	23.80	20.59	58.00	520.00	25.00	343.00
	40	30.52	62.50	6.01	2.51	2.62	2.29	1.09	16.35	7.72	4.05	6.63	11.44	15.51	21.34	23.26	79.00	897.00		
	40																56.00	639.00		
	55	30.59	59.50	5.64	4.04	4.68	4.47	2.02	27.72	6.24	4.59	8.71	17.34	25.96	40.85	37.64	130.00	1047.00	32.30	605.00
steel fibres	55	42.02	59.50	5.89	2.85	2.95	2.55	1.57	20.00	7.27	4.42	7.76	14.01	20.30	32.73	30.66	54.00	866.00	27.40	466.00
	55	36.77	52.50	5.82	3.30	3.85	3.41	1.87	22.54	8.46	4.34	7.52	13.61	19.27	28.32	29.24	70.00	1018.00		
	55																104.00	1051.00		
	70	55.79	60.50	8.16	5.14	5.25	5.37	3.35	34.76	8.38	4.70	9.17	18.39	27.04	41.51	37.53	84.00	1245.00	44.40	664.00
steel fibres	70	54.10	62.50	9.07	5.70	4.75	3.59	2.00	27.74	9.31	4.23	7.03	12.19	17.10	25.44	28.50	110.00	1404.00	47.70	678.00
	70	58.93	60.50	8.12	5.28	4.75	3.69	2.11	28.09	9.52	4.43	7.99	14.85	20.84	29.74	37.61	85.00	1206.00	40.80	568.00
	70																130.00	1446.00	38.90	696.00